FUNCTIONALIZATION OF TITANIUM SURFACES WITH LYSINE, ASPARTIC ACID, VITAMINS C AND D_3: A MICRO RAMAN STUDY OF INTERMOLECULAR INTERACTIONS

by

Cesar Augusto Manrique Bastidas

A dissertation submitted in partial fulfillment of the requirements for the degree of

DOCTOR OF PHILOSOPHY

in

BIOENGINEERING

UNIVERSITY OF PUERTO RICO – MAYAGÜEZ

2019

Approved by:

_____	_____
Samuel P. Hernández-Rivera, Ph.D. President of Graduate Committee	Date
_____	_____
Nairmen Mina Camilde, Ph.D. Member of Graduate Committee	Date
_____	_____
Pedro J. Resto Irizarry, Ph.D. Member of Graduate Committee	Date
_____	_____
Paul A. Sundaram, Ph.D. Member of Graduate Committee	Date
_____	_____
Arturo J. Hernández-Maldonado, PhD Representative of Graduate Studies	Date
_____	_____
Eduardo J. Juan, Ph.D. Chairperson of the Department	Date

Abstract

Titanium (Ti) has been used since 1964 in manufacturing of Ti implants because of its optimal mechanical properties and good biocompatibility. Nevertheless, this biomaterial can have failures due to poor osseointegration caused by the spontaneous formation of a passive layer of titanium dioxide (TiO_2) when exposed to air. This amorphous TiO_2 layer does not promote very well the development of hydroxyapatite (HA) nor the new growing of bone onto the Ti surface implant. The above in conjunction with biological microorganisms lead to malfunction and many times to removal of orthopedic and dental implants based on Ti. Therefore, the compromised patient will be affected in different ways: financially, socially, and psychologically.

The work presented describes some processes that can be used to functionalize TiO_2/Ti surfaces aimed at to promoting its bioactivity when developing an HA layer on the functionalized Ti surface. The functionalization of Ti surface has been verified by using the Micro Raman Spectroscopy, which provides relevant spectroscopic information that can be used to infer possible intermolecular interactions between adsorbate (biological molecule) and substrate (Ti surface or functionalized Ti surface) leading to bonding.

In order to achieve a very good functionalization of Ti surface four target molecules (biomolecules) were used: lysine (Lys), aspartic acid (Asp), ascorbic acid (Vit-C) and cholecalciferol (Vit-D3). They were chosen based on their chemical, physical, and physiological properties conferring to Ti surface the capacity of *"in vitro"* formation of an HA layer onto it, improving in such way its biocompatibility and durability. Likewise, it will

impact directly the bioengineering field because Ti based implants could be manufactured with a better osseointegration and a lower cost than right now, and the patients will be improved their finances regarding the above issue.

In summary, the functionalization of Ti surfaces with bioactive molecules and hence biocompatible coatings is a technique that will incidence the clinical success associate to bone-anchored Ti implants, due to the interface stability between Ti implant and bone will be improved.

Resumen

El titanio (Ti) se ha utilizado desde 1964 en la fabricación de implantes de Ti debido a sus óptimas propiedades mecánicas y buena biocompatibilidad. Sin embargo, este biomaterial puede tener fallas debido a una mala oseointegración causada por la formación espontánea de una capa pasiva de dióxido de titanio (TiO_2) cuando se expone al aire. Esta capa de TiO_2 amorfo no promueve muy bien el desarrollo de hidroxiapatita (HA) ni el nuevo crecimiento de hueso en la superficie del implante de Ti. Lo anterior, aunado a los microorganismos biológicos, conduce a un mal funcionamiento y muchas veces a la extracción de los implantes ortopédicos y dentales fabricados a base de Ti. Por lo tanto, el paciente comprometido se verá afectado económica, social y psicológicamente.

La investigación doctoral realizada ha permitido funcionalizar la superficie de TiO_2 / Ti a fin de promover su bioactividad al desarrollar una capa de HA sobre la superficie de Ti funcionalizada. La funcionalización de la superficie de Ti se ha verificado utilizando la espectroscopia Micro Raman, la cual proporciona información espectroscópica relevante útil para poder inferir las interacciones intermoleculares entre el adsorbato (molécula biológica) y el sustrato (superficie de Ti o superficie de Ti funcionalizada). Para lograr una muy buena funcionalización de la superficie de Ti, se usaron cuatro moléculas biológicas a saber: lisina, ácido aspártico, ácido ascórbico y colecalciferol. Las anteriores fueron elegidas debido a sus buenas propiedades químicas, físicas y

biológicas que le confieren a la superficie de Ti la capacidad "in vitro" de formar una capa de HA sobre ella, mejorando de esta manera su biocompatibilidad y durabilidad. Del mismo modo, esto afectará directamente al campo de la bioingeniería porque los implantes a base de Ti se podrán fabricar con una mejor oseointegración y menores costos de producción con relación a los que se producen en este momento. De tal manera, que los pacientes afectados mejorarán sus finanzas en ese aspecto.

Para finalizar, la funcionalización de las superficies de Ti con moléculas bioactivas y, por lo tanto, con recubrimientos biocompatibles es una técnica que incidirá en el éxito clínico asociado a los implantes de Ti anclados en los huesos, debido a la estabilidad de la interfaz entre el implante de Ti y el hueso.

Thesis submitted in partial fulfillment of the requirements for the degree of Doctor of Philosophy in Bioengineering at University of Puerto Rico – Mayaguez.

Mayagüez, Puerto Rico, USA, 2019

Acknowledgements

First of all, I want to thank God for giving me the privilege being alive and carry out the duties entrusted by him. Likewise, I would like to thank Dr. Samuel P. Hernández for his great advices and for allowing me to belong to his excellent research group. Thanks are also expressed to Dr. Paul Sundaram, Dr. Pedro Resto and Dr. Nairmen Mina for their guidance and advices.

To my friends Annette Colón, Francheska Colón, and Luis Perez for their friendship. Thanks to all. Thanks to my best friend Rubén D. Mera for encouraging me to pursue my PhD studies away from home.

Thanks to the Faculty and Staff of the Department of Bioengineering at University of Puerto Rico, particularly Dr. Eduardo J. Juan for your great collaboration and guidance. To Mrs Aracelis Rosado I am very grateful for your generous and kindly assistance in the administrative processes during these years in my doctoral studies.

Thanks to my family, specially my children, my wife, my parents, and my brothers for trusting on me.

Table of Contents

List of Tables

List of Figures

Acronyms

AAs	amino acids
Asp	aspartic acid
BCC	body-centered cubic structure
CHA	carbonated hydroxyapatite crystals
CKD	chronic kidney disease
DI	deionized
ECM	extracellular matrix
HA	hydroxyapatite
HCP	hexagonal close packed structure
Lys	lysine
NCPs	non-collagenous proteins
RS	Raman scattering
SBF	simulated body fluid
SiC	silicon carbide
Ti	titanium
Vit-C	vitamin C
Vit-D	vitamin D

Chapter 1

Introduction

1.1 Overview

The element titanium was discovered independently in 1791 by William Gregor, and in 1795 by Martin Heinrich Klaproth. It was found confined in a rutile ore. In Greek mythology, the giant Titan, son of Uranus (Father Heaven) and Gaia (Mother Earth) was confined in the underground dark world because he lost the wars against the Olympic Gods. This served as inspiration to Klaproth to name the new element titanium (Ti).

Ti is the fourth most abundant metal (0.6%), preceded by aluminum, iron, and magnesium, and the ninth among all elements in the earth's crust. It has atomic number 22, and atomic weight of 47.88 g mol^{-1}. Ti has five naturally occurring isotopes: ^{46}Ti, ^{47}Ti, ^{48}Ti (most abundant, 73.72%), ^{49}Ti and ^{50}Ti. It is a lustrous metal with high melting point (1667 °C). Pure Ti crystallizes at low temperatures in a hexagonal close packed structure (HCP) identified as α-titanium. At high temperatures, the stable body-centered cubic structure (BCC) called β-titanium, predominates.

There is a wide spectrum for applications of Ti and its alloys, mainly in the aerospace industry. However, they have also been adapted and widely employed as implantable medical devices in dentistry and restorative surgery. The main reasons for this is that Ti has good biocompatibility due to its lightness, excellent mechanical properties, lack of toxicity, extremely low corrosion rate, and spontaneously oxidation of titanium surface yielding a passivating titanium dioxide (TiO_2) layer of 5-6 nm. [1-11]

Titanium(IV) oxide (TiO_2) is referred to as titania. It is extracted from ilmenite, rutile and anatase minerals. Titanium dioxide has three main crystal structures: rutile, anatase, and brookite, which is the least stable common crystal structure. TiO_2 is relatively inert, both chemically and physiologically. This was first demonstrated by Heaton in 1929, when he ate TiO_2 dust sweetened with glucose. Heaton eliminated it in 24 h without any adverse or collateral reactions. These facts are very important

because they provide information for TiO_2 naturally occurring layer on titanium surfaces used in biomedical devices without health risks. Besides, Ti has a tetragonal rutile crystal structure TiO_2 as an oxidation product resulting of air exposure. Notwithstanding Ti is chemically labile, the thin TiO_2 film protects the metal (passivating it) and promotes a good resistance to corrosion as long as its integrity can be maintained. However, it is useful consider the type of chemistry which might be involved in the biological system of human body. For the most part, the body is a reducing environment, and under these conditions it is likely it contributes to decrease the protective nature of the oxide film, causing problems of osseointegration and fixation of Ti implants into the body. [12-14]

The main medical applications of Ti and its alloys are as follows: screws, plates, hip and knee joints, vascular endoprosthetics, heart valves, dental implants, and so forth. At present, the most used compositions are commercial elemental Ti, α+β and β; and Ti-6Al-4V alloys. Nevertheless, there are issues with vanadium (V), due to the fact that V can be toxic in a long term exposure. [15]

The goal in physiological applications is to design and develop implants based on Ti that work for a long time, without the need of surgical interventions directed to fix problems due to failures or lack of compatibility issues. Normally, the service period is about 15 to 20 y for older patients, and over 20 y for younger patients. [16]

Consequently, the main concern of using Ti implants has been the inmunoresistance and bio-inertness of Ti based prosthesis. That is, prosthesis should not yield toxic substances nor tissue interactions. Notwithstanding, recent studies reveled that Ti based prosthesis have considerable limitations as biomaterials because of there was no direct chemical bond with the host bone after implantation and its performance was reduced, while the mobilization of the titanium prostheses was increased. In fact, in some cases the Ti based prostheses had to be removed, resulting in additional health and financial costs for the patients. [16,17]

Research in the field allowed to design and develop new biomaterials to overcome the above-mentioned problem. Because of the interface between host bone and synthetic devices has a remarkable influence on the clinical efficacy of implant, protocols directed to improve implant materials with coating have been developed to

promote the osseointegration of the titanium prostheses with the living bone tissue and form new harder tissue. [17,18]

For a material be successfully biocompatible there must be an improvement on the chemical and physical surface properties of the implanted devices, since the surfaces that will be in contact with the biological system in body implants must foster tissue-implant bonding. Current coated Ti surfaces are based on TiO_2 to improve biocompatibility and corrosion resistance. Nevertheless, these can be degraded by some physiological conditions such as bacterial contamination and corrosion, resulting in device failure. [19, 20] To address these problems an innovative functionalization of Ti surfaces with lysine, aspartic acid, vitamins C and D_3, and a subsequent micro Raman study of intermolecular interactions promoted were performed. As is known, implanted materials in the human body have interactions with blood and tissues, and they must possess a high wear resistance in this corrosive biological environment. If the wear resistance is low a wear debris in the surrounding tissue can be formed promoting inflammatory reactions carrying to osteolysis. Finally, implant loosening due to biological system starts to digest the wear debris and the bonds implant-bone are destroyed. [21]

As regards to the above, the exposed Ti surface was coated with lysine, aspartic acid, vitamin C, and vitamin D_3. These compounds constitute a versatile class of substances, due to their excellent biological, chemical and physical properties, make them biocompatible.

1.2 Amino acids

The amino acids (AAs) are the fundamental building blocks for vast quantity of biomolecules. Likewise, their chemical structures and functional groups determine the physical and chemical properties needed for surface interactions with Ti and specifically with TiO_2 (Figure 1.1). Regarding the presence of functional groups, such as basic amine and acidic carboxyl groups, it is therefore expected to be an interaction via formation of covalent bonds and/or hydrogen bonds with TiO_2. Besides, their

zwitterionic or ampholytic character is crucial for enhancing and promoting the adsorption process on the Ti/TiO_2 surface. [22]

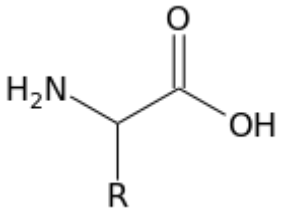

Figure 1.1. Chemical structure of amino acids

Biomineralization is a term related to the process followed by living organisms to produce biominerals that have exceptional properties such as high mechanical properties, among others. These properties are directly controlled by biomolecules. Formation of bone tissue involves one of the most complex examples of biomineralization, since an organic-inorganic hybrid material is produced based on collagen, non-collagenous proteins (NCPs) and carbonated hydroxyapatite (CHA) crystals. CHA nucleates and grows in extracellular matrix (ECM) provided by collagen fibers. ECM determines the ultimate structure and orientation of CHA. However, CHA is not able to initiate HA mineralization, although body fluids are supersaturated in HA. A set of negatively charged phosphorylated NCPs associated with the ECM initiate HA nucleation. NCPs attract Ca^{2+} and PO_4^{3-} ions using their AAs domains in order to create an increment of the local super saturation to produce nuclei with a critical size and promote formation of HA crystals. [23-26] AAs and peptides have been investigated to know their effect on HA mineralization. Both, positively and negatively charged AAs are present in the hole zone of collagen responsible for HA nucleation. This appears to be important in order to carry out the required interactions with both Ca^{2+} and PO_4^{3-} ions to induce HA precipitation. [25, 26]

In a similar way studies carried out *in vitro*, have shown that charged AAs induce HA mineralization modifying the morphology and crystalline structure of HA, due to their carboxylate and phosphate groups. When AAs are compared with proteins and peptides, it can be seen that AAs do not have long molecular chains and their three-dimensional conformations are simpler; besides, AAs are much smaller (about 7 nm).

These steric properties give advantages to AAs over proteins and peptides since a single AA can interact with only one HA facet. [27-36] *In vivo* studies aimed at elucidating the effect of AAs on HA precipitation under similar conditions to the physiological ones were performed, taking into account factors such as collagen, mineralization inhibitors, and cells that markedly impact HA precipitation. [37, 38]

1.3 Vitamin C

Ascorbic acid or vitamin C known has a lactone structure which is a cyclic ester of hydro carboxylic acids. In fact, it does not belong directly to the family of carboxylic acids. Hence, its acidity is due to ionization of hydroxyl group present on C-3, yielding an anion stabilized by resonance (Figure 1.2). It has many uses, mainly in pharmaceutical, cosmetic, food and chemical industries, where it has been widely employed because of its antioxidant properties. It is very important for the biosynthesis of collagen due to its role as antioxidant that prevents oxidative damage caused by reactive oxidative species. *In vitro* studies suggest that local application of vitamin C in periodontal health enhances the production of collagen. [39] It is a biological compound that has been investigated in dental implants due to its properties related to accelerate bone regeneration, substantially improve implant-bone response in osteoporotic and healthy conditions, and augment implant osseointegration. Besides, there is evidence about vitamin C speeding up the precipitation of HA due to its agglomeration, under physiological conditions. [40] Ascorbic acid is characterized by its hydroxyl functional group that confers it a good molecular site to chemically bond to TiO_2, mediated by hydrogen bond, and therefore to promote formation of HA over Ti/TiO_2 surfaces. [39-45]

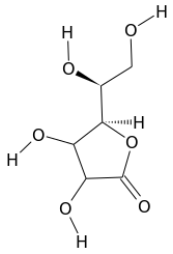

Figure 1.2. Chemical structure of ascorbic acid

Also, vitamin C has been used as a surface modifier in material science. [46] Notwithstanding, vitamin C has been rarely reported as an agent to control the morphology of material surfaces.

1.4 Vitamin D

Vitamin D is necessary to support normal levels of phosphate and calcium needed to carry out bone mineralization, nerve conduction, muscle contraction and control general cellular function into the human body. Vitamin D, refers to a group of fat-soluble vitamins. It exists in five diverse forms; however, the principal two forms are vitamin D_2 (ergocalciferol) and vitamin D_3 (cholecalciferol) illustrated in Figure 1.3. Structural differences between ergocalciferol and cholecalciferol are as follows: the side chain of ergocalciferol contains a double bond between carbons located in position 22 and 23, and a methyl group on carbon 24.

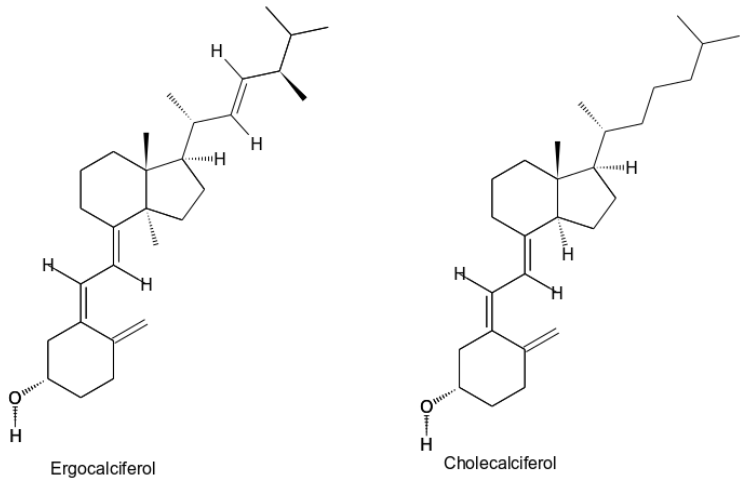

Figure 1.3. Chemical structure of ergocalciferol and cholecalciferol.

Plants produce vitamin D_2, while vitamin D_3 is produced by the skin of animals after exposition to sunlight. Calcitriol, the active form of vitamin D that it is synthesized from vitamin D_3, binds and activates vitamin D receptors located in the nuclei of target cells. Vitamin D_3 has been studied as a bone-resorbing agent. *In vitro* experiments

demonstrate that vitamin D_3 inhibits bone resorption regulating intestinal calcium absorption. Production of alkaline phosphatase and type I collagen, needed for bone growth, in osteoblastic cells are stimulated by vitamin D_3. [47, 48] In fact, vitamin D_3 has been used in treatments of osteoporosis. Also, research has suggested that vitamin D_3 participates in acceleration of bone regeneration, in such manner that its deficiency exerts negative effects on implant osseointegration. [49-59] In this regard, vitamin D deficiency is common in chronic kidney disease (CKD) which is a highly prevalent disease affecting diverse systems such as cardiovascular, osseous and renal. [60] In CKD patients bone regeneration and fracture healing are negatively affected by vitamin D deficiency, due it is required in bone metabolism. [61] Research carried out by investigators have proven that vitamin D insufficiency is not favorable for osseointegration of Ti implants in male Sprague-Dawley rats. [62] However, researchers have found that vitamin D supplementation is relevant to obtain a meaningful survival advantage in patients suffering CKD, and improvement in the process of fracture healing. [60]

The above suggests that vitamin D supplementation is an effective approach that can be used to improve implant-bone integration and fixation of Ti implants. It is worth considering that the chemical structure of vitamin D has a hydroxyl group that can be interact with TiO_2 to chemically form a hydrogen bond in order to promote growing of HA onto Ti surfaces, and so functionalized it.

AAs, and vitamins C and D_3 are promising bioactive molecular candidates that can promote osseointegration due to their osteogenic potential. The properties of these compounds can provide Ti with good biocompatibility, resulting in better molecular interactions with biological system to form HA coating on Ti surfaces and osseointegration needed to fix the Ti prostheses in the body and prevent its failure and future removal.

1.5 Intermolecular interactions of AAs, vitamins C and D_3 with Ti and TiO_2

Research on interactions of AAs, vitamins C and D_3 molecules with Ti and TiO_2 can give an essential comprehension of the Ti based implants. Nonetheless, experimental techniques able to measure the affinity of single AAs or vitamin to a given surface are still few. In this regards, the research was focused on spectral measurements based on Raman Scattering (RS) spectroscopy since the technique has many advantages over others, such as: non-destructive, non-invasive, label free, highly specificity, very small sample quantity needed (about few µL), and compatible with physiological measurements (weak interferences from water). Moreover, RS can be used to identify specific chemical bonds that are present on Ti surfaces, as well as structural information of the surfaces layers. RS also, supplies simple and specific data about biological and chemical composition of samples, and required practically no sample preparation. Furthermore, the data obtained requires very little preprocessing, and the results can be obtained immediately (in near real time) allowing to make decisions and act according to the situation. Each RS spectrum is unique, due to this technique is chemically-specific and sensitive to variations in molecular composition and structure. If the substance under study changes in chemical/physiological environment because of some chemical and/or physical situations, it can be anticipated that this will be reflected in the RS spectrum.

The spectroscopic phenomenon known as Raman scattering was postulated in 1923 by Smekal. Nevertheless, the recognition and Nobel prize was awarded to C.V. Raman and K.S. Krishnan for the discovery, spreading and explanation of the technique. In order to understand the Raman effect, it is necessary to establish that scattering is a two-photon process: one incoming into the molecular system and another outgoing from it. Rayleigh scattering and the related Raman scattering are related to the molecular polarizability, which is a measure of the susceptibility of electrons in atoms or molecules to be distorted by an externally applied electric field. In Rayleigh scattering the photons are elastically scattered: a molecule absorbs a photon and simultaneously emits a photon of the same energy, frequency, and wavelength in any direction. In Raman

scattering the photons are inelastically scattered: the molecules are changing their polarizabilities (for example, the molecule may be vibrating, inducing a change in polarizability), so a photon can be absorbed and then simultaneously emitted, but the energy, frequency and wavelength of the outgoing photon are different from those of the incoming photon. Generally, the incoming photon loses energy, so the outgoing photon has less energy. This process occurs for about one photon in a 10 million photons. [63]

Raman microspectroscopy uses a microscope operating in confocal mode to collect all the light scattered by the sample and filters out any photons that are at the original frequency (Rayleigh scattering), leaving only those with shifted frequencies. A spectrometer is used to analyze the shifted frequency photons, and then their exact frequency shift is determined. As the frequency shift is directly related to the induced rotational and vibrational motions of the molecule, the structure of any compounds can be investigated.

1.6 Benefits

According to the above, this dissertation research proposal offers benefits related to a better comprehension of HA mineralization mediated by AAs, vitamins C and D_3. This knowledge will improve the current background information on bone formation onto Ti implants. Moreover, AAs, vitamins C and D_3 are inexpensive and stable, making them better cost-effective candidates for fast development and design of coating onto the Ti surface, solving difficulties associated to high-tech, high-cost equipment. The above displays an economical potential in bioengineering.

Chapter 2

Hypothesis and Research Objectives

2.1 Hypothesis

Ti surfaces can be functionalized with biological molecules to produce HA on them, and intermolecular interactions adsorbate–surface. The information required to confirm this can be acquired by a vibrational spectroscopic technique with high sensitivity and specificity: Raman spectroscopy.

2.2 Research Objectives

This research deals mainly with the micro Raman study of intermolecular interactions that occur on functionalized Ti surfaces. Concomitant to the mentioned in the previous section to carry out the research the main objective was as follows:

To functionalize Ti/TiO_2 surfaces using coatings based on AAs, and vitamin C and D_3 with specific physical and chemical properties that meet requirements, such as: good adsorption, promote intermolecular interactions, non-volatility, trigger development of a layer of HA, and so forth. To perform micro RS studies to characterize the intermolecular interactions resulting from coated Ti with AAs, and vitamin C and D_3, and evidence development of layer of HA on the substrate after its exposition to simulated body fluid (SBF).

To attain the proposed objective several sub-aspects were investigated:

1. Reviewing and use of adequate techniques of coating on Ti/TiO_2
2. Confirmation of AAs, and vitamins C and D_3 based Ti/TiO_2 coating
3. Study the effects of specific AAs, and vitamin C and D_3 in triggering development of layer of HA on the Ti/TiO_2 surfaces in SBF
4. Elucidate intermolecular interactions resulting from coated Ti/TiO_2 surfaces with AAs, and vitamin C and D_3.

Chapter 3

Methodology

3.1 Functionalization of TiO_2 / Ti surfaces

Functionalization of the Ti surfaces involved the following methodology:

3.1.1 Ti surfaces cleaning

Ti surfaces were abraded progressively using SiC grinding paper. After that, they were cleaned with acetone, alcohol, and distilled water consecutively about 15 min. Then, the cleaned surfaces were dried by exposing them to air.

3.1.2 Ti surfaces modification

Ti surfaces were modified to yield a TiO_2 layer using HNO_3 to etch the surfaces, and subsequently H_2O_2–oxidation were performed. [64] The general procedure was as follows:

3.1.2.1 Etching of Ti surfaces

After being dried in air, the cleaned Ti surfaces were etched for 2 min each one, using a mixture composed of 30 mL of nitric acid (HNO_3, 40 wt.%) and 70 mL of DI water.

3.1.2.2 Oxidation of Ti surfaces

Oxidation of etched Ti surfaces were performed by immersing and soaking the samples in 30% mass solution H_2O_2 for 24 h.

3.1.3 Adsorption of AAs, and vitamins C and D_3 onto Ti surfaces

AAs, and vitamins C and D_3 were adsorbed on Ti surfaces according to incubation techniques described in the literature. [65] The general procedure was as follows: the samples were prepared by incubating oxidized Ti surfaces in solutions of biological compounds for time needed to produce adsorption at room temperature. After incubation Ti samples were rinsed with water and ethanol to eliminate any interferences. Then, they were immersed again for another incubation at room

temperature. Finally, Ti samples were dried exposing them to air, to produce a film that coats the modified oxidized Ti surface.

3.1.4 HA formation on functionalized Ti surfaces

To evaluate the bioactivity of functionalized Ti surfaces with AAs, and vitamins C and D_3, samples were immersed in SBF, a solution that was developed by Kokubo and coworkers for testing the bone bonding capability of materials, that is, to form HA on bioactive materials *in vitro*. [66]

The preparation of SBF solutions were carried out according to methodology described therein. Afterward, the functionalized Ti surfaces were immersed in SBF for determined periods of time in order to induce the development of an HA layer onto them, and therefore, an HA composite coating on Ti substrates.

3.2 Coating characterization and study of intermolecular interactions by RS

Functional coating of a Ti surface was a very important step required to enhance the formation and adsorption of target molecules such as biological molecules, and HA onto it. Functionalization involved the intermolecular interactions of adsorbates (biological molecules) with Ti surface, and with HA. High speed analysis and chemical selectivity are both feasible if rapid spectroscopic methods are used, such as RS, which provides direct chemical information about the coating on Ti surface.

The information that can be derived from a Raman spectrum is influenced by the frequency location of a Raman band, which is affected by the masses of the atoms in a molecule or crystal. Besides, their spatial arrangement, and displacements that occur during a vibration and the bond force constants exert an effect on observed and predicted characteristic frequencies. Another important aspect has to do with the intensity, which depends on change in polarizability during the vibration.

Intermolecular interactions can be influenced by the above, because some changes in the equilibrium conformation, the atomic masses, or the force constants can change both the frequency and intensity of a band. Also, it is important to mention that in a molecule different parts of it can be strongly coupled, and a single atom can produce

perturbations in its vibrational modes. Therefore, subtle variations in molecular structure can impact the intermolecular interactions, which can be reflected in the RS spectrum due to its sensitivity to chemical and physical structure.

As regards to the aforementioned, Micro RS were used to identify and characterize the specific chemical bonds and intermolecular interactions present at the functionalized Ti surfaces with AAs. Therefore, the impact of functionalization of Ti surfaces with AAs, and vitamin C and D_3 on development of HA were studied based on spectroscopic measurements. [67-69]

3.3 REFERENCES

[1] M. D. Pierschbacher and E. Ruoslahti, “Cell attachment activity of fibronectin can be duplicated by small synthetic fragments of the molecule,” *Nature*, **309**: 30-33, 1984.

[2] E. Ruoslahti and M. D. Pierschbacher, “New perspectives in cell adhesion: RGD and integrins,” *Science*, **238**(4826): 491-497, 1987.

[3] X. Liu, P. K. Chu, and C. Ding, “Surface modification of titanium, titanium alloys, and related materials for biomedical applications,” *Mater. Sci. Eng. R Reports*, **47**(3): 49-121, 2004.

[4] L. Carlsson, T. Röstlund, B. Albrektsson, T. Albrektsson, and P.-I. Brånemark, “Osseointegration of titanium implants,” *Acta Orthop. Scand.*, **57**(4): 285-289, 1986.

[5] P. Tengvall and I. Lundström, “Physico-chemical considerations of titanium as a biomaterial,” *Clin. Mater.*, **9**(2): 115-134, 1992.

[6] D. G. Castner and B. D. Ratner, “Biomedical surface science: Foundations to frontiers,” *Surf. Sci.*, **500**(1): 28-60, 2002.

[7] J. E. Ellingsen, “A study on the mechanism of protein adsorption to TiO_2,” *Biomaterials*, **12**(6): 593-596, 1991.

[8] K. E. Healy and P. Ducheyne, “Hydration and preferential molecular adsorption on titanium in vitro,” *Biomaterials*, **13**(8): 553-561, 1992.

[9] E. A. B. Effah P. D. Bianco P. Ducheyne., “Crystal structure of the surface oxide layer on titanium and its changes arising from immersion,” *J. Biomed. Mater. Res.*, **29**(1): 73-80, 1995.

[10] D. F. Williams, “Titanium as a metal for implantation Part 1,” *J. Med. Eng. Technol.*, **1**(4): 195-198, 1977.

[11] D. C. Rodrigues, R. M. Urban, J. J. Jacobs, J. L. Gilbert., “In vivo severe corrosion and hydrogen embrittlement of retrieved modular body titanium alloy hip implants,” *J. Biomed. Mater. Res. Part B Appl. Biomater.*, **88B**(1): 206-219, 2008.

[12] K. A. Davis, “Titanium dioxide,” *J. Chem. Educ.*, **59**(2): 158, 1982.

[13] Jones, D.A., "Principles and Prevention of Corrosion", Second ed. Upper Saddle River, NJ 07458, Prentice Hall, pp. 1-8, 40-48, 75-84, 146-156, 1996.

[14] Textor, M., Sittig, C., Frauchiger, V., Tosatti, S., Brunette, D. M., "Properties and Biological Significance of Natural Oxide Films on Titanium and Its Alloys", in Titanium in Medicine, M. D., Brunette, P., Tengvall, M., Textor, P., Thomsen, Editor, Springer - Verlag Berlin, pp. 171-230, 2001.

[15] K.L. Wapner, Implications of metallic corrosion in total knee arthroplasty, *Clinical Orthopaedics and Related Research*. **271**: 12-20, 1991.

[16] M. Abdel-Hady Gepreel and M. Niinomi, “Biocompatibility of Ti-alloys for long-term implantation,” *J. Mech. Behav. Biomed. Mater.*, **20**: 407–415, 2013.

[17] N. Drnovšek, S. Novak, U. Dragin, M. Čeh, M. Gorenšek, and M. Gradišar, “Bioactive glass enhances bone ingrowth into the porous titanium coating on orthopaedic implants,” *Int. Orthop.*, **36**(8): 1739-1745, 2012.

[18] R. Narayanan, S. K. Seshadri, T. Y. Kwon, and K. H. Kim, “Calcium phosphate-based coatings on titanium and its alloys,” *J. Biomed. Mater. Res. Part B Appl. Biomater.*, **85B**(1): 279-299, 2008.

[19] S.-M. Zhang, J. Qiu, F. Tian, X.-K. Guo, F.-Q. Zhang, and Q.-F. Huang, “Corrosion behavior of pure titanium in the presence of Actinomyces naeslundii,” *J. Mater. Sci. Mater. Med.*, **24**(5): 1229-1237, 2013.

[20] L. Hall-Stoodley, J. W. Costerton, and P. Stoodley, “Bacterial biofilms: from the Natural environment to infectious diseases,” *Nat. Rev. Microbiol.*, **2**(2): 95-108, 2004.

[21] M. Geetha, A. K. Singh, R. Asokamani, and A. K. Gogia, “Ti based biomaterials, the ultimate choice for orthopaedic implants – A review,” *Prog. Mater. Sci.*, **54**(3): 397–425, 2009.

[22] D. L. Nelson and Michael M. Cox *Lehninger Principles of Biochemistry*. Fourth edition. New York: W.H. Freeman, pp. 75-85, 2005.

[23] J. Song, V. Malathong, and C. R. Bertozzi, “Mineralization of Synthetic Polymer Scaffolds: A Bottom -Up Approach for the Development of Artificial Bone,” *J. Am. Chem. Soc.*, **127**(10): 3366–3372, 2005.

[24] A. George and A. Veis, “Phosphorylated Proteins and Control over Apatite Nucleation, Crystal Growth, and Inhibition,” *Chem. Rev.*, **108**(11): 4670–4693, 2008.

[25] W. J. Landis and R. Jacquet, “Association of Calcium and Phosphate Ions with Collagen in the Mineralization of Vertebrate Tissues,” *Calcif. Tissue Int.*, **93**(4): 329–337, 2013.

[26] F. H. Silver and W. J. Landis, “Deposition of apatite in mineralizing vertebrate extracellular matrices: A model of possible nucleation sites on type I collagen,” *Connect. Tissue Res.*, **52**(3): 242–254, 2011.

[27] K. S. Jack, T. G. Vizcarra, and M. Trau, “Characterization and Surface Properties of Amino-Acid-Modified Carbonate-Containing Hydroxyapatite Particles,” *Langmuir*, **23**(24): 12233–12242, 2007.

[28] B. Palazzo, D. Walsh, M. Iafisco, E. Foresti, L. Bertinetti, G. Martra, C. L. Bianchi, G. Cappelletti, N. Roveri, “Amino acid synergetic effect on structure, morphology and surface properties of biomimetic apatite nanocrystals,” *Acta Biomater.*, **5**(4): 1241–1252, 2009.

[29] D. Rautaray, S. Mandal, and M. Sastry, “Synthesis of Hydroxyapatite Crystals Using Amino Acid-Capped Gold Nanoparticles as a Scaffold,” *Langmuir*, **21**(11): 5185–5191, 2005.

[30] N. Almora-Barrios and N. H. de Leeuw, “A Density Functional Theory Study of the Interaction of Collagen Peptides with Hydroxyapatite Surfaces,” *Langmuir*, **26**(18): 14535–14542, 2010.

[31] A. Sugino, T. Miyazaki, and C. Ohtsuki, “Apatite-forming ability of polyglutamic acid hydrogels in a body-simulating environment,” *J. Mater. Sci. Mater. Med.*, **19**(6): 2269–2274, 2008.

[32] H. Pan, J. Tao, X. Xu, and R. Tang, “Adsorption Processes of Gly and Glu Amino Acids on Hydroxyapatite Surfaces at the Atomic Level,” *Langmuir*, **23**(17): 8972–8981, 2007.

[33] A. Takeuchi, C. Ohtsuki, M. Kamitakahara, S. Ogata, T. Miyazaki, and M. Tanihara, “Biomimetic deposition of hydroxyapatite on a synthetic polypeptide with β sheet structure in a solution mimicking body fluid,” *J. Mater. Sci. Mater. Med.*, **19**(1): 387–393, 2008.

[34] A. Takeuchi,C. Ohtsuki, T. Miyazaki, M. Kamitakahara, S. Ogata, M. Yamazaki, Y. Furutani, H. Kinoshita, M. Tanihara., “Heterogeneous nucleation of hydroxyapatite on protein: structural effect of silk sericin,” *J. R. Soc. Interface*, **2**(4): 373–378, 2005.

[35] N. J. Greenfield and G. D. Fasman, “Computed circular dichroism spectra for the evaluation of protein conformation,” *Biochemistry*, **8**(10): 4108–4116, 1969.

[36] M. Kresak, E. C. Moreno, R. T. Zahradnik, and D. I. Hay, “Adsorption of amino acids onto hydroxyapatite,” *J. Colloid Interface Sci.*, **59**(2): 283–292, 1977.

[37] I. Yoshinori, C. J. E., S. E. M., and W. R. E., “Effect of amino acid levels on matrix vesicle formation by epiphyseal growth plate chondrocytes in primary culture,” *J. Cell. Physiol.*, **126**(3): 399–406, 2018.

[38] A. Jennings, A. MacGregor, T. Spector, and A. Cassidy, “Amino Acid Intakes Are Associated With Bone Mineral Density and Prevalence of Low Bone Mass in Women: Evidence From Discordant Monozygotic Twins,” *J. Bone Miner. Res.*, **31**(2): 326–335, 2016.

[39] H. S. Alghamdi, R. Bosco, J. J. J. P. van den Beucken, X. F. Walboomers, and J. A. Jansen, “Osteogenicity of titanium implants coated with calcium phosphate or collagen type-I in osteoporotic rats,” *Biomaterials*, **34**(15): 3747–3757, 2013.

[40] R. Vani, E. K. Girija, K. Elayaraja, S. Prakash Parthiban, R. Kesavamoorthy, and S. Narayana Kalkura, “Hydrothermal synthesis of porous triphasic hydroxyapatite/(α and β) tricalcium phosphate,” *J. Mater. Sci. Mater. Med.*, **20**(1): 43–48, 2009.

[41] S. J. Padayatty, A. Katz, Y. Wang, P. Eck, O. Kwon, J. H. Lee, S. Chen, C. Corpe, A. Dutta, S. K. Dutta, and M. Levine, “Vitamin C as an Antioxidant: Evaluation of Its Role in Disease Prevention,” *J. Am. Coll. Nutr.*, **22**(19): 18–35, 2003.

[42] H. W. Meng, E. Y. Chien, and H. H. Chien, “Dental implant bioactive surface modifications and their effects on osseointegration: a review,” *Biomark. Res.*, **4**(1): 1-14, 2016.

[43] J. Li, Z. Lin, Q. Zheng, X. Guo, S. Lan, S. Liu, S. Yang, “Repair of rabbit radial bone defects using true bone ceramics combined with BMP-2-related peptide and type I collagen,” *Mater. Sci. Eng. C*, **30** (8): 1272–1279, 2010.

[44] K. Tsutsumi, H. Fujikawa, T. Kajikawa, M. Takedachi, T. Yamamoto, S. Murakami, “Effects of L-ascorbic acid 2-phosphate magnesium salt on the properties of human gingival fibroblasts,” *J. Periodontal Res.*, **47**(29): 263–271, 2012.

[45] J.-L. Ravanat, T. Douki, and J. Cadet, “Direct and indirect effects of UV radiation on DNA and its components,” *J. Photochem. Photobiol. B Biol.*, **63**(1): 88–102, 2001.

[46] S. Mallakpour and M. Javadpour, “An innovative strategy for the production of novel magnetite poly(vinyl alcohol) nanocomposite films with double-capped synthesized Fe_3O_4 nanoparticles with citric acid and vitamin C,” *Compos. Interfaces*, **22**(9): 867–884, 2015.

[47] L. G. Rao, J. N. Wylie, M. S. Kung Sutherland, and T. M. Murray, “17β-Oestradiol enhances the stimulatory effect of 1,25-dihydroxyvitamin D_3 on alkaline phosphatase activity in human osteosarcoma SaOS-2 cells in a differentiation-dependent manner,” *J. Endocrinol.* , **148**(1): 181–187, 1996.

[48] E. F. Barroga, T. Kadosawa, M. Okumura, and T. Fujinaga, “Influence of Vitamin D and Retinoids on the Induction of Functional Differentiation In Vitro of Canine Osteosarcoma Clonal Cells,” *Vet. J.*, **159**(2): 186–193, 2000.

[49] L. G. Raisz, C. L. Trummel, M. F. Holick, and H. F. Deluca, “1,25-Dihydroxycholecalciferol: A Potent Stimulator of Bone Resorption in Tissue Culture,” *Science*, **175**(4023): 768-769, 1972.

[50] T. Suda, N. Takahashi, N. Udagawa, E. Jimi, M. T. Gillespie, and T. J. Martin, “Modulation of Osteoclast Differentiation and Function by the New Members of the Tumor Necrosis Factor Receptor and Ligand Families,” *Endocr. Rev.*, **20**(3): 345–357, 1999.

[51] K. G. Seshadri, B. Tamilselvan, and A. Rajendran, “Role of Vitamin D in Diabetes,” *J. Endocrinol. Metab.* **1**(2): 47-56, 2011.

[52] A. Shiraishi, S. Higashi, H. Ohkawa. N. Kubodera, T. Hirasawa, I. Ezawa, K. Ikeda, and E. Ogata, “The Advantage of Alfacalcidol Over Vitamin D in the Treatment of Osteoporosis,” *Calcif. Tissue Int.*, **65**(4): 311–316, 1999.

[53] H. Orimo, M. Shiraki, Y. Hayashi, T. Hoshino, T. Onaya, S. Miyazaki, H. Kurosawa, T. Nakamura, and N. Ogawa, “Effects of 1α-hydroxyvitamin D_3 on lumbar bone mineral density and vertebral fractures in patients with postmenopausal osteoporosis,” *Calcif. Tissue Int.*, **54**(5): 370–376, 1994.

[54] S. Sairanen, M. Kärkkäinen, R. Tähtelä, K. Laitinen, P. Mäkelä, C. Lamberg-Allardt, and M. J. Välimäki, “Bone Mass and Markers of Bone and Calcium Metabolism in Postmenopausal Women Treated with 1,25-Dihydroxyvitamin D (Calcitriol) for Four Years,” *Calcif. Tissue Int.*, **67**(2): 122–127, 2000.

[55] D. Gabriella, F. Alexander, W. Georg, T. Stefan, P. Petra, and G. Reinhard, “Impact of dietary vitamin D on osseointegration in the ovariectomized rat,” *Clin. Oral Implants Res.*, **23**(11): 1308–1313, 2012.

[56] K. James, L. Audrey, W. C. J., P. Sil, and N. Ichiro, “Vitamin D and Bone Physiology: Demonstration of Vitamin D Deficiency in an Implant Osseointegration Rat Model,” *J. Prosthodont.*, **18**(6): 473–478, 2009.

[57] D. Baas, K. Prüfer, M. E. Ittel, S. Kuchler-Bopp, G. Labourdette, L. L. Sarliève, and P. Brachet, “Rat oligodendrocytes express the vitamin D_3 receptor and respond to 1,25-dihydroxyvitamin D_3,” *Glia*, **31**(1): 59–68, 2000.

[58] P. B. Rapuri, J. C. Gallagher, and Z. Nawaz, “Caffeine decreases vitamin D receptor protein expression and $1,25(OH)_2D_3$ stimulated alkaline phosphatase activity in human osteoblast cells,” *J. Steroid Biochem. Mol. Biol.*, **103**(3): 368–371, 2007.

[59] M. F. McCarty, “Poor vitamin D status may contribute to high risk for insulin resistance, obesity, and cardiovascular disease in Asian Indians,” *Med. Hypotheses*, **72**(6): 647–651, 2018.

[60] P. Chandra, J. N. G. Binongo, T. R. Ziegler, L. E. Schlanger, W. Wang, J. T. Someren, V. Tangpricha., “Cholecalciferol (Vitamin D3) Therapy and Vitamin D Insufficiency in Patients with Chronic Kidney Disease: A Randomized Controlled Pilot Study,” *Endocr. Pract.*, **14**(1): 10–17, 2008.

[61] M. R Brinker, D. P O’Connor, Y. T Monla, and T. P Earthman, *Metabolic and Endocrine Abnormalities in Patients With Nonunions*, **21**(8): 557-570, 2007.

[62] K. James, L. Audrey, W. C. J., P. Sil, and N. Ichiro, “Vitamin D and Bone Physiology: Demonstration of Vitamin D Deficiency in an Implant Osseointegration Rat Model,” *J. Prosthodont.*, **18**(6). 473–478, 2009.

[63]. Ferraro, J.R. y Nakamoto, K., *Introductory Raman Spectroscopy*. Academic Press, California, pp 13-26. 1994.

[64] L. Nádai, B. Katona, A. Terdik, and E. Bognár, “Chemical etching of titanium samples,” *Period. Polytech. Mech. Eng.*, **57**(2): 53-57, 2013.

[65] K. Sugimoto, S. Tsuchiya, M. Omori, R. Matsuda, M. Fujio, K. Kuroda, M. Okido, and H. Hibi, “Proteomic analysis of bone proteins adsorbed onto the surface of titanium dioxide,” *Biochem. Biophys. Reports*, **7**: 316–322, 2016.

[66] T. Kokubo and H. Takadama, “How useful is SBF in predicting in vivo bone bioactivity?,” *Biomaterials*, **27**(15): 2907–2915, 2006.

[67] U. Balachandran and N. G. Eror, “Raman spectra of titanium dioxide,” *J. Solid State Chem.*, **42**(3): 276–282, 1982.

[68] P. E. Timchenko, E. V. Timchenko, E. V. Pisareva, M. Yu. Vlasov, N. A. Red’kin, and O. O. Frolov, “Spectral analysis of allogeneic hydroxyapatite powders,” *J. Phys. Conf. Ser.*, **784**(1): 1-8, 2017.

[69] T. Roliński, S. Gawinkowski, A. Kamińska, and J. Waluk, “Raman Spectra of Solid Amino Acids: Spectral Correlation Analysis as the First Step Towards Identification by Raman Spectroscopy. Optical Spectroscopy and Computational Methods in Biology and Medicine,” M. Baranska, Ed. Dordrecht: Springer Netherlands, pp. 329–354, 2014**.**

Chapter 4

Functionalization of Titanium Surfaces with Lysine: a Micro Raman Study of the Intermolecular Interactions of Lysine-TiO_2

Abstract

Raman scattering (RS) was used as a powerful, efficient, and sensitive technique for studying intermolecular interactions between an organic ligand adsorbate and a metallic substrate. Functionalization of titanium (TiO_2/Ti) surfaces was performed using lysine (Lys) as adsorbate and later developing a hydroxyapatite (HA) layer onto this functionalized surface. The functionalization process was performed at different pH values of the interacting chemical species. Chemisorption onto the TiO_2/Ti substrates through the Lys carboxylic group was demonstrated spectroscopically. Analysis of vibrational spectra showed that the CH side chain of Lys was relatively distant from the (TiO_2/Ti) surface, preventing direct contact with the surface. Additionally, the signals corresponding to the unbound γ-NH_2 group indicate that it is available for additional complexation. *In vitro* bioactivity of the Lys–TiO_2/Ti surface was achieved, developing an HA layer onto already functionalized TiO_2/Ti surfaces at various pH values. Spectroscopic data using the spectral markers of HA and Lys provided a decisive role in establishing the necessary baseline data for evidencing the intermolecular bonding. The functionalized TiO_2/Ti surface reactivity is linked to the specific intermolecular

interactions of $–COO^-$ (pH 7.0) with Ca^{2+} ions, as well as the –COOH (pH 2.0 and 12.0) groups of Lys, with the –OH groups of PO_4 belonging to HA.

Keywords

Titanium (Ti) functionalization, titanium dioxide, lysine (Lys), hydroxyapatite (HA), Raman spectroscopy (RS), intermolecular interactions

4.1 Introduction

Titanium (Ti) is the 9th most abundant element in the Earth's crust. Commercially pure Ti has many applications in modern society and is extensively used in bone implants due to its properties. Ti produces a spontaneous thin layer of titanium dioxide (TiO_2) of approximately 5 to 6 nm that confers unique characteristics, such as nontoxicity, bioinertness, resistance to corrosion, and biocompatibility (via osseointegration). The above properties position Ti as a "gold standard" for orthopedic and dental prostheses. [1–3] Formation of TiO_2 can be explained based on the electronic structure of Ti: $[^{18}Ar]3d^2 4s^2$. Electrons in the $3d^2$ and $4s^2$ shells are relatively loose and therefore highly reactive, thereby leading to the formation of TiO_2 when the conditions are favorable, such as in the presence of water (or humidity) and air. Nonetheless, there is a risk of negative effects on the formation of biological tissues in the event of an increased formation of the TiO_2 layer. Normally, Ti implants are packed in vacuo, sustaining contact with oxygen only when the practicing physician carries out the surgical procedure to insert the Ti implant into a patient's body. [4]

Although biological inertness makes Ti appropriate for use in bone implants, some issues related to inefficient direct chemical bonding with the host bone after implantation

(osseointegration) exist; therefore, immobilization of Ti prostheses is reduced, resulting in additional health and financial costs to the patients. [5, 6] To contribute to improving the efficacy of osseointegration of Ti surfaces, a new generation of biocoatings are customized to promote bioactivity and improve the performance in the healing process, since the Ti surface is in direct contact with the surrounding tissues. In this study, lysine (Lys) was chosen as a functionalization agent and tested for *"in vitro"* formation of hydroxyapatite (HA) onto TiO_2/Ti surfaces due to its high adsorption on the surface. [7, 8]

Adsorption of a biocompatible organic ligand at the TiO_2/Ti surface possesses relevance, given that it could interact at the molecular level with TiO_2, thereby contributing to the important function of promoting the formation of HA on the TiO_2/Ti surface. Therefore, the functionalization and biocompatibility of TiO_2/Ti for use as medical implants and prosthetic materials could be mediated by an organic ligand. This work focused on the identification of such an organic ligand adsorbate (Lys) which could play an important role in the osseointegration process of Ti-based implants via its structure and the type of interaction that occurs between it and the substrate (TiO_2/Ti surface). Confocal Raman scattering (RS) was employed as the sensing tool required for elucidating the intermolecular interactions between Lys and the TiO_2/Ti surface in order to understand the adsorption process, which can take place when a TiO_2/Ti surface is immersed in an aqueous Lys solution.

4.2 Materials and methods

Chemically or physically untreated Ti plates (99.99%, Thermo-Fisher Scientific, Waltham, MA, USA) with dimensions of 10 mm x 10 mm x 2 mm were used as

substrates for functionalization. The Ti surfaces were roughened using silicon carbide (SiC) grinding paper. The plates were then consecutively bathed with acetone, absolute ethanol, and deionized (DI) water in an ultrasonic bath for 15 min each. Once the Ti surfaces were cleaned, they were dried in a desiccator overnight before modification and functionalization. A mixture of 30 mL nitric acid (HNO_3, 40 wt.%) and 70 mL DI water was used for etching the Ti surfaces. The dried Ti substrates were etched for 2 min. Etched Ti surfaces were oxidized by immersing and soaking them in a hydrogen peroxide solution (H_2O_2, 30% wt.) for 24 h.

The functionalization process of Ti surfaces proceeded as follows: the oxidized Ti substrates were incubated in 10.0 mM Lys solution, adjusting the pH to the values of 2.0, 7.0, and 12.0 by adding small aliquots of dilute HCl and NaOH solutions at room temperature when required. The incubation proceeded for 72 h. Then, TiO_2/Ti samples were rinsed with DI water and ethanol to eliminate any chemical interference. Then, the TiO_2/Ti plates were immersed again for another incubation period of 72 h at room temperature. Finally, the plates were dried again.

To assess the *in vitro* bioactivity of the Lys–TiO_2/Ti plates to develop a hydroxyapatite (HA) coating, a simulated body fluid (SBF) was prepared according to the methodology described by Kokubo and coworkers. [9] According to their procedure, Na^+, K^+, Mg^{2+}, Ca^{2+}, Cl^-, HCO_3^-, HPO_4^{2}, and SO_4^{2-} ions were used, and their ion concentrations were nearly equal to those of human blood plasma. In addition, the SBF solution was buffered at pH 7.4 with tris(hydroxymethyl)aminomethane and HCl. Afterward, Lys–TiO_2/Ti plates were immersed and soaked in SBF for 28 days, and the precipitation of HA from SBF was observed and controlled.

RS spectra were acquired to analyze the following samples: nontreated Ti substrates, oxidized Ti substrates, Lys, Lys–TiO_2/Ti plates, and the developed HA layer on functionalized Lys–TiO_2/Ti plates. The two principal polymorphs of TiO_2 (anatase and rutile) were used as references for determining the oxide phase formed on the Ti substrates. Confocal micro RS spectra were acquired by employing an InVia Raman microspectrometer (Renishaw, LLC, West Dundee, IL, USA). The spectrometer was interfaced to a Leica DM2500 microscope, and a Leica 50x objective was used to focus the laser beam onto the sample surface for collecting the scattered light. Each acquisition consisted of 10 averaged accumulations with an acquisition time of 10 s each. A 532 nm diode pumped laser (Cobolt AB, Solna, Sweden) was used as the excitation source. The spectrometer was calibrated before each set of measurements using the 520.65 cm^{-1} Raman shift peak of silicon (110). Characteristic RS signatures were marked, and a baseline correction was applied to all spectra. The laser power at the samples was controlled to avoid sample degradation upon laser irradiation.

4.3 Results and discussion

4.3.1 Functionalization of TiO_2/Ti surface with Lys

Results from RS measurements were used to identify band shifts, changes in relative intensities, new bands, and the disappearance of bands that would provide evidence for the formation/breakage of specific chemical bonds resulting from intermolecular interactions between the TiO_2/Ti surface and adsorbate. Spectroscopic analyses enabled acquisition of structural information regarding Ti surface layers. The reference RS spectra of room temperature stable polymorphs of TiO_2 are shown in Figures 4.1a and 4.1b for anatase and rutile, respectively. The Raman shifts of the

major five Raman bands for the crystalline anatase phase were observed at 136, 188, 398, 509, and 631 cm^{-1}, and they can be tentatively assigned to the five active modes of the anatase polymorph with symmetries of E_g, E_g, B_{1g}, A_{1g}, and B_{1g}, respectively (Figure 4.1a). [12] There is also a weak and broad peak centered at approximately 825 cm^{-1}. The anatase polymorph of TiO_2 shows an intense vibrational marker (E_g) at approximately 136 cm^{-1} that differentiates it from the crystalline rutile phase. This band corresponds to the lattice vibrational mode of the anatase structure and indicates the presence of the crystalline phase with a well-developed crystal structure. Figure 4.1b shows the main Raman shift bands of the rutile polymorph of TiO_2 located at 142, 239, 449, 610, and 830 cm^{-1}. The bands have been tentatively ascribed to B_{1g} two-phonon scattering, E_g, A_{1g}, and B_{1g} modes, respectively, for the first 4 Raman shift signals. The peak at 830 cm^{-1} is broad and of low intensity. [13] The situation here is contrary to that observed for anatase. The strongest peaks characteristic of rutile are located at 449 and 610 cm^{-1}. These spectroscopic features are used to indicate the presence of anatase or rutile on modified Ti surfaces. [14]

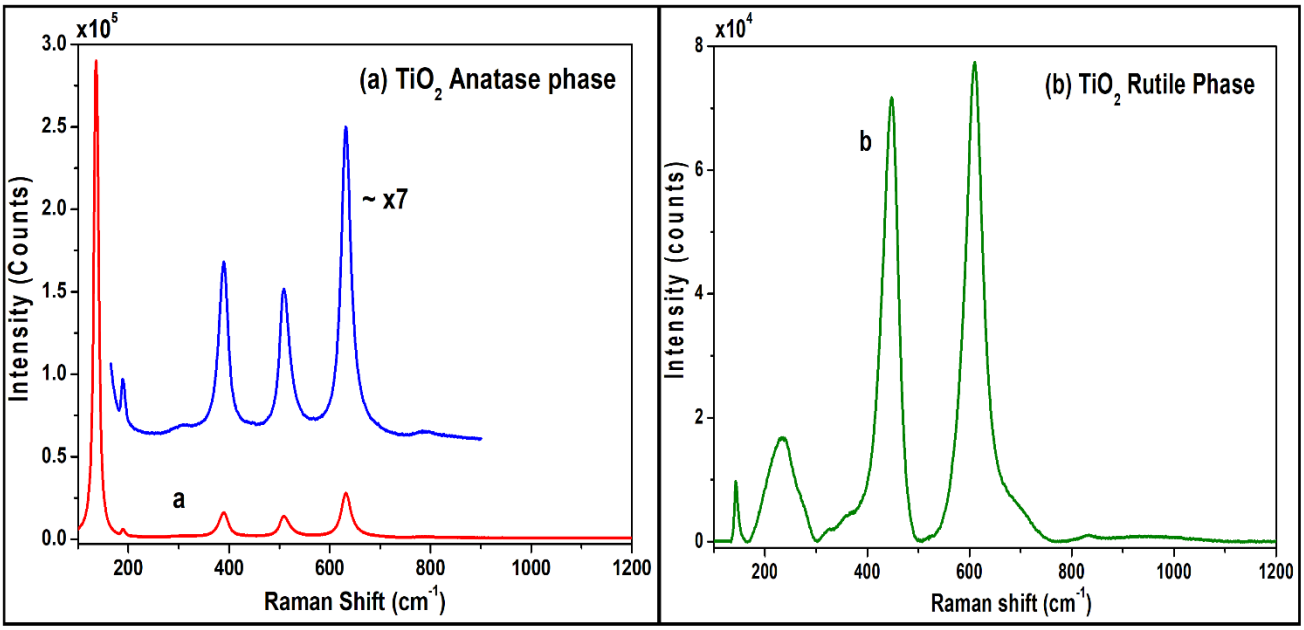

Figure 4.1. RS spectrum of crystalline TiO_2: (a) anatase phase; (b) rutile phase

RS spectra were obtained at numerous locations of several washed and dried plates to confirm the possible presence of a layer of crystalline TiO_2 phase on the surface of the untreated Ti plates. The results are shown in Figure 4.2a. The plates were kept in desiccators at low relative humidity. The crystallinity or the degree of structural order of this naturally oxidized Ti layer can be determined by the RS spectrum, since the scattering of the laser light is sensitive to the degree of crystallinity of the sample. Normally, a crystalline compound produces a Raman spectrum with very sharp and intense Raman bands, while an amorphous substance exhibits broader and less intense Raman peaks. In addition, the Raman spectra of amorphous compounds are relatively featureless. According to the above, the broad band centered at approximately 800 cm^{-1} indicates that a highly amorphous native form of TiO_2 is present on the untreated Ti plates in the form of a thin film, evidencing the spontaneous oxidation of the neat Ti surfaces at room temperature. The amorphous phase is due to the high solubility of oxygen in Ti that produces the rapid formation of a passivation layer onto the metallic surface within seconds of exposure to air. [10, 11] Figure 4.2b shows the Raman spectrum of a chemically oxidized Ti plate. As can be observed, there are five bands centered at approximately 148, 252, 442, 612, and 804 cm^{-1}. When the observed peaks of the RS spectra of the laboratory oxidized Ti plates were compared with those belong to rutile, it was inferred that the layer on the Ti surface corresponds to rutile. This procedure is illustrated in Figures 4.2c-d. The above finding confirms that the Ti surface was modified and that it primarily contains one crystalline TiO_2 phase: rutile with some degree of noncrystallinity (amorphous phase), as can be deduced from the relatively high intensity of the broad peak near 804 cm^{-1}. [14]

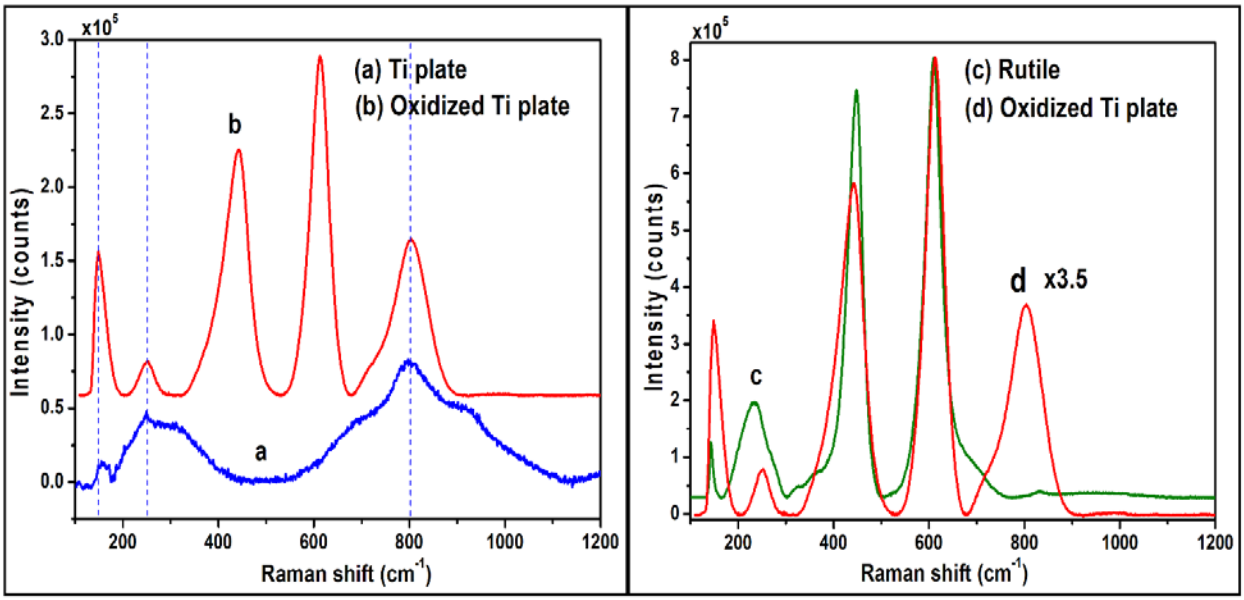

Figure 4.2. RS spectra of (a) neat, non-chemically treated Ti plate; (b) chemically oxidized Ti plate. Comparison of (c) rutile phase TiO_2 and (d) chemically oxidized Ti plate.

Lys, the organic ligand used in this study, is a basic, polar amino acid (Figure 4.3a). The RS spectrum of Lys in the region from 100 to 3800 cm^{-1} is shown in Figure 4.4a. Table 1 contains the Raman shifts with their tentative assignments. Strong bands corresponding to the C-H stretching mode can be observed within the 2800-3000 cm^{-1} region. The peaks at 2985, 2950, 2905, and 2878 cm^{-1} have been tentatively assigned to aliphatic hydrocarbon stretching bands. Additionally, there are medium intensity peaks related to N-H stretching vibrational modes in the range of 3200 to 3400 cm^{-1}. The vibrations corresponding to methylene groups (CH_2) in the lateral chain predominate on the RS spectrum. Tentative band assignments are based on published data on related compounds and characteristic group frequencies. [15-19]

Figure 4.4b shows the Raman spectrum of Lys in the region of 100–2000 cm^{-1}. The antisymmetric stretching group vibrations of COO^- were observed at 1580 and 620 cm^{-1}. The symmetric stretching vibration mode of COO^- was located at 1405 cm^{-1}. The group of bands from 1420 to 1480 cm^{-1} with a maximum at 1439 cm^{-1} is tentatively assigned to deformations of the NH_3^+ group. Bands observed in the region of 1306-1360 cm^{-1} are related to NH_2 and CH_2 bending modes coupled to CH_2 twisting vibrations. The antisymmetric rocking vibrations of NH_3^+ were observed at 1139 and 1178 cm^{-1}. The aliphatic skeletal stretching vibrational modes of C-C and C-N are observed in the region of 860-1100 cm^{-1}. The vibrational C-COO^- mode was located at approximately 936 cm^{-1}. Bands at 663, 559 and 473 cm^{-1} were tentatively assigned to deformation modes of the COO^- group. [20]

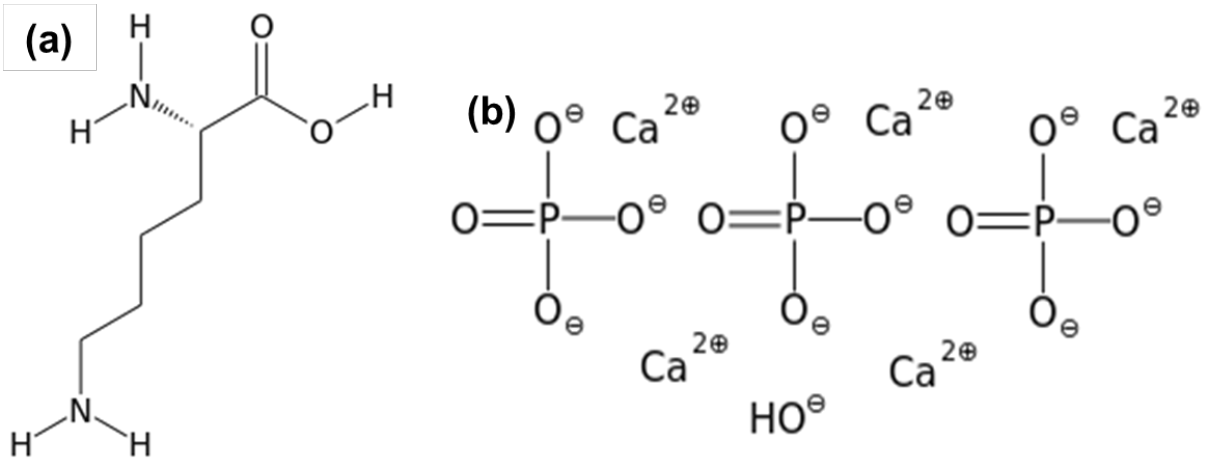

Figure 4.3. Chemical structures of (a) lysine (Lys); (b) HA

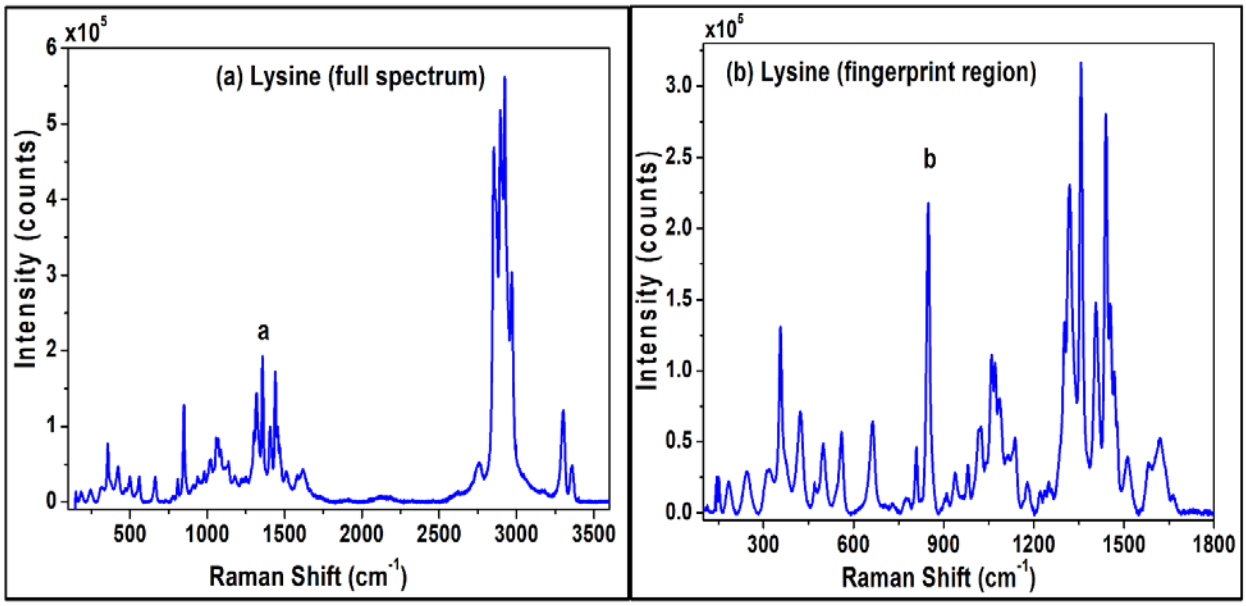

Figure 4.4.RS spectra of Lys: (a) full range; (b) zoom view of the 100 – 1800 cm^{-1} range

Table 4. 1. Raman shift observed and tentative assignment frequencies for Lys

Raman Shift (cm^{-1})	Proposed Assignment
3200-3400(m)	N-H stretching
2800-3000(s)	C-H stretching mode
1620(w) and 1580(w)	asymmetric stretching of COO^-
1405(m)	symmetric stretching of COO^-
1420-1480	deformations of NH_3^+ group
1306-1360	NH_2 and CH_2 bending coupled to CH_2 twisting
1139(w) and 1178(vw)	antisymmetric rocking of NH_3^+
860-1100	aliphatic skeletal stretching of C-C and C-N
936(w)	vibrational C-COO^- mode
663(m), 559(m) and 499(m)	deformation of the COO^- group

(vs) = very strong, (s) = strong, (m) = medium, (w) = weak, (vw) = very weak

The RS spectra offer insight into the molecular structure of the Lys layer upon the TiO_2/Ti surface and evidence the structural changes that occur when the modified Ti substrate interacts with Lys. To test the effect of the pH of the medium on the interaction between Lys and TiO_2/Ti substrates, the pH was modified from its nominal value (pH=9.5 for aqueous solutions of Lys) to acidic, neutral, and basic. Then, RS spectra were acquired as a function of time for fixed pH values of the interacting system. Figure 4.5 shows typical RS spectra obtained displayed in a stacked form that allows easier comparison of the spectra.

Figures 4.5b-d show the RS spectra of the Lys–TiO_2/Ti substrate at pH values of 2.0, 7.0, and 12.0, respectively. The RS spectrum of the Lys in its solid state is also shown as a reference in the bottom trace (Fig. 4.5a). The spectrum shown in Figure 4.5b

(pH=2.0) shows some bands that are characteristic for Lys. The weak intensity band at 320 cm^{-1} can be assigned to the skeletal deformation of the Lys molecule, while the medium intensity signals at 417 and 587 cm^{-1}, and the weak band at 540 cm^{-1}, correspond to the wagging deformation modes of the COO^- group. [21] A very weak band at 724 cm^{-1} is assigned to the CH_2 rocking vibration in the aliphatic chain of Lys. Two new bands appeared at 827 (shoulder) and 880 (mid) cm^{-1}, and they can be assigned to the aliphatic skeletal stretching vibrational modes of C-C and C-N in the Lys–TiO_2/Ti complex. The medium intensity peak at 981 cm^{-1} and the strong band at 1039 cm^{-1} are associated with the C-COO^- vibration modes, and they are assigned to the bridged Ti-O-R species. [22] The bands in the region from 1100 to 1400 cm^{-1} are assigned to vibrations which are characteristic of CH_2 and NH_2 groups of the Lys molecule, as explained above. Comparing the spectra, aside from the bands of the carboxylic group, the spectrum is dominated by vibrational modes that correspond to methylene groups in the lateral chain of Lys. The peaks in the 1300-1500 cm^{-1} range are all relatively in the same position as in the normal RS spectrum of neat Lys, although their intensities vary to some extent. The above evidence suggests that no direct interaction occurs between the CH_2 groups and the TiO_2/Ti substrate. The peak at 1446 cm^{-1} corresponds to deformations of the NH_3^+ group. The shoulder at 1505 cm^{-1} and a weak band at 1599 cm^{-1} correspond to symmetric and asymmetric NH_3^+ deformation vibrations, respectively. The presence of a medium intensity band at 1737 cm^{-1} indicates the presence of the $^+NH_3$-R-COOH cation. When comparing the spectra of Figures 4.5a and 4.5b, it can be inferred that no Raman band is found near 1737 cm^{-1} in the free amino acid. However, when the $^+NH_3$-R-COOH cation was formed, the

presence of the corresponding band was evident. The above can be corroborated by analyzing the RS spectra of Figures 4.5c and 4.5d, in which the band at 1737 cm^{-1} does not appear, since the high pH condition prevents the formation of the $^{+}NH_3$-R-COOH cation.

Comparing the Raman spectra shown in Figures 4.5b-d of the modified substrate and the spectrum for the neat Lys ligand (Fig. 4.5a) suggests that the surface layer is now composed of Ti oxide, with the modifying Lys ligand forming bridged complexes with the surfaces via the carboxylic group to accomplish the complexation. The neighboring ammonium group of Lys is protonated at pH=2.0 (Figure 4.5b). The new peaks at 827 and 880 cm^{-1} are associated with C-H stretching vibrations. Frequencies in the region from 1100 to 1400 cm^{-1}, assignable to amino groups, indicate that the γ-NH_2 is not bound to the TiO_2 and is available for further coordination. Analyzing the RS of Figures 4.5b-d, a broadening of the 1599 cm^{-1} band, which arises from COO^-, can be observed. Generally, band broadening can occur as a consequence of adsorption and the range of different chemical environments that the adsorbate occupies: that is, changes result from the hydration sphere of the molecule and interaction with the Ti surface. [23] This finding further suggests that the carboxylic group is interacting with the modified TiO_2/Ti surface when Lys is adsorbed onto it.

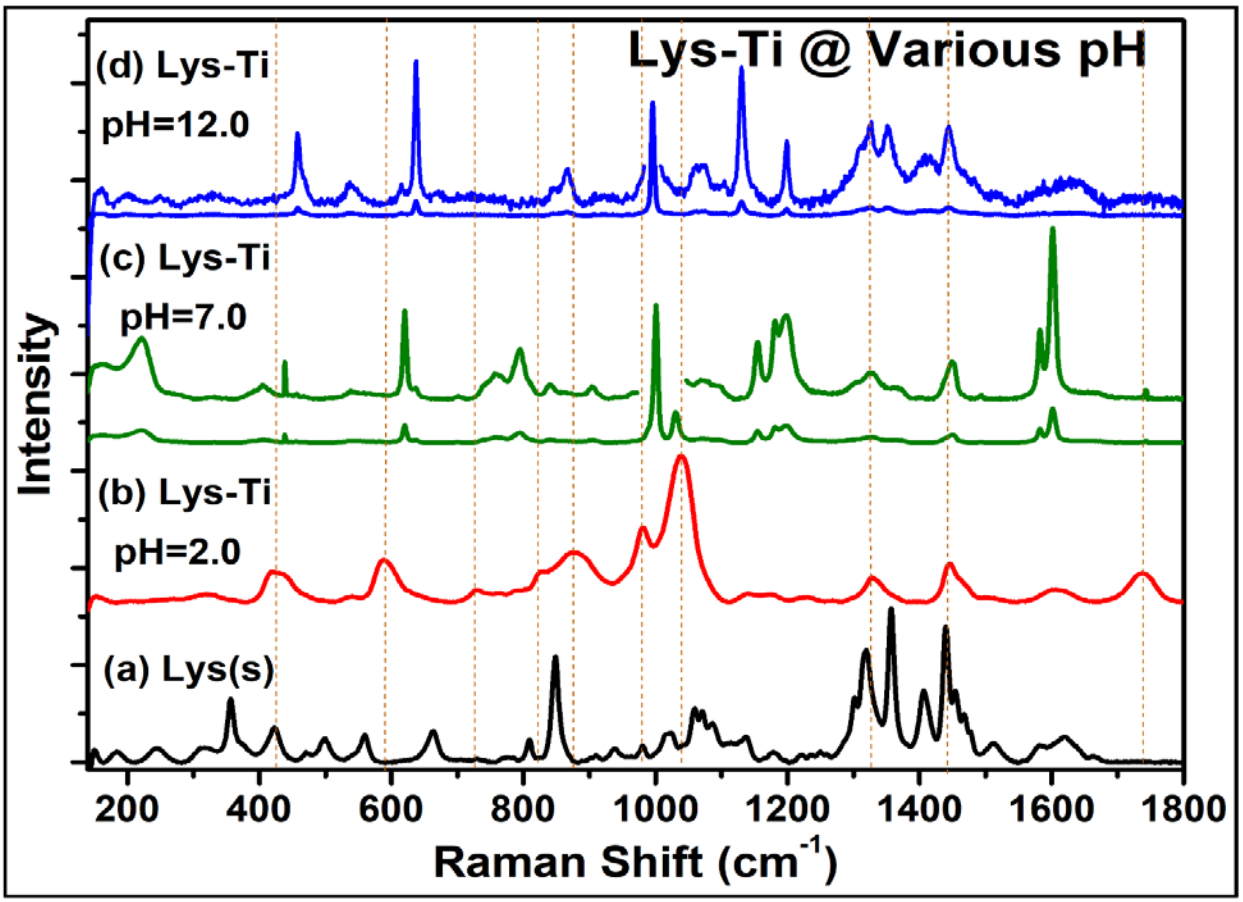

Figure 4.5. RS spectra of functionalized TiO_2/Ti surface with Lys at several pH values: (a) pH=2.0; (b) pH=7.0; (c) pH=12.0. The bottom trace corresponds to the RS spectrum for solid Lys

Based on the above information, it is proposed that the coating of the Ti surface can exist as a bridged surface complex of Lys–TiO_2, where the Lys ligand is bound to the TiO_2 through the carboxylic group (Figure 4.6). As seen, further coordination with TiO_2 could be possible through the neighboring ammonium group of the amino acid. In addition, the orientation of the aliphatic chain of Lys can be parallel or tilted relative to the TiO_2 surface. Signals corresponding to the unbound γ-NH_2 group indicate that it is available for additional complexation.

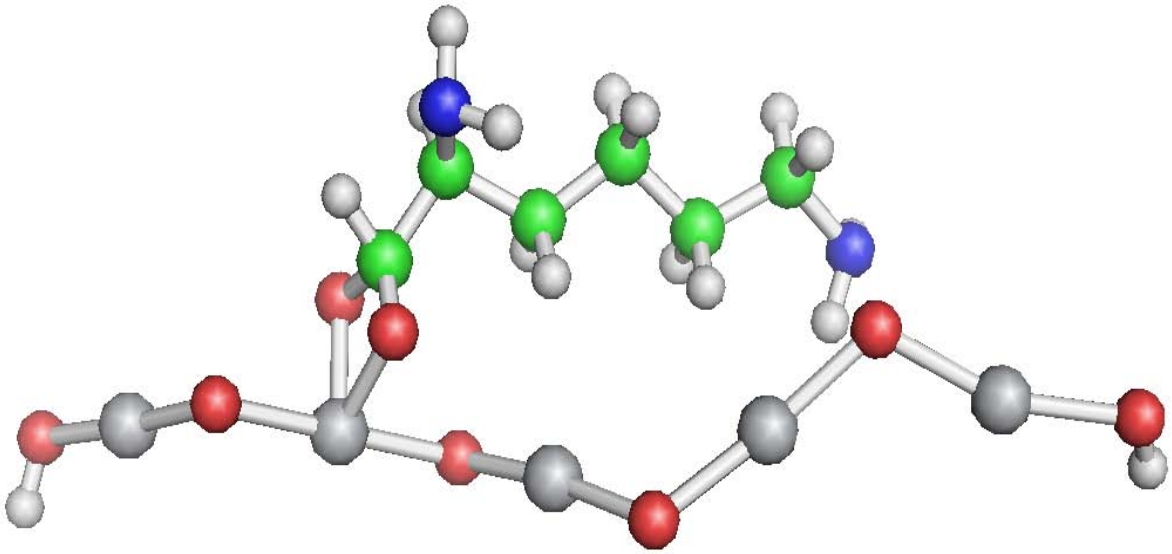

Figure 4.6. Proposed orientation of Lys on the TiO_2/Ti surface

4.3.2 “In vitro” bioactivity of Lys–TiO_2/Ti surfaces

The RS spectra of HA on the Lys–TiO_2/Ti surfaces were acquired under pH conditions of 2.0, 7.0, and 12.0. As in Figure 4.5, the reference spectrum of HA is shown in Figure 4.7a. At pH 2.0 (Figure 4.7b), the RS spectrum of HA–Lys–TiO_2 is characterized by a very strong peak at 1007 cm^{-1} corresponding to the symmetric stretching vibrational mode (v_1) of P-O in PO_4^{3-}. The band at 1044 cm^{-1} is assigned to the asymmetric stretching mode (v_3) of the PO_4^{3-} group (P-O bond). The peaks at 599 and 619 cm^{-1} correspond to vibrational bending modes of the O-P-O bond in the phosphate group. Similarly, a medium intensity peak at 415 cm^{-1} is attributed to the bending mode (v_2) of the PO_4^{3-} group (O-P-O). [24–29] The bond-stretching mode associated with –OH groups was observed at 3494 cm^{-1}, corresponding to a sharp medium intensity peak. Vibrational modes of the –OH group at 630 cm^{-1} belonging to water molecules are absent. However, the RS spectrum of HA at pH 2.0 displays another sharp band of medium intensity at 3398 cm^{-1} for which no report has been found in the literature. It can be related to the O-H···O stretching mode of water molecules. Additionally, the relatively larger width of RS spectrum peaks upon increasing from pH 2.0 to 12.0 indicates that there are structurally disordered phosphate groups. [30] Raman bands below 320 cm^{-1} can be associated with vibrational modes involving translational motion of the Ca^{2+} and PO_4^{3-} sublattices, as well as vibrational modes of the PO_4^{3-} ion. [31–33] The proposed chemical structure of HA–Lys on the functionalized Ti surface is shown in Figure 4.8.

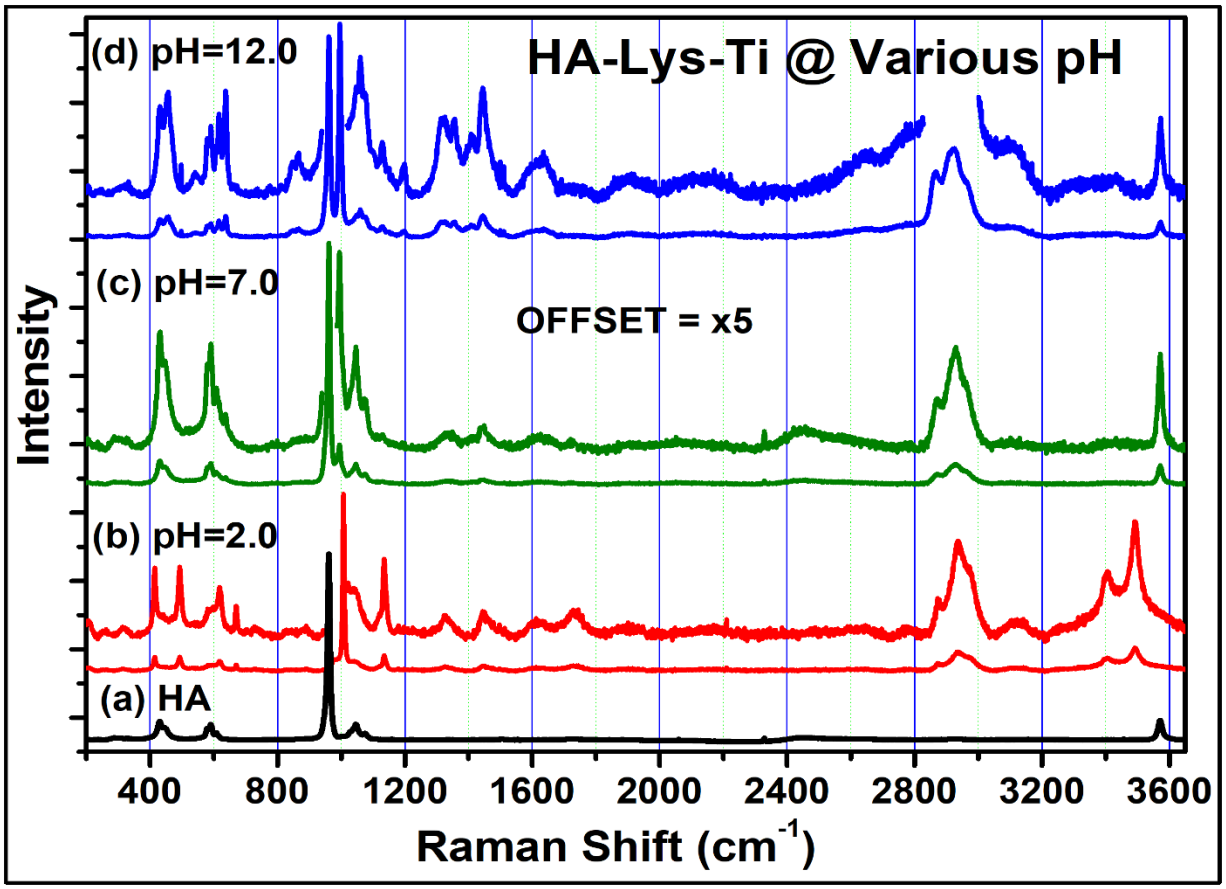

Figure 4.7. RS spectra of HA produced on Lys-TiO_2/Ti surface at different pH values: (a) pH=2.0; (b) pH=7.0; (c) pH=12.0. The bottom trace corresponds to the RS spectrum for solid HA

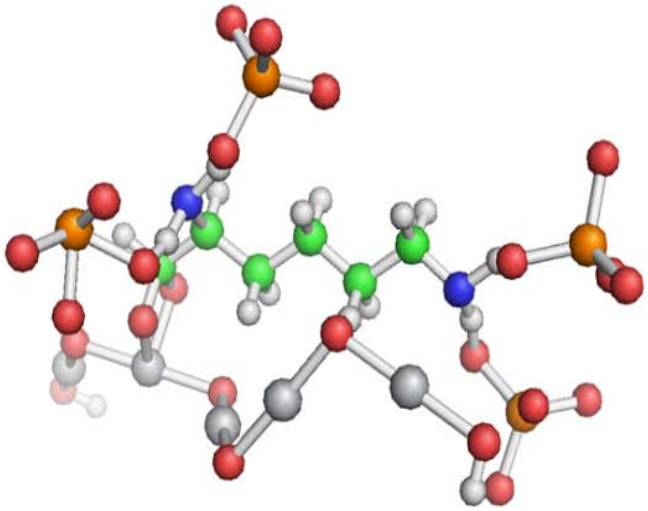

Figure 4.8. Proposed chemical structure of HA-Lys on the TiO_2/Ti surface

RS confirms the adsorption and interaction of HA with Lys. It provides information related to –COOH and $–NH_2$ groups upon the Lys–TiO_2/Ti surface; therefore, explanations regarding the bonding of HA with Lys can be suggested. The presence of characteristic bands at 1720 cm^{-1} in the Raman spectra at pH 2.0 and 12.0 indicates the existence of the $–COO^-$ group. A possible interpretation for this is that the fixation of HA onto the Lys-TiO_2/Ti surface is due to H-bonds between the –COOH of lysine and oxygen atoms of the PO_4^{3-} group.

Conversely, the features of the Raman spectrum acquired at pH 7.0 are similar to those of the spectrum at pH 2.0. Hence, the adsorption of HA is primarily due to the electrostatic interaction between the $–COO^-$ groups of Lys and Ca^{2+} ions of the HA. It is important to mention that the fixation of HA on Lys–TiO_2/Ti can be due to two factors: the simultaneous presence of $–COO^-/Ca^{2+}$ electrostatic interactions and H-bonds between NH_3 protons and oxygen atoms of the PO_4^{3-} group belonging to HA. [34–36]

4.4 Conclusions

Neat, chemically/physically untreated Ti plates were used as substrates for functionalization experiments, in which the essential amino acid Lys was used as an organic ligand adsorbate. As the first step, the Ti substrates were characterized using Raman microspectroscopy: a spontaneously formed layer of TiO_2 was detected, and its amorphous nature was confirmed by comparison with room temperature stable phases of the oxide (rutile and anatase). After that step, the Ti substrates were chemically oxidized to obtain a consistent TiO_2 layer. The results obtained provided information

regarding the TiO_2 phase formed, showing that it was spectroscopically consistent with the rutile phase.

The TiO_2/Ti surfaces were then modified with Lys. RS allowed identification of the chemical bonds between Lys and TiO_2/Ti, obtaining structural and chemical information about the intermolecular interactions between the adsorbate and the host TiO_2/Ti substrate. By comparing the Raman spectra of the modified substrate with the organic ligand adsorbate at different pH values, it was confirmed that Lys used its carboxylic group to form a complex with the TiO_2/Ti surface, forming a bridged structure. RS vibrational spectra indicate that further complexation with TiO_2/Ti and the neighboring ammonium group belonging to Lys is still possible. Further analysis leads to the conclusion that the aliphatic chain of Lys can be oriented in a parallel position or tilted relative to the TiO_2/Ti surface.

To establish the *in vitro* bioactivity of the Lys–TiO_2/Ti surface, an HA layer was developed onto it. RS measurements confirmed that the adsorption of HA on Lys–TiO_2/Ti surfaces is influenced by the pH value of the medium. Vibrational spectra suggest that H-bonds or electrostatic forces involving calcium ions are responsible for adhesion of the important mineralization HA layer on the Lys–TiO_2/Ti surfaces.

In conclusion, micro RS was employed to investigate the intermolecular interactions of Lys with the TiO_2/Ti surface. Raman signals from exterior layers could be detected, and analysis and comparisons of the Raman bands from the organic ligand and modified coated Ti surface enables tentative assignments in order to infer the behaviors of substrate-adsorbate at the molecular level. Moreover, the Raman spectral information of

Lys–TiO_2/Ti with HA at various pH values was utilized to extract valuable information regarding the type of intermolecular interactions of Lys and HA.

Acknowledgments

The authors express sincere appreciation to the faculty members and supporting personnel of the Departments of Bioengineering and Chemistry of the Mayagüez Campus of the University of Puerto Rico for their collaboration during all project stages.

Conflict of Interest

The authors report there are no conflicts of interest.

4.5 References

[1] L. E. Carneiro-Campos, C. P. Fernandes, A. Balduíno, M. E. Leite Duarte, and M. Leitão, “The effect of titanium topography features on mesenchymal human stromal cells’ adhesion,” Clin. Oral Implants Res., **21**(2): 250–254, 2010.

[2] L. T. de Jonge, S. C. G. Leeuwenburgh, J. G. C. Wolke, and J. A. Jansen, “Organic–Inorganic Surface Modifications for Titanium Implant Surfaces,” Pharm. Res., **25**(10): 2357–2369, 2008.

[3] M. D. Pierschbacher and E. Ruoslahti, “Cell attachment activity of fibronectin can be duplicated by small synthetic fragments of the molecule,” Nature, **309**(5963): 30-33, 1984.

[4] K. Heydenrijk, G. M. Raghoebar, H. J. A. Meijer, W. A. Van Der Reijden, A. J. Van Winkelhoff, and B. Stegenga, “Two-stage IMZ implants and ITI implants inserted in a single-stage procedure,” Clin. Oral Implants Res., **13**(4): 371–380, 2002.

[5] M. Abdel-Hady Gepreel and M. Niinomi, “Biocompatibility of Ti-alloys for long-term implantation,” J. Mech. Behav. Biomed. Mater., **20**: 407–415, 2013.

[6] N. Drnovšek, S. Novak, U. Dragin, M. Čeh, M. Gorenšek, and M. Gradišar, “Bioactive glass enhances bone ingrowth into the porous titanium coating on orthopaedic implants,” Int. Orthop., **36**(8): 1739–1745, 2012.

[7] S. Monti and T. R. Walsh, “Free Energy Calculations of the Adsorption of Amino Acid Analogues at the Aqueous Titania Interface,” J. Phys. Chem. C, **114**(50): 22197–22206, 2010.

[8] A. M. Sultan, Z. E. Hughes, and T. R. Walsh, “Binding Affinities of Amino Acid Analogues at the Charged Aqueous Titania Interface: Implications for Titania-Binding Peptides,” Langmuir, **30**(44): 13321–13329, 2014.

[9] T. Kokubo and H. Takadama, “How useful is SBF in predicting in vivo bone bioactivity?,” Biomaterials, **27**(15): 2907–2915, 2006.

[10] S. H. Flint, J. D. Brooks, and P. J. Bremer, “Properties of the stainless steel substrate, influencing the adhesion of thermo-resistant streptococci,” J. Food Eng., **43**(4): 235–242, 2000.

[11] F. D. Hardcastle, H. Ishihara, R. Sharma, and A. S. Biris, “Photoelectroactivity and Raman spectroscopy of anodized titania (TiO2) photoactive water-splitting catalysts as a function of oxygen-annealing temperature,” J. Mater. Chem., **21**(17): 6337–6345, 2011.

[12] T. Ohsaka, F. Izumi, and Y. Fujiki, “Raman spectrum of anatase, TiO2,” J. Raman Spectrosc., **7**(6): 321–324, 1978.

[13] S. P. S. Porto, P. A. Fleury, and T. C. Damen, “Raman Spectra of TiO2, MgF2, ZnF2, FeF2, and MnF2” Phys. Rev., **154**(2): 522–526, 1967.

[14] X. Wang, J. Shen, and Q. Pan, Raman spectroscopy of sol-gel derived titanium oxide thin films, **42**(7): 1578-1582, 2011.

[15] H. I. Lee, S. W. Suh, and M. S. Kim, “Raman spectroscopy of L-tryptophan-containing peptides adsorbed on a silver surface,” J. Raman Spectrosc., **19**(7): 491–495, 1998.

[16] E. Podstawka, R. Borszowska, M. Grabowska, M. Drąg, P. Kafarski, and L. M. Proniewicz, “Investigation of molecular structures and adsorption mechanisms of

phosphonodipeptides by surface-enhanced Raman, Raman, and infrared spectroscopies," Surf. Sci., **599**(1-3): 207–220, 2005.

[17] E. Podstawka, Y. Ozaki, and L. M. Proniewicz, "Part III: Surface-Enhanced Raman Scattering of Amino Acids and Their Homodipeptide Monolayers Deposited onto Colloidal Gold Surface," Appl. Spectrosc., **59**(12): 1516–1526, 2005.

[18] C. Jing and Y. Fang, "Experimental (SERS) and theoretical (DFT) studies on the adsorption behaviors of l-cysteine on gold/silver nanoparticles," Chem. Phys., **332**(1): 27–32, 2007.

[19] J. S. Suh and M. Moskovits, "Surface-enhanced Raman spectroscopy of amino acids and nucleotide bases adsorbed on silver," J. Am. Chem. Soc., **108**(16): 4711–4718, 1986.

[20] A. E. Aliaga, I. Osorio-Roman, C. Garrido, P. Leyton, J. Cárcamo, E. Clavijo, J. S. Gómez-Jeria, G. Díaz, M. M. Campos-Vallete, "Surface enhanced Raman scattering study of l-lysine," Vib. Spectrosc., **50**(1): 131–135, 2009.

[21] T. Roliński, S. Gawinkowski, A. Kamińska, and J. Waluk, "Raman Spectra of Solid Amino Acids: Spectral Correlation Analysis as the First Step Towards Identification by Raman Spectroscopy. Optical Spectroscopy and Computational Methods in Biology and Medicine," M. Baranska, Ed. Dordrecht: Springer Netherlands, pp. 329–354, 2014.

[22] U. Schubert, S. Tewinkel, and F. Moeller, "Metal Complexes in Inorganic Matrixes. 13. Nickel Complexes with Lysinate-Substituted Titanium Alkoxides as Ligands. X-ray Structure Analysis of [(EtO)3Ti(glycinate)]2," Inorg. Chem., **34**(4): 995–997, 1995.

[23] K. D. Dobson, P. A. Connor, and A. J. McQuillan, "Monitoring Hydrous Metal Oxide Surface Charge and Adsorption by STIRS," Langmuir, **13**(10): 2614–2616, 1997.

[24] W. P. Griffith, "Raman studies on rock-forming minerals. Part II. Minerals containing MO3, MO4, and MO6 groups," J. Chem. Soc. A Inorganic, Phys. Theor., (0): 286–291, 1970.

[25] D. C. O'Shea, M. L. Bartlett, and R. A. Young, "Compositional analysis of apatites with Laser-Raman spectroscopy: (OH,F,Cl)apatites," Arch. Oral Biol., **19**(11): 995–1006, 1974.

[26] R. Cuscó, F. Guitián, S. d. Aza, and L. Artús, "Differentiation between hydroxyapatite and β-tricalcium phosphate by means of μ-Raman spectroscopy," J. Eur. Ceram. Soc., **18**(9): 1301–1305, 1998.

[27] S. Koutsopoulos, "Synthesis and characterization of hydroxyapatite crystals: A review study on the analytical methods," J. Biomed. Mater. Res., **62**(4): 600–612, 2002.

[28] A. Antonakos, E. Liarokapis, and T. Leventouri, "Micro-Raman and FTIR studies of synthetic and natural apatites," Biomaterials, **28**(19): 3043–3054, 2007.

[29] G. Penel, G. Leroy, C. Rey, and E. Bres, "MicroRaman Spectral Study of the PO4 and CO3 Vibrational Modes in Synthetic and Biological Apatites," Calcif. Tissue Int., **63**(6): 475–481, 1998.

[30] B. Mihailova, B. Kolev, C. Balarew, E. Dyulgerova, and L. Konstantinov, "Vibration spectroscopy study of hydrolyzed precursors for sintering calcium phosphate bio-ceramics," J. Mater. Sci., **36**(17): 4291–4297, 2001.

[31] Z. Iqbal, V. P. Tomaselli, O. Fahrenfeld, K. D. Möller, F. A. Ruszala, and E. Kostiner, "Polarized Raman scattering and low frequency infrared study of hydroxyapatite," J. Phys. Chem. Solids, **38**(8): 923–927, 1977.

[32] V. Devarajan and W. E. Klee, "A potential model for fluorapatite," Phys. Chem. Miner., **7**(1): 35–42, 1981.

[33] D. M. Adams and I. R. Gardner, "Single-crystal vibrational spectra of apatite, vanadinite, and mimetite," J. Chem. Soc. Dalt. Trans., (0): 1505–1509, 1974.

[34] N. Almora-Barrios and N. H. de Leeuw, "A Density Functional Theory Study of the Interaction of Collagen Peptides with Hydroxyapatite Surfaces," Langmuir, **26**(18): 14535–14542, 2010.

[35] N. Almora-Barrios, K. F. Austen, and N. H. de Leeuw, "Density Functional Theory Study of the Binding of Glycine, Proline, and Hydroxyproline to the Hydroxyapatite (0001) and $(01\bar{1}0)$ Surfaces," Langmuir, **25**(9): 5018–5025, 2009.

[36] A. Rimola, M. Corno, C. M. Zicovich-Wilson, and P. Ugliengo, “Ab Initio Modeling of Protein/Biomaterial Interactions: Glycine Adsorption at Hydroxyapatite Surfaces,” J. Am. Chem. Soc., **130**(48): 16181–16183, 2008.

Chapter 5

Functionalization of Titanium Surfaces with Aspartic Acid: Intermolecular Interactions Assisting Osseointegration

Abstract

Aspartic acid (Asp) was used to functionalize modified titanium dioxide/titanium (Ti) substrates. *In vitro* bioactivity was performed by developing a hydroxyapatite (HA) layer on the functionalized Ti surface. It was found that the chemisorption of Asp was carried out through the carboxylic group with NH_3^+ oriented out of the modified Ti surface, in such way that the possibility exists that the carbon skeleton is oriented parallel to the Ti surface, and –COOH groups are not parallel nor perpendicular to the modified Ti surface. Therefore, the Asp molecules are oriented at an angle with respect to the modified Ti surface, forming Ti-O-R species. Analyzing the spectral features of HA and Asp, it was observed that the Ti surface reactivity depends on the specific intermolecular interactions of –COOH of HA and TiO_2 layer. Furthermore, the –OH groups of PO_4^{3-} play a very important role in the developing of HA onto functionalized Ti surface.

Keywords

Aspartic acid (Asp), titanium (Ti) substrates, hydroxyapatite, Raman spectroscopy, osseointegration

5.1 Introduction

Titanium (Ti) is a bio-inert element that has been used in implant materials due to its spontaneous capability to form a passivating TiO_2 layer on its surface, which after implantation is linked to the surrounding bone tissue (osseointegration). [1] Although the TiO_2 layer is important to bone implants, a series of problems can arise from an ineffective immobilization of Ti implants due to diverse factors such as the formation of a weak chemical bond with the bone host, and others. [2,3] To enhance the biocompatibility of Ti implants with its physiological environment in a person, covering the Ti surface with bioactive layers, such as amino acids, that can exert an improved effect on the fixation of implants by promoting the development of a hydroxyapatite (HA) layer on the implant surface. This, in turn, can result in improving the interaction between the implant and the host bone tissue.

L-Aspartic acid or (S)-(+)-aminosuccinic acid or (S)-aminobutanedioic acid (Asp; Figure 5.1) is an alpha-amino acid whose amino group is protonated forming $–NH_3^+$ form under physiological conditions (pH = 7.4), while its α-carboxylic acid group is deprotonated $–COO^-$. This property confers it an essential role in matrix proteins to nucleate calcium phosphate growth to stimulate biomineralization. [4] Intermolecular interactions between Asp and TiO_2/Ti surfaces are critical in the functionality of Ti implant-bone prostheses. Amino acids can self-organize on surfaces such as TiO_2/Ti; therefore, they can functionalize implants, leading to specific properties characteristic such as assisting in osseointegration. [5, 6] Binding of Asp to modified TiO_2/Ti surfaces

is fundamental to the design of templates that can be useful to bind additional molecules in special arrangements, for instance, HA. Raman scattering (RS) coupled to an optical microscope is very useful to obtain a better understanding about the potential binding of Asp to the modified TiO_2 /Ti surfaces, and it can be used to study the intermolecular interactions among chemical species in detail, resulting in a better comprehension of the behavior adsorbate-substrate.

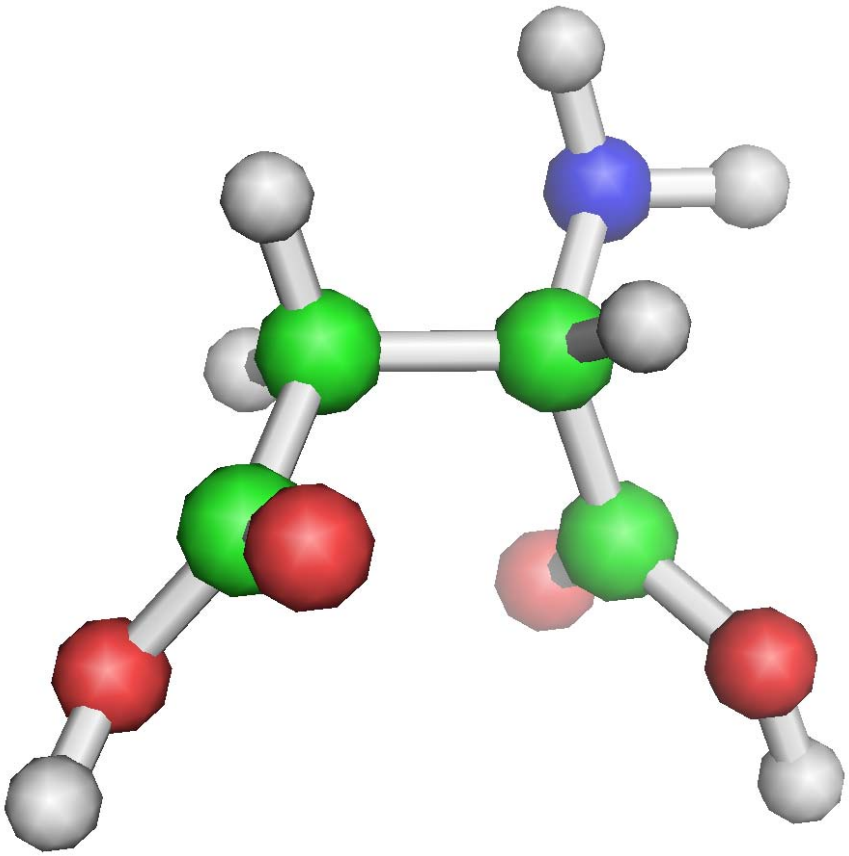

Figure 5. 1. Chemical structure of Asp

5.2 Materials and methods

Neat Ti plates (10 mm x 10 mm x 2 mm) used as substrates in functionalization were acquired from Thermo-Fisher Scientific Ti plates (99.99%, Waltham, MA, USA). Silicon carbide grinding paper was used to erode the Ti surfaces. Once the Ti surfaces were roughened. they were washed with acetone, absolute ethanol, and deionized (DI) water sequentially, in an ultrasonic bath for 15 min each time. Cleaned surfaces were dried in a desiccator overnight, to use them after to modification and functionalization. A mixture of 30 mL nitric acid (HNO_3, 40 wt.%) and 70 mL DI water was used for etching the Ti surfaces. Dried substrates were etched for 2 min. Etched surfaces were oxidized by immersing and soaking them in hydrogen peroxide solution (H_2O_2, 30% wt.) for 24 h.

To functionalize the Ti surfaces, the oxidized surfaces were incubated in 10.0 mM Asp solution, keeping the pH constant at 2.0 by adding small portions of a dilute HCl solution at room temperature. The total incubation process lasted 6 days. However, at the end of 3rd day, Ti samples were rinsed with water and ethanol to eliminate any chemical interferences produced. Finally, functionalized Asp-TiO_2 surfaces were left to dry overnight in a desiccator. A simulated body fluid (SBF) was prepared according to the methodology described by Kokubo and coworkers. [7] Samples were immersed and soaked in SBF for 28 d, monitoring the precipitation of HA from SBF. The above procedure was aimed at evaluating the bioactivity *in vitro* of Asp-TiO_2 to form HA on them.

Raman scattering (RS) microspectroscopy was used to analyze the Asp-TiO_2 substrates. The reference samples were the two crystalline phases of TiO_2 (anatase and rutile). Their RS analysis was described in a previous contribution. [8] RS spectra

were acquired employing an InVia Raman microspectrometer (Renishaw, LLC., West Dundee, IL, USA). The spectrometer was interfaced to a Leica DM2500 microscope, and a 50x Leica objective was used to focus the laser beam on the sample surface to excite the RS and for collecting the scattered light. Ten accumulations were averaged with an exposure time of 10 s. A 532 nm diode pumped laser (Cobolt AB, Solna, Sweden) was used as the excitation source.

The spectrometer was calibrated before each set of measurements using the 520.65 cm^{-1} Raman shift peak of silicon (110). Characteristic RS signatures were marked, and a baseline correction was applied to all spectra. The laser power at the samples was controlled to avoid sample degradation upon laser irradiation.

5.3 Results and discussion

5.3.1 Raman spectroscopic features of Asp

RS of Asp is shown in Figure 5.2. The observed frequencies with their relative intensities and assignments are listed in Table 1. To discuss in detail the tentative assignments of the observed vibrational bands, three regions were considered: a high-frequency (CH, NH, OH) region (3800–2500 cm^{-1}), a medium-frequency or fingerprint region (1800–500 cm^{-1}), and a low-frequency region (below 500 cm^{-1}).

Table 5. 1. Raman shift observed and tentative assignment frequencies for Asp

Raman Shift (cm^{-1})	Proposed Assignment
3080	symmetric NH_3^+ stretching
3012	CH_2 asymmetric stretching
2995	CH asymmetric stretching
2954	CH_2 symmetric stretching
1690 (m)	asymmetric stretching vibration of COO^-
1639 (w)	asymmetric in-plane bending vibration of NH_3^+ moiety
1614 (w)	asymmetric stretching vibration of COO^-
1553	symmetric in-plane bending of NH_3^+
1407 (s)	symmetric COO^- stretching
1359 and 1334	vibrational bending modes of C-H group
1249	bending vibrations of methylene
1261	coupling of the C-O stretching vibration with the hydroxyl in-plane deformation vibration
1144	rocking vibration modes of NH_3^+
950-1100	C-C and C-N skeletal stretching
937 (vs)	hydroxyl out-of-plane bending of the carboxylic group
870	rocking vibration mode of CH_2
777 and 599	carboxylate bending vibrations modes
661 and 550	in-plane bending vibrations of COOH moiety
500-200	skeletal bending and skeletal torsional vibrations; includes C-C-C and C-C-N modes
467	torsional vibration of NH_3^+
187	torsional vibration of carboxylate (COO^-)

(vs) = very strong; (s) = strong, (m) = medium; (w) = weak; (vw)= very weak

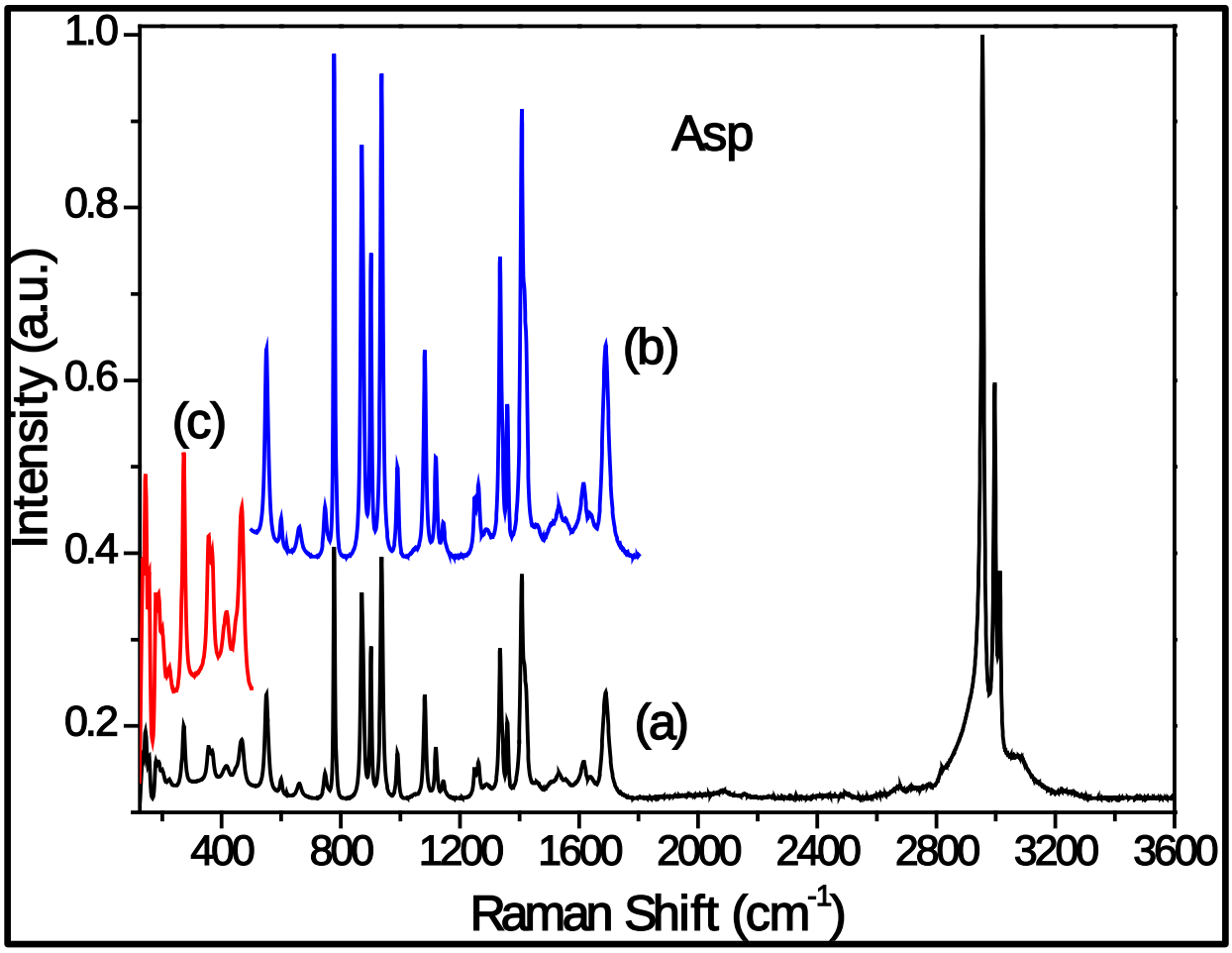

Figure 5.2. Raman spectrum of Asp: (a) full range; (b) fingerprint region; (c) low frequency range.

5.3.1.1 High-frequency region (3800-2500 cm^{-1})

N-H, C-H, and OH stretching vibrations characterize this region, where bands corresponding to $\nu(NH_3^+)$, $\nu(CH)$, and $\nu(OH)$ modes, both symmetric and fundamental asymmetric vibrations can be located. The highest intensity bands related to $\nu_a(CH_2)$, $\nu(CH)$, and $\nu_s(CH_2)$ appear at 3012, 2995, and 2954 cm^{-1}, respectively. The weak band observed at 3080 cm^{-1} has been assigned to symmetrical NH_3^+ stretching vibrations. [9]

5.3.1.2 Medium-frequency region (1800-500 cm^{-1})

Three bands were observed between 1700 and 1600 cm^{-1} in the RS spectrum of, specifically at 1690, 1639, and 1614 cm^{-1} with medium intensity the first and weak intensities the other two bands. The peak at 1639 cm^{-1} is assigned to asymmetric in-plane bending vibration of the NH_3^+ moiety. [10,11] The $\nu(C=O)$ vibrations were observed at 1690 and 1614 cm^{-1}. They correspond to the asymmetric stretching vibration of the carboxylate group, COO^-. [10,12] It is important to mention that the broadening of the above bands belonging to C=O and NH_3^+ groups, respectively, can be due to couplings of vibrations of –COOH with vibrations of the neighboring NH_3^+ group. [13,14]

Symmetric in-plane bending of NH_3^+ was observed at 1553 cm^{-1}. A strong band was observed at 1407 cm^{-1}, and it was assigned to symmetric COO^- stretching vibration characteristic of some amino acids such as Asp. [10,15] Furthermore, the bands at 1407 and 1261 cm^{-1} are assigned to the coupling of the C-O stretching vibration with the hydroxyl in-plane deformation vibration. [16,17]. Bending vibrations of methylene appear

at 1249 cm^{-1}. Two bending vibrational modes of the C-H group were observed at 1359 and 1334 cm^{-1}. Rocking vibration modes of NH_3^+ appeared at 1144 and 1119 cm^{-1} in a similar way to other amino acids reported. [12,15] Finally, bands assigned to C-C and C-N skeletal stretching vibrations are observed between 950 and 1100 cm^{-1}. At 937 cm^{-1} a relatively strong band corresponding to hydroxyl out-of-plane bending vibration of the carboxylic group was observed, similar to that reported for glutamic acid. [12] A rocking vibration mode of CH_2 was observed at 870 cm^{-1} The carboxylate bending vibrations modes were observed at 777 and 599 cm^{-1} and they are related to intermolecular associations. Based on previous studies about correlations on carboxylic acids, bands at 661 and 550 cm^{-1} were assigned to in-plane bending vibrations of COOH moiety. [16]

5.3.1.3 Low-frequency region (below 500 cm^{-1})

This region is characterized by the existence of remaining bending and torsional vibrations of Asp. The band at 467 cm^{-1} indicates a torsional vibration of NH_3^+. Between 500 and 200 cm^{-1}, there are four skeletal bending and three skeletal torsional vibrations that involved mainly C-C-C and C-C-N modes. Finally, a carboxylate torsional vibration of COO^- was observed at 187 cm^{-1}, according to previous frequencies reported for amino acids such as glutamic and alanine. [10,12]

5.3.2 Functionalization of Ti surface with Asp

RS measurements were instrumental in identifying and interpreting specific chemical bonds arising between intermolecular interactions of modified Ti surface with Asp.

Structural information about the Asp layer on the modified Ti surface was obtained according to the above. The RS spectrum of Asp-TiO_2/Ti is dominated by two strong peaks at 1047 and 2948 cm^{-1}, assigned to CH bending vibration and stretching vibration of CH_2, respectively. In the same way in the 3050 – 3300 cm^{-1} region exists a band corresponding to symmetric stretching of NH_3^+. Another broad band in 3350 – 3600 cm^{-1} is present, and it could be correlated to O-H···O stretching mode of water molecules. [18,19] In the 2550 – 2750 cm^{-1} region exists a broad band corresponds to $–NH_3^+$ symmetric stretching, which can be corroborated observing another broad band in 2050 – 2110 cm^{-1}. [9]

Figure 5.3b shows the Raman spectrum of Asp-TiO_2/Ti in the region of 100 – 1800 cm^{-1}. At 1737 cm^{-1} there is a medium vibration band that can be assigned to the –C=O stretching mode of –COOH group. This spectrum helps to corroborate that Asp molecules are adsorbed onto the modified Ti surface using the carboxylic group since this band does not appear in the RS spectrum of Asp (Figure 5.3a). Furthermore, it indicates the existence of the $^+NH_3$-R-COOH cation, having in mind that this band is not characteristic of the $–COO^-$ ion. A broad band centered at about 1601 cm^{-1} and a sharp peak at 1406 cm^{-1} are related to asymmetric NH_3^+ deformation and $–COO^-$ symmetrical stretching vibration mode, respectively. Interestingly, when comparing the Asp spectrum (Figure 5.3a) with Asp-TiO_2/Ti spectrum (Figure 5.3b), the band at 1334 cm^{-1} associated to CH bending vibration has drastically decreased in intensity, and it has been displaced to lower wavenumber (1324 cm^{-1}) this could be due to atomic interactions of neighboring –COOH and NH_3^+ groups with $–CH_2$ since, it is in the middle of them. The low-intensity band at 1361 cm^{-1} supports the inferred regarding band at 1324 cm^{-1}.

Besides, the high-intensity band at 1407 cm^{-1}, belonging to Asp, has strongly decreased its intensity in the Asp-TiO_2/Ti spectrum, and now it is a broader band displaced one lower wavenumber, due possibly to the interaction between TiO_2 and –COOH group of Asp on the modified Ti surface. Analyzing the 1300 – 1130 cm^{-1} region there are two broad weak bands, indicating that the NH_3^+ group is far away from the modified Ti surface, in comparison to –COOH groups and side chain which are near the Ti surface. It is worth mentioning the emergence of two new bands at 981 and 1047 cm^{-1} with medium and high intensities, respectively. They are associated with C-COO^- vibration modes and correspond to bridged Ti-O-R species. [20] It can be noted the absence of a band at 937 cm^{-1} assigned to –OH belonging to COOH group, which can be correlated to the sharp medium band at 926 cm^{-1} corresponding to the interaction of –OH with TiO_2 of modified Ti surface. Interestingly, two new strong, sharp bands are located at 817 and 887 cm^{-1}, which are related to aliphatic skeletal stretching vibration modes of C-C and C-N in the complex formed between TiO_2 of Ti surface and Asp. [20] The strong band at 780 cm^{-1} of Asp is now a weak band at 777 cm^{-1} and displaced a lower wavenumber due to the interaction of –COOH with TiO_2/Ti surface. The medium broad band at 589 cm^{-1} corresponding to wagging deformation mode of –COO^- group, it indicates the interaction of another carboxylic group with TiO_2/Ti surface. The skeletal deformation vibration mode of Asp molecule and wagging deformation mode of –COO^- can be observed at 430 and 381 cm^{-1}, respectively. [20] As mentioned above, at 2948 cm^{-1} the broad, strong peak corresponds to C-H stretching vibration mode, but it also indicates the proximity of –CH group to the modified Ti surface.

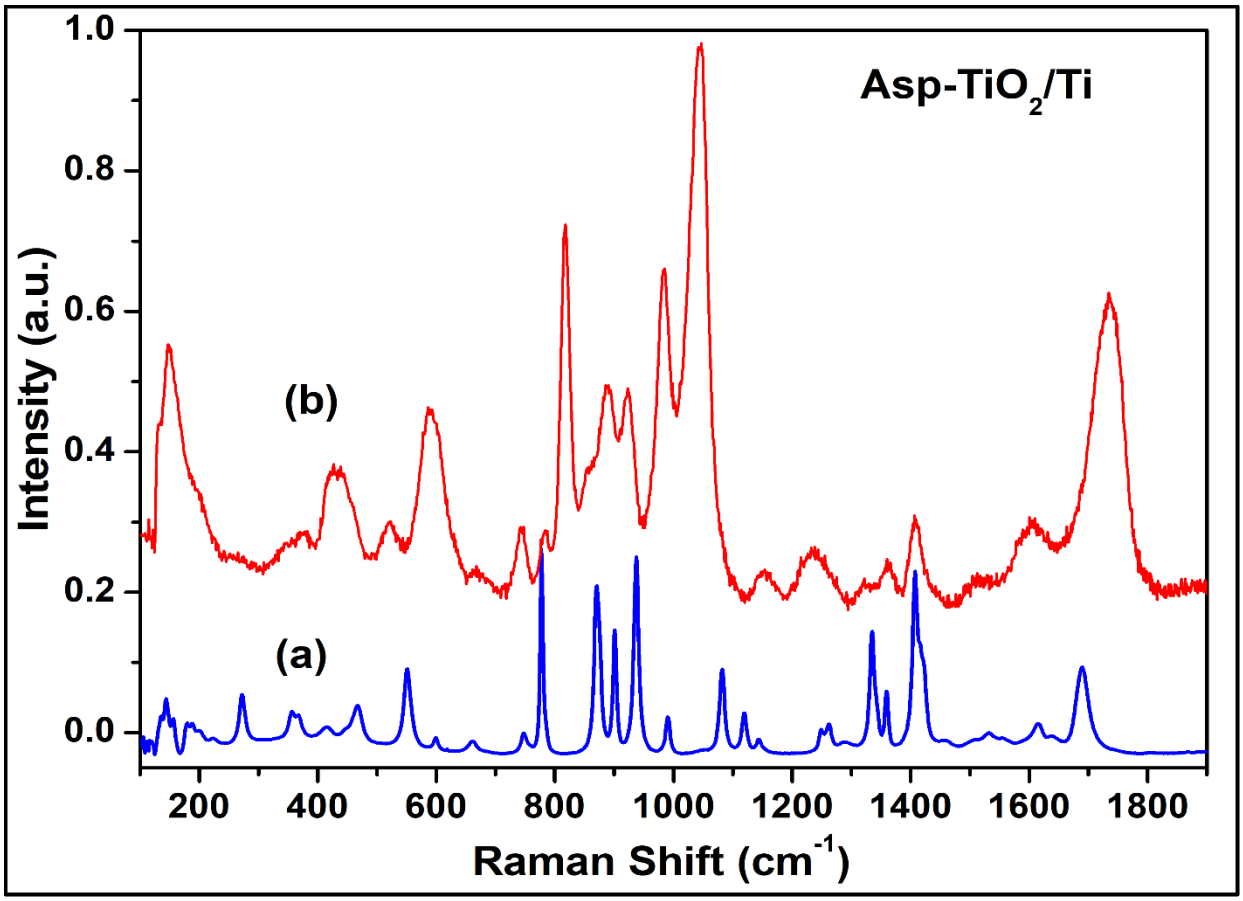

Figure 5. 3. RS spectra of functionalized Ti surface with Asp (region 100-1800 cm^{-1}): (a) RS of Asp; (b) RS of Asp-TiO_2/Ti.

Comparing both RS spectra of modified Ti substrate and organic ligand adsorbate, it can be evidenced that TiO_2 layer on the Ti surface is interacting chemically with Asp through its –COOH groups, developing bridged surface complexes. Furthermore, the broad weak bands in the 1300 – 1130 cm^{-1} region provide indications of that ammonium group of Asp is protonated, and it is far from the TiO_2/Ti surface. In the same way, the strong, sharp band at 817 cm^{-1} indicates the possibility of carbon skeletal has a parallel orientation relative to Ti surface, which is corroborated with the new band at 887 cm^{-1}. According to the frequency of the two new bands at 981 and 1047 cm^{-1} and their intensities in the RS spectrum of Asp-TiO_2/Ti, it can be inferred that the –COOH functional groups are not parallel nor perpendicular relative to Ti surface, reinforcing the fact of NH_3^+ is distant from TiO_2/Ti surface, and it does not take direct part in the bonding with the TiO_2/Ti surface. Therefore, the Asp molecules are oriented at an angle with respect to TiO_2/Ti surfaces, forming Ti-O-R species. The broadening of the band at 1601 cm^{-1} suggests confirmation of the mentioned above, indicating that carboxylic group is directly interacting with the TiO_2/Ti surface. Therefore, Asp seems to be adsorbed onto the modified TiO_2/Ti surface. Also, the –OH out-of-plane bending vibration corresponding to the strong band at 937 cm^{-1} is absent in the RS spectrum of Asp-TiO_2/Ti, evidencing that all hydroxyl groups of carboxyl group have reacted with the TiO_2/Ti surface, confirming again the interchange reactions of ligands between modified TiO_2/Ti surface and Asp.

RS analysis enables to deduce that Asp reacts through its carboxylic acid functional groups. Finally, based on the above discussion, all spectroscopic evidence points to the coating in the functionalized TiO_2/Ti surface is a bridged surface complex of Asp-

TiO_2/Ti, where the chemical bonding is carried out using carboxylic group, taking into account that the spatial orientation of aliphatic chain relative to the TiO_2/Ti surface is parallel. Consequently, the most probable chemical structure for the adsorption of Asp onto modified Ti surface is indicated in Figure 5.4, where it can be noted the interaction between the two carboxylic groups of Asp and Ti ions of the modified TiO_2/Ti surface.

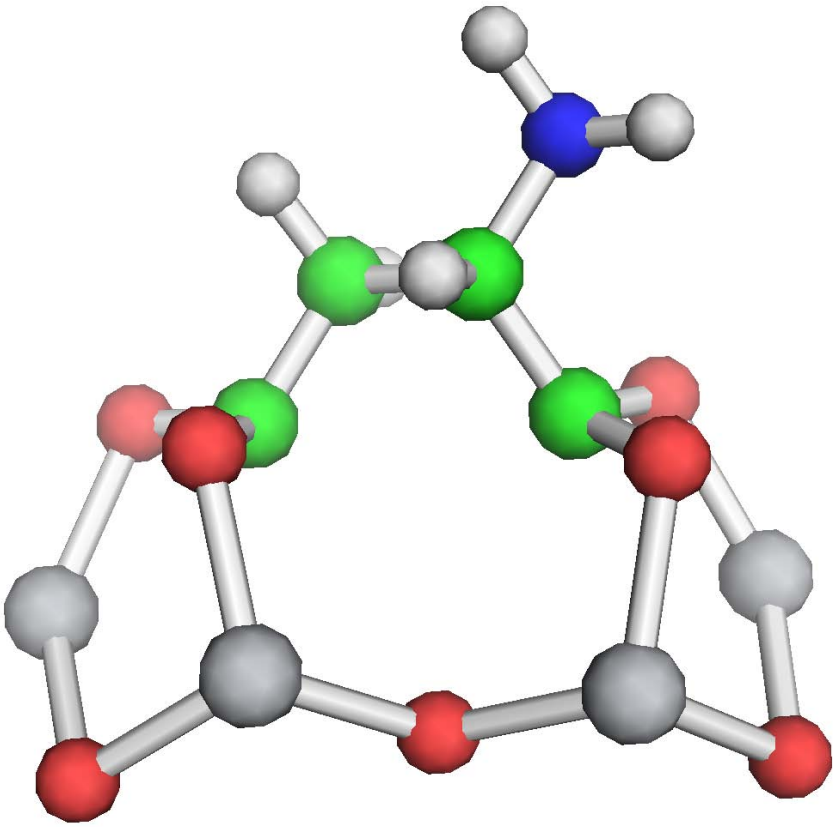

Figure 5.4. Proposed orientation of Asp onto the TiO_2/Ti surface

5.3.3 Bioactivity *"in vitro"* of Asp-Ti surface

Figure 5.5 shows the RS spectrum of the HA layer formed on the Asp-TiO_2/Ti surface. The RS measurements were useful when elucidating the chemical bonds and intermolecular interactions of Asp with developed HA onto functionalized TiO_2/Ti surface. The sharp, strong peak at 1007 cm^{-1} (the most intense signal) and a shoulder at 980 cm^{-1} correspond to symmetric stretching vibration mode of P-O of the phosphate ion. At this point, it is worth to mention that fine structure and intensities of bands belonging to PO_4^{3-} are representative of a good crystallinity of developed HA coating. [21-25] The weak band located at 618 cm^{-1} corresponds to bending vibrational mode of PO_4^{3-} group (O-P-O bond). Similarly, the medium peak centered at 413 cm^{-1} is also assigned to bending mode of PO_4^{3-}. [26-31] The bands located at 493 and 670 cm^{-1} are assigned as corresponding to out-of-plane CO deformation vibration. [9] The weak and very weak bands at 817 and 927 cm^{-1}, respectively, are related to aliphatic skeletal vibration mode of C-C and C-N in the complex formed between TiO_2 of TiO_2/Ti surface and Asp, and the interaction of –OH of carboxylic group of Asp with TiO_2/Ti surface. [20] The weak peak at 1134 cm^{-1} can be associated with NH_3^+ rocking vibration. [9] Another very weak band related to the interaction between TiO_2 and –COOH group of Asp on the modified TiO_2/Ti surface, is located at 1402 cm^{-1}. At 1726 cm^{-1} exists a weak broad band associated to –C=O stretching mode of carboxylic group complexed to TiO_2/Ti surface. The medium broad peak located at 2950 cm^{-1} is related to stretching vibration of CH_2. The strong band at 3403 and the medium peak at 3491 cm^{-1} correspond to the bond-stretching mode associated to –OH of HA. The broadening and overlapping of

them indicate the existence of disordered structural phosphate groups. [32] The vibrational modes involving translational motion of Ca^{2+} and PO_4^{3-} sublattices, and librational modes of the PO_4^{3-} are associated with the very weak band at 313 cm^{-1}. [33-35]

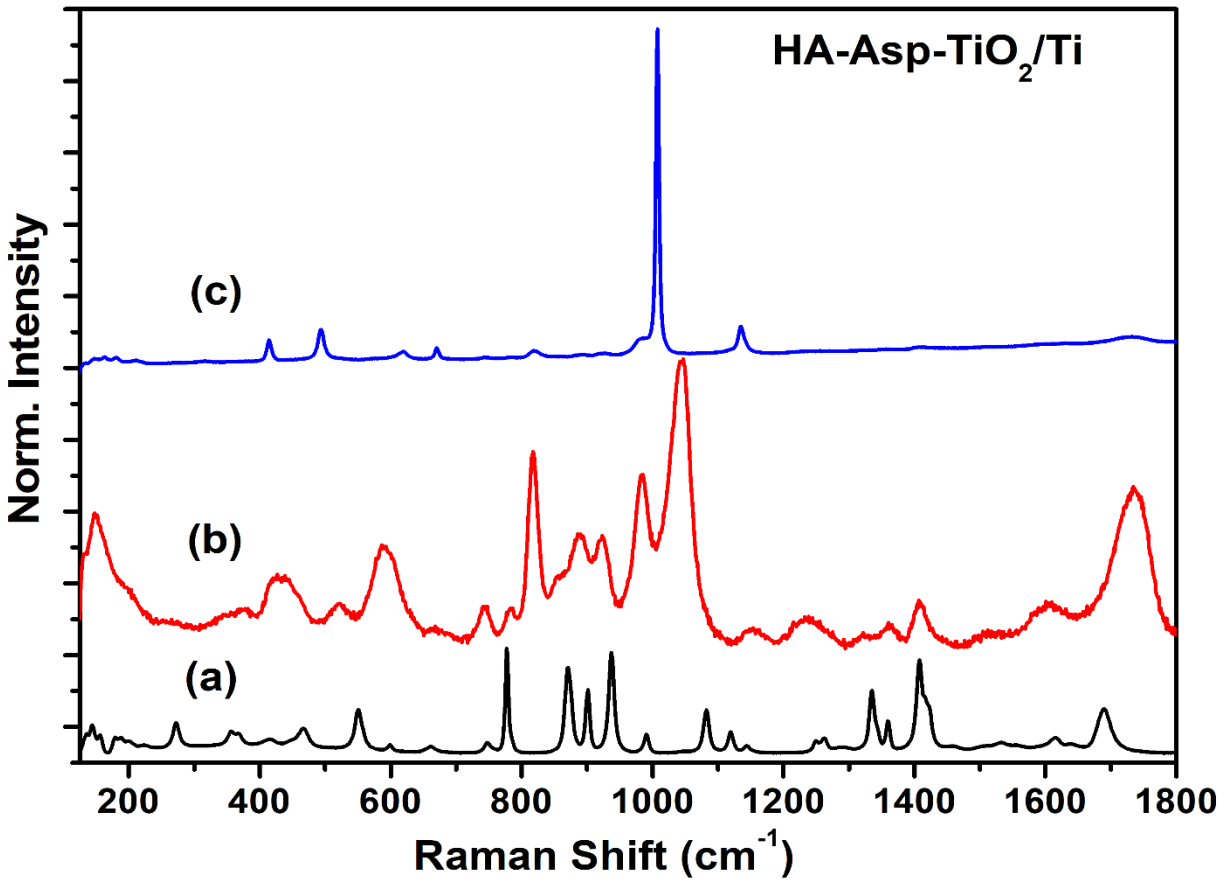

Figure 5. 5. RS spectrum of developed HA layer on Asp functionalized TiO_2/Ti surface: (a) Asp; (b) Asp-TiO_2/Ti; (c) HA-Asp-TiO_2/Ti.

Finally, based on RS and observing the decreasing of intensities and shifting of bands to lower wavenumbers for carboxylic group (1402 and 1726 cm^{-1}), and broadening of bands at 3403 and 3491 cm^{-1} it can be suggested that fixation of HA onto Asp-TiO_2/Ti surface is carried out through Hydrogen bond between –COOH group of Asp and oxygen atoms belonging to PO_4^{3-} (Figure 5.6). [36-38]

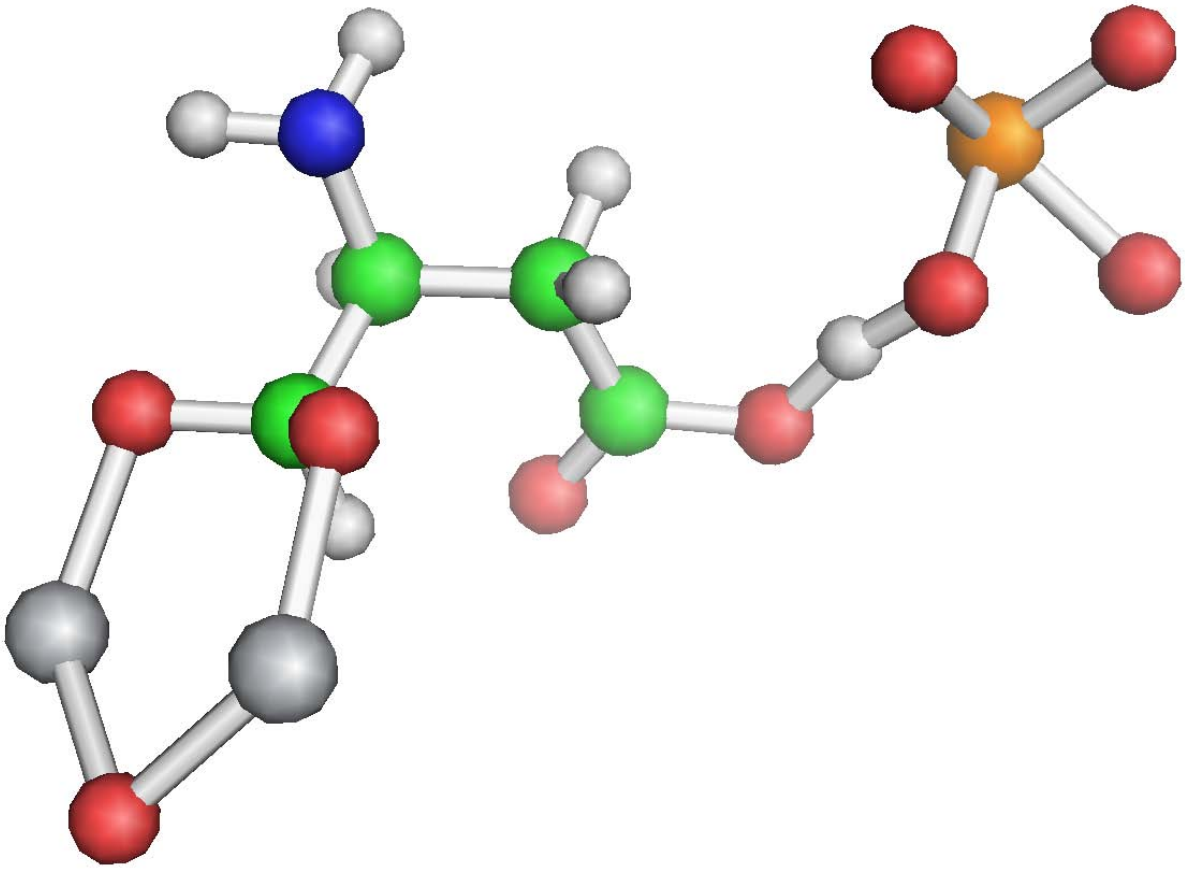

Figure 5.6. Proposed chemical structure of HA-Asp on the functionalized TiO_2/Ti surface.

5.4 Conclusions

Neat pure Ti plate was chemically oxidized to produce a TiO_2 / Ti surface. Functionalization of TiO_2 / Ti surface was carried out by adsorbing Asp on it. RS spectroscopy was employed to elucidate the specific chemical bonds present and the intermolecular interactions that there are between Asp and TiO_2 / Ti surface, in order to get structural information about adsorbate-substrate layers. To accomplish the above, ASP was spectroscopically analyzed using RS spectroscopy in order to obtain its Raman spectroscopic features in the three vibrational regions: high-frequency, medium-frequency (fingerprint region) and low-frequency. RS spectra of neat Asp and Asp-TiO_2/Ti were compared to extract important information related to the chemical environment between the organic ligand adsorbate and the functionalized substrate. At this point it is worthwhile to mention that there is a chemical interaction between TiO_2 layer on the Ti surface and Asp through its -COOH groups forming bridged surface complexes. Besides, the ammonium group belonging to Asp is protonated and it is found far away from the TiO_2 / Ti surface. In the same way, exists a possibility that the orientation of aliphatic chain of Asp relative to TiO_2 / Ti surface be parallel. Based on the mentioned above it can be deduced that the -COOH functional groups are not parallel nor perpendicular relative to TiO_2 / Ti surface, and NH_3^+ is distant from it avoiding any chemical bonding. Thence, the Asp molecule has an angular orientation with respect to TiO_2 / Ti surface.

The bioactivity of Asp-TiO_2 / Ti surface was evaluated "*in vitro*" by developing a HA layer onto it. Observing and analyzing the RS measurements it was possible to suggest

that the adsorption of HA on TiO_2 / Ti surface was due to formation of hydrogen bonds between –COOH group of Asp and oxygen atoms belonging to PO_4^{3-}.

Finally, it is very important to take into account the spectroscopic evidence and molecular structure of each compound to provide clarity about specific chemical bond and the intermolecular interactions in order to suggest and make tentative assignments to understand the behavior of complex substrate-adsorbate at molecular level.

Acknowledgments

The authors express sincere appreciation to the faculty members and supporting personnel of the Departments of Bioengineering and Chemistry of the Mayagüez Campus of the University of Puerto Rico for their collaboration during all project stages.

Conflict of Interest

The authors report there are no conflicts of interest.

5.5 References

[1]. T. Albrektsson and H.-A. Hansson, “An ultrastructural characterization of the interface between bone and sputtered titanium or stainless steel surfaces,” *Biomaterials*, **7**(3): 201–205, 1986.

[2]. M. Abdel-Hady Gepreel and M. Niinomi, “Biocompatibility of Ti-alloys for long-term implantation,” *J. Mech. Behav. Biomed. Mater.*, **20**: 407–415, 2013.

[3]. N. Drnovšek, S. Novak, U. Dragin, M. Čeh, M. Gorenšek, and M. Gradišar, “Bioactive glass enhances bone ingrowth into the porous titanium coating on orthopaedic implants,” *Int. Orthop.*, **36**(8): 1739-1745, 2012.

[4]. A. Tsortos and G. H. Nancollas, “The Adsorption of Polyelectrolytes on Hydroxyapatite Crystals,” *J. Colloid Interface Sci.*, **209**(1): 109–115, 1999.

[5]. Z. Pászti and L. Guczi, “Amino acid adsorption on hydrophilic TiO2: A sum frequency generation vibrational spectroscopy study,” *Vib. Spectrosc.*, **50**(1): 48–56, 2009.

[6]. S. M. Barlow and R. Raval, “Complex organic molecules at metal surfaces: bonding, organisation and chirality,” *Surf. Sci. Rep.*, **50**(6): 201–341, 2003.

[7]. T. Kokubo and H. Takadama, “How useful is SBF in predicting in vivo bone bioactivity?,” *Biomaterials*, **27**(15): 2907–2915, 2006.

[8]. C. A. Manrique-Bastidas, P. Sundaram, P. R., N. Mina, and S. P. Hernandez-Rivera, “Functionalization of Titanium Surfaces with Lysine: a Micro Raman Study of TiO_2 -Lysine Intermolecular Interactions”, Manuscript in progress, 2019.

[9]. G. Socrates, “Infrared and Raman Characteristic Group Frequencies, Tables and Charts.” Third Ed., John Wiley & Sons, Ltd., pp.331, 2001.

[10]. M. Diem, P. L. Polavarapu, M. Oboodi, and L. A. Nafie, “Vibrational circular dichroism in amino acids and peptides. 4. Vibrational analysis, assignments, and solution-phase Raman spectra of deuterated isotopomers of alanine,” *J. Am. Chem. Soc.*, **104**(12): 3329–3336, 1982.

[11]. H. Susi, D. M. Byler, and W. V Gerasimowicz, “Vibrational analysis of amino acids: cysteine, serine, β-chloroalanine,” *J. Mol. Struct.*, 102(1-2): 63–79, 1983.

[12]. P. Dhamelincourt and F. J. Ramírez, “Polarized micro-Raman and Fourier transform infrared spectra of L-glutamic acid,” *J. Raman Spectrosc.*, **22**(10): 577–582, 1991.

[13]. J. T. López-Navarrete, J. J. Quirante, and F. J. Ramírez, “Harmonic force field for the glycine molecule by semiempirical methods,” *J. Mol. Struct.*, **268**(1-3): 249–261, 1992.

[14]. V. Hernández, F. J. Ramírez, and J. T. López Navarrete, “Comparison between semiempirical and experimental force fields of oligothiophenes as an approach for

the calculations of the vibrational spectrum of the polymer," *J. Mol. Struct.*, **294**: 37–40, 1993.

[15]. P. Dhamelincourt and F. J. Ramirez, "Polarized Micro-Raman and FT-IR Spectra of L-Glutamine," *Appl. Spectrosc.*, **47**(4): 446–451, 1993.

[16]. D. Hadzi, N. Sheppard, "The infrared absorption bands associated with the COOH and COOD groups in dimeric carboxylic acids. I. The region from 1500 to 500 cm^{-1}" *Proc. R. Soc. London. Ser. A. Math. Phys. Sci.*, **216**(1125): 247-266, 1953.

[17]. T. Shimanouchi, M. Tsuboi, T. Takenishi, and N. Iwata, "A strong band at 1200 cm−1, characteristic of the $-CH_2-COOH$ group," *Spectrochim. Acta*, **16**(11-12): 1328–1332, 1960.

[18]. R. M. Silverstein, F. X. Webster, D. J. Kiemle and D. L. Bryce, "Spectrometric identification of organic compounds," John Wiley & Sons, 2014.

[19]. M. Badertscher, P. Bühlmann and E. Pretsch, "Structure determination of organic compounds," Springer, Berlin, Heidelberg, 2008.

[20]. U. Schubert, S. Tewinkel, and F. Moeller, "Metal Complexes in Inorganic Matrixes. 13. Nickel Complexes with Lysinate-Substituted Titanium Alkoxides as Ligands. X-ray Structure Analysis of $[(EtO)_3Ti(glycinate)]_2$," *Inorg. Chem.*, **34**(4): 995–997, 1995.

[21]. G. R. Sauer, W. B. Zunic, J. R. Durig, and R. E. Wuthier, "Fourier transform Raman spectroscopy of synthetic and biological calcium phosphates," *Calcif. Tissue Int.*, **54**(5): 414–420, 1994.

[22]. H. Tsuda and J. Arends, "Raman Spectra of Human Dental Calculus," *J. Dent. Res.*, **72**(12): 1609–1613, 1993.

[23]. B. O. Fowler, M. Markovic, and W. E. Brown, "Octacalcium phosphate. 3. Infrared and Raman vibrational spectra," *Chem. Mater.*, **5**(10): 1417–1423, 1993.

[24]. G. Penel *et al.*, "Raman microspectrometry studies of brushite cement: in vivo evolution in a sheep model," *Bone*, **25**(2), Supplement 1, p. 81S–84S, 1999.

[25]. F. Barrere, C. A. van Blitterswijk, K. de Groot, and P. Layrolle, "Nucleation of biomimetic Ca–P coatings on Ti6Al4V from a SBF×5 solution: influence of magnesium," *Biomaterials*, **23**(10): 2211–2220, 2002.

[26]. W. P. Griffith, “Raman studies on rock-forming minerals. Part II. Minerals containing MO_3, MO_4, and MO_6 groups,” *J. Chem. Soc. A Inorganic, Phys. Theor.* , **0**: 286–291, 1970.

[27]. D. C. O’Shea, M. L. Bartlett, and R. A. Young, “Compositional analysis of apatites with Laser-Raman spectroscopy: (OH,F,Cl)apatites,” *Arch. Oral Biol.*, **19**(11): 995–1006, 1974.

[28]. R. Cuscó, F. Guitián, S. d. Aza, and L. Artús, “Differentiation between hydroxyapatite and β-tricalcium phosphate by means of μ-Raman spectroscopy,” *J. Eur. Ceram. Soc.*, **18**(9): 1301–1305, 1998.

[29]. S. Koutsopoulos, “Synthesis and characterization of hydroxyapatite crystals: A review study on the analytical methods,” *J. Biomed. Mater. Res.*, **62**(4): 600–612, 2002.

[30]. A. Antonakos, E. Liarokapis, and T. Leventouri, “Micro-Raman and FTIR studies of synthetic and natural apatites,” *Biomaterials*, **28**(19): 3043–3054, 2007.

[31]. G. Penel, G. Leroy, C. Rey, and E. Bres, “MicroRaman Spectral Study of the PO4 and CO3 Vibrational Modes in Synthetic and Biological Apatites,” *Calcif. Tissue Int.*, **63**(6): 475–481, 1998.

[32]. B. Mihailova, B. Kolev, C. Balarew, E. Dyulgerova, and L. Konstantinov, “Vibration spectroscopy study of hydrolyzed precursors for sintering calcium phosphate bio-ceramics,” *J. Mater. Sci.*, **36**(17): 4291–4297, 2001.

[33]. Z. Iqbal, V. P. Tomaselli, O. Fahrenfeld, K. D. Möller, F. A. Ruszala, and E. Kostiner, “Polarized Raman scattering and low frequency infrared study of hydroxyapatite,” *J. Phys. Chem. Solids*, **38**(8): 923–927, 1977.

[34]. V. Devarajan and W. E. Klee, “A potential model for fluorapatite,” *Phys. Chem. Miner.*, **7**(1): 35–42, 1981.

[35]. D. M. Adams and I. R. Gardner, “Single-crystal vibrational spectra of apatite, vanadinite, and mimetite,” *J. Chem. Soc. Dalt. Trans.*, **0**(14): 1505–1509, 1974.

[36]. N. Almora-Barrios and N. H. de Leeuw, “A Density Functional Theory Study of the Interaction of Collagen Peptides with Hydroxyapatite Surfaces,” *Langmuir*, **26**(18): 14535–14542, 2010.

[37]. N. Almora-Barrios, K. F. Austen, and N. H. de Leeuw, “Density Functional Theory Study of the Binding of Glycine, Proline, and Hydroxyproline to the Hydroxyapatite (0001) and (0110) Surfaces,” *Langmuir*, **25**(9): 5018–5025, 2009.

[38]. A. Rimola, M. Corno, C. M. Zicovich-Wilson, and P. Ugliengo, “Ab Initio Modeling of Protein/Biomaterial Interactions: Glycine Adsorption at Hydroxyapatite Surfaces,” *J. Am. Chem. Soc.*, **130**(48): 16181–16183, 2008.

Chapter 6

Adsorption of Vitamin C to TiO_2 / Ti Surfaces: Experimental Evidence of Intermolecular Interactions using Raman Scattering Spectroscopy: Implications for Osseointegration

Abstract

Neat Ti surfaces were modified and subsequently functionalized to develop hydroxyapatite (HA) layer onto it. Raman scattering (RS) spectroscopy coupled to an optical microscope was used to carry out the elucidation of intermolecular interactions between L-ascorbic acid or vitamin C (Vit-C) and modified Ti surfaces. An HA layer was formed on functionalized Ti surface. In the interaction of Ti surfaces modified with Vit-C, evidence of the formation of a bond between oxygen atoms of 2,3-enediole was observed. This was confirmed by analyzing the bands at 1652, 1666 and 1749 cm^{-1} belonging to C=C and C=O. The formation of hydrogen bond between HA and Vit-C could occur through hydrogen atom of the -OH group of Vit-C with oxygen atoms of phosphate ion of HA, and oxygen atoms of C-O group of Vit-C with the hydrogen of $^{-}$OH with HA.

Keywords

Functionalization, L-ascorbic acid (Vit-C), TiO_2/Ti surfaces, hydroxyapatite (HA), Raman scattering (RS), osseointegration

6.1 Introduction

L-Ascorbic acid also known as vitamin-C (Vit-C) is a cyclic lactone containing an enediol group (Figure 6.1). Its acidic character is due to electron delocalization in the ring system, and therefore it is a potent reducing agent that prevents oxidation of physiological components (an antioxidant) by destructing the reactive oxygen species and hence offering protection to tissues from damage free radicals. It is present in redox biochemical and physiological reactions in the human body, and it can be found naturally in fruits and vegetables. [1-9] It has good water solubility and plays a relevant role in human nutrition and other mammals. [10] Neurons use Vit-C in chemical and enzymatic reaction and can also act as a neuromodulator. [11]

Vit-C can be used as a preservative in food and beverages, and it protects the human skin from the danger of exposure to UV light. [1-9] Research has demonstrated that Vit-C can act as a cytotoxic agent against some types of cancer cells such as melanoma, human leukemia, neuroblastoma, and tumor ascites cells. [12,13] The powerful and versatile chemical can help to increase the power of the immune system of HIV-positive patients by killing the HIV-positive cells. [14]

Medical implants based on titanium (Ti) are used in dental and orthopedic reconstructive surgery, where surface science is impacting biomaterials research searching for a good osseointegration material with excellent long-term clinical outcome

for bone implants. In this regards, functionalization of Ti surfaces with Vit-C could be very important to improve and optimize the positive response of human bodies to Ti implants, allowing to form a hydroxyapatite (HA) layer onto Ti surfaces and getting better recognition from the immune system, and enhancing the fixation of Ti implants.

In this research work, the interaction between the TiO_2 layer of modified Ti surfaces (TiO_2/Ti) and Vit-C, in the functionalized Ti surface, was studied using Raman scattering (RS) spectroscopy. Vit-C was chosen as a coating agent to functionalize the Ti surfaces because it has two significant functional groups: carbonyl and hydroxyl, which can be hydrogen bonded to the TiO_2 layer that exists on the oxidized Ti surface. On the other hand, the formation of HA on the functionalized Ti surfaces and characterization by RS was used to elucidate intermolecular interactions between Vit-C and HA.

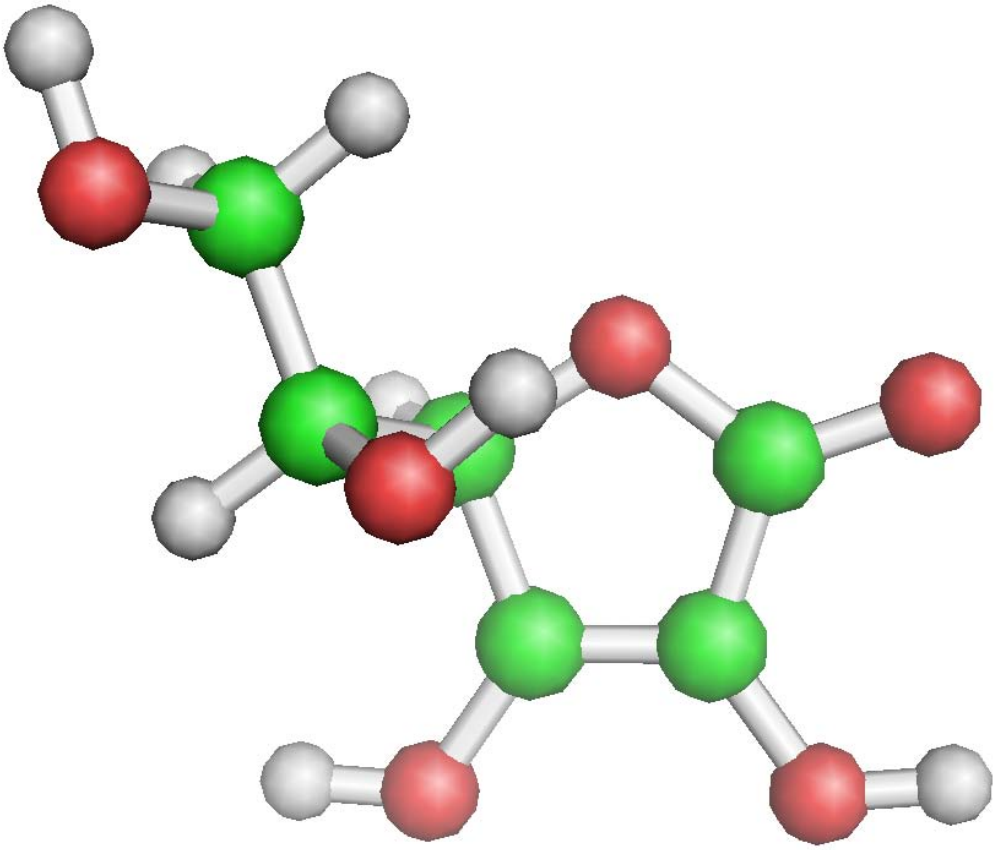

Figure 6. 1. Chemical structure of L-ascorbic acid or vitamin-C (Vit-C)

6.2 Materials and methods

Substrates employed in functionalization were all neat Ti plates with dimensions of 10 mm x 10 mm x 2 mm. They were acquired from Fisher Scientific (99.99%, Thermo-Fisher Scientific, Waltham, MA, USA). Roughened using silicon carbide (SiC) grinding paper. The plates were then consecutively bathed with acetone, absolute ethanol, and deionized (DI) water in an ultrasonic bath for 15 min each. Once the Ti surfaces were cleaned, they were dried in a desiccator overnight before modification and

functionalization. Etching was carried out for 2 min. A mixture of 30 mL nitric acid (HNO_3, 40 wt.%) and 70 mL DI water was prepared. A 30% mass solution H_2O_2 was used to oxidize the etched Ti surfaces. They were immersed and soaked for 24 h.

Functionalization of oxidized Ti surfaces implied incubated them in 10.0 mM Vit-C solution at room temperature. The complete incubation process lasted 6 days, eliminating any interferences after the 3rd day of incubation, by rinsing with water and ethanol. After that, functionalized Vit-C-TiO_2/Ti surfaces were left to dry overnight.

The *in vitro* bioactivity of Vit-C-TiO_2/Ti to develop an HA layer onto it was carried out using a Simulated Body Fluid (SBF) which was prepared according to the methodology described by Kokubo and coworkers. [15] Vit-C-TiO_2/Ti samples were immersed and soaked in SBF for 28 days monitoring the precipitation of HA from SBF.

Samples were studied by micro RS. The reference samples were the two room temperature stable crystalline phases of TiO_2 (anatase and rutile). Spectroscopic analysis of these phases has been described previously. [16] Confocal micro RS spectra were acquired by employing an InVia Raman microspectrometer (Renishaw, LLC, West Dundee, IL, USA). The spectrometer was interfaced to a Leica DM2500 microscope, and a Leica 50x objective was used to focus the laser beam onto the sample surface for collecting the scattered light. Ten (10) accumulations were averaged with an exposure time of 10 s each. A 532 nm diode pumped laser (Cobolt AB, Solna, Sweden) was used as the excitation source. The spectrometer was calibrated before each set of measurements using the 520.65 cm-1 Raman shift peak of silicon (110). Characteristic RS signatures were marked, and a baseline correction was applied to all

spectra. The laser power at the samples was controlled to avoid sample degradation upon laser irradiation.

6.3 Results and discussion

6.3.1 Raman spectroscopic features of Vit-C

RS spectrum of Vit-C is shown in Figure 6.2. Band assignments are listed in Table 6.1. The three weak bands in the 3300-3600 cm^{-1} correspond to stretching modes of O-H bond in the hydroxyl group. [17] The different C-H stretching modes yield four bands located at 2863, 2916, 2978 and 3002 cm^{-1} each one.

The very intense doublet at 1653 and 1666 cm^{-1} indicates the stretching vibration of C=C in the Vit-C molecule. Likewise, the weak band at 1749 cm^{-1} is related to the stretching mode of the C=O group. [17-19] The band observed in the 1500-1200 cm^{-1} region is corresponding to scissors, twisting and wagging of CH_2 group, especially bands at 1497 and 1320 cm^{-1} (scissors vibration mode), and the C-H deformation modes. The C-O-C stretching mode can be correlated to the band at 1128 cm^{-1}, which gives information about ring deformation. It can be corroborated with a weak peak at 1064 cm^{-1}.

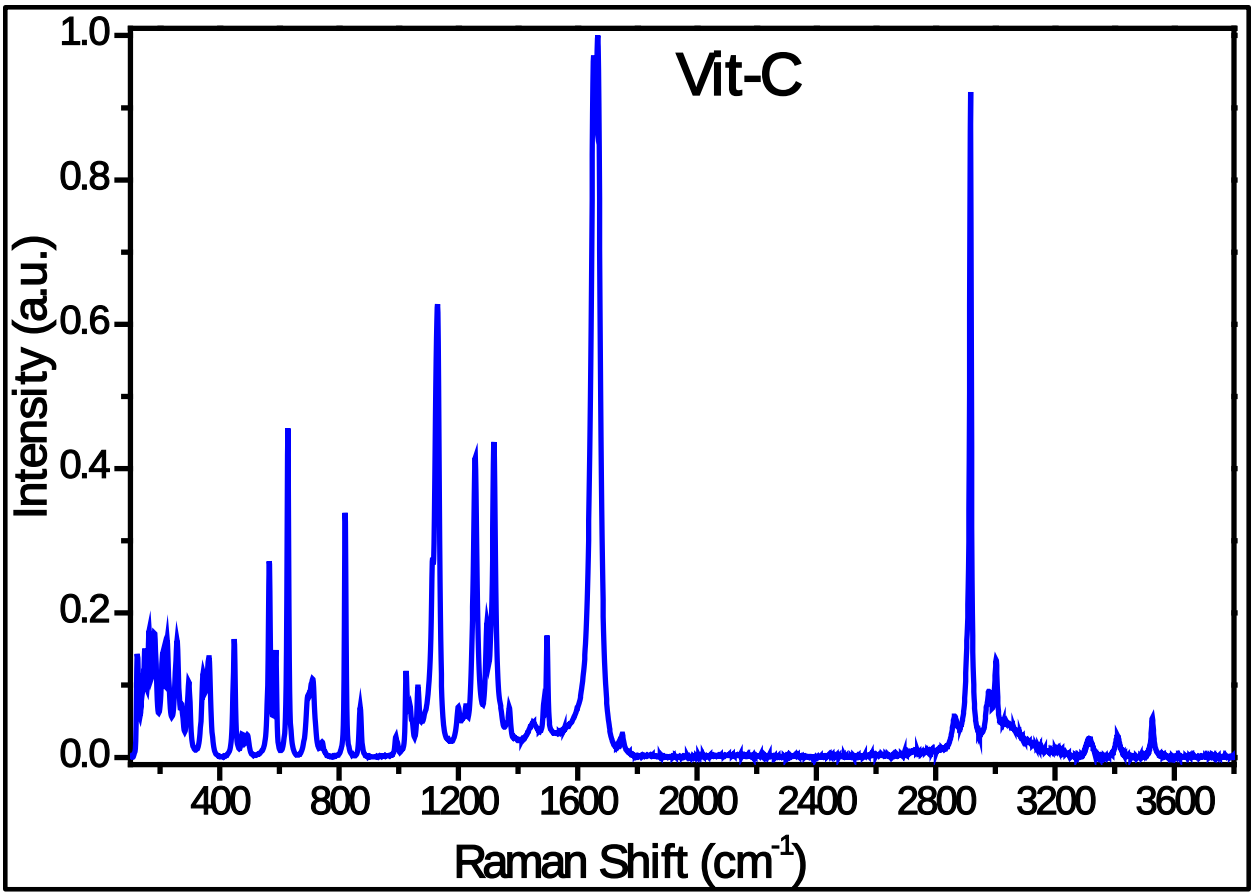

Figure 6. 2. RS spectrum of Vit-C.

Table 6. 1. Raman frequencies of Vit-C

Raman Shift (cm^{-1})	Proposed Assignment
3300-3600	stretching modes of O-H bond in the hydroxyl
2863, 2916, 2978, 3002	C-H stretching modes
1653, 1666	stretching vibration of C=C
1749 (w)	stretching mode of C=O group
1500-1200	scissors, twisting and wagging of CH_2 group
1450 (vw)	-C-OH in-plane bending
1256 (m)	C-O-H bending vibrational mode
1128, 1064	C-O-C stretching mode
1198, 989	CH_2 torsional and rocking vibration modes
1295, 1225	CH deformation bond
1112	stretch of C-O-C bond
1064 (w)	C-O-C stretching and C-OH bending modes
1024 (w)	ring O-H bend
870 (ms)	C-C ring stretching mode
587, 694, 820	planar ring deformation
870 (ws)	C-C ring stretching mode
448 (w)	O-H wagging
362 and 344	-OH wagging mode
257 (w)	-C-C-OH in-plane bending
222	C-OH bonding mode

A very weak band at 1571 cm^{-1} corresponds to CH_2 wagging mode. [17-19] In the same way, bands at 1198 and 989 cm^{-1} are related to CH_2 torsional and rocking vibration modes, respectively. The wavenumbers at 1295 and 1225 cm^{-1} have been assigned to CH deformation bond. Regarding lactone ring, it can be observed seven bands as a follows: one shoulder at 1112 cm^{-1} corresponding to stretch of C-O-C bond. [17,18] a weak band at 1024 cm^{-1} related to ring O-H bend, another medium sharp peak at 870 cm^{-1} corresponds to C-C ring stretching mode, three weak bands at 587, 694 and 820 cm^{-1} related to planar ring deformation, and a weak sharp band at 870 cm^{-1} assigned to C-C ring stretching mode. [17,18] As regards to four –OH groups the RS spectrum of Vit-C presents four weak bands located in the 3200-3600 cm^{-1} as mentioned above. Besides, the following peaks can be observed: a very weak band at 1450 cm^{-1} associated to -C-OH in-plane bending, a medium peak at 1256 cm^{-1} corresponding to C-O-H bending vibrational mode, another weak band at 1064 associated to C-O-C stretching mode and C-OH bending modes, one weak peak located at 448 cm^{-1} corresponds to O-H wagging, one weak band at 257 cm^{-1} related to -C-C-OH in-plane bending, and two weak bands at 362 and 344 cm^{-1} related both to -OH wagging mode. The band at 222 cm^{-1} corresponds to C-OH bonding mode. Bands located under 222 cm^{-1} are related to the crystal lattice. [17-19]

6.3.2 Functionalization of TiO_2/Ti surface with Vit-C

Figure 6.3a shows the RS spectrum of Vit-C and Figure 6.3b shows the RS spectrum of Vit-C-TiO_2/Ti in the 200-3600 cm^{-1} region. Figure 6.4a shows the RS spectrum of Vit-C

and Figure 6.4b shows the RS spectrum of Vit-C-TiO_2/Ti at 2700-3600 cm^{-1} region. As can be seen after functionalizing of the modified surface, two broad bands appear as a follows: a weak broad band is located from 3250-3450 cm^{-1} corresponding to the four weak peaks observed. However, the bands are overlapping among them indicating the possibility of formation of complexes between hydroxyl groups of Vit-C and the hydrated TiO_2 of modified Ti surface. The band centered at 2916 cm^{-1} remained unshifted but broader possibly due interactions between -C-O of the ring lactone with TiO_2/Ti surface. This can be attributed to the fact that the bond order reduced the decrease in the electronic density about the C=C and C=O bonds by delocalization.

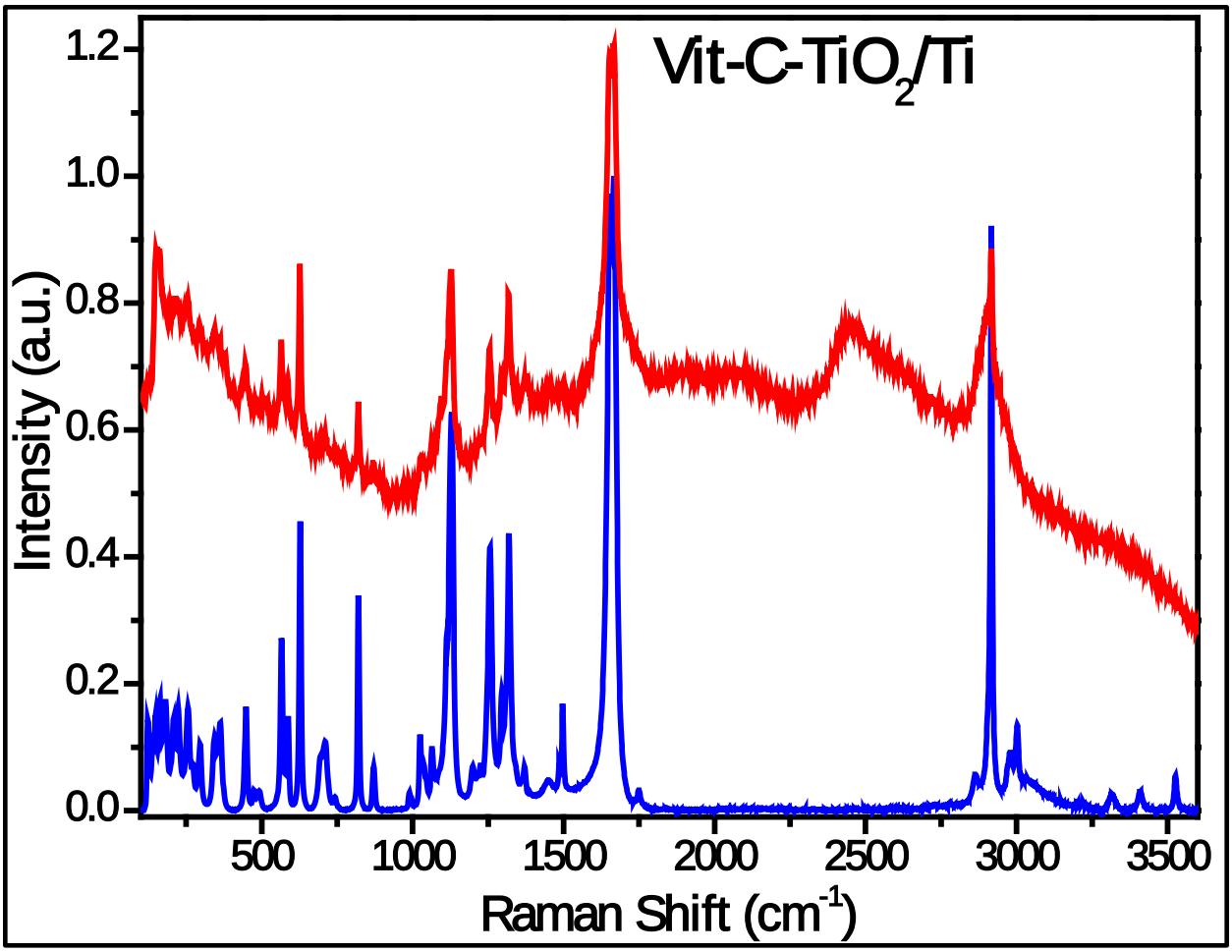

Figure 6. 3. Raman spectra of RS spectrum of a) Vit-C and b) Vit-C-TiO_2/Ti.

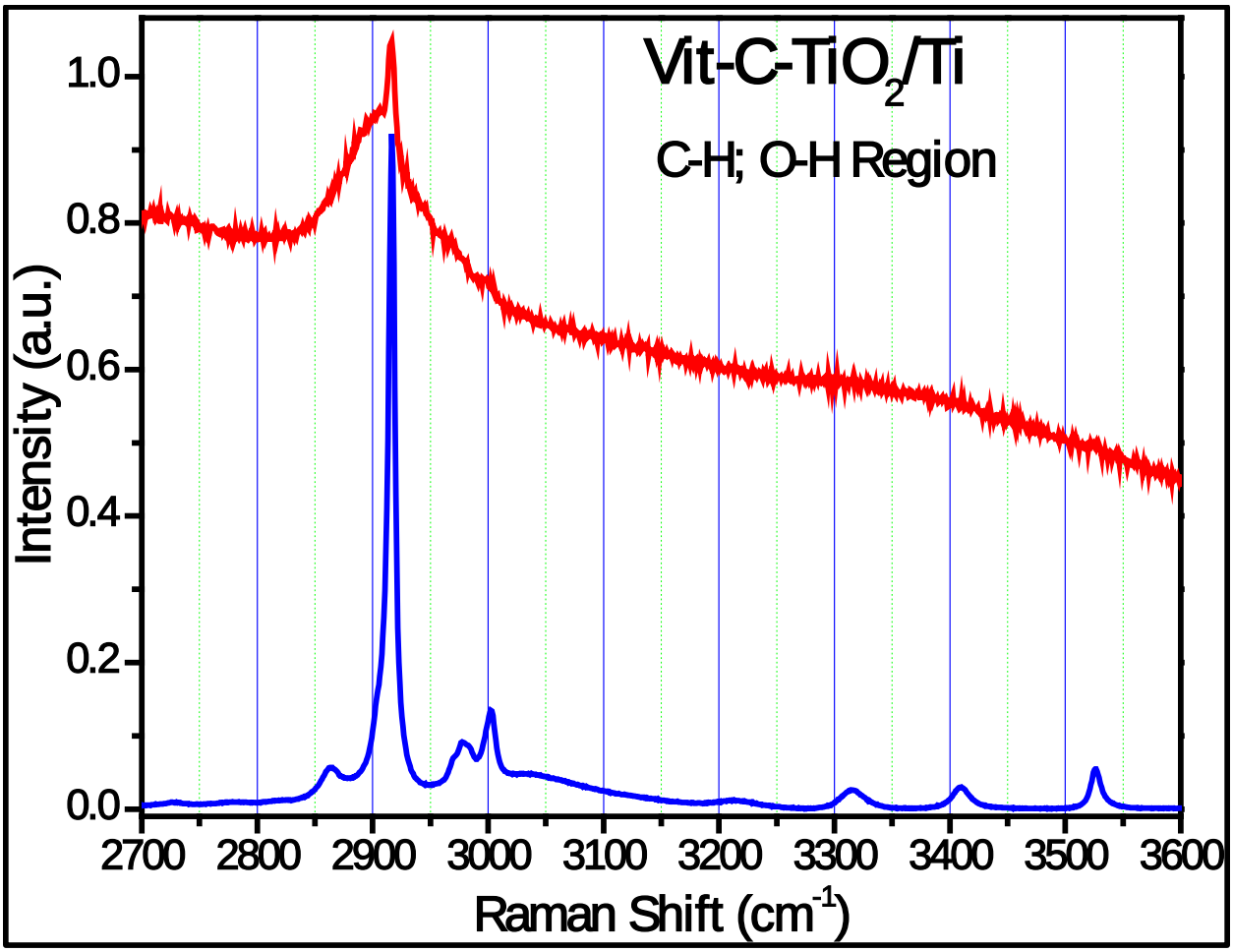

Figure 6. 4. Region of 2700-3600 cm^{-1} of the RS spectrum of a) Vit-C and b) Vit-C-TiO_2/Ti.

This can be corroborated by analyzing Figure 6.5b where it can be appreciated that weak band corresponding to stretching vibration of C=O group at 1749 cm^{-1} is now practically overlapped by the stronger band of C=C of the ring lactone upon adsorption on the substrate. Furthermore, the intensity and location of the bands at 1653 and 1666 cm^{-1} are the same. However, a broadening of the base of the doublet overlapping other bands can be observed, which is consistent above discussion. A new band in the form of a shoulder is located at 1554 cm^{-1}. This band corresponds to the partial double bond between C-C, which is not unsaturated and supports the proposed delocalized electron cloud in the 2,3-enediole bond of the furan ring of Vit-C. [20] The broadening, decreasing of intensities and shifting to lower frequencies for bands at 1497 and 1450 cm^{-1} indicate the important role played by the *ortho*-substituted hydroxyl groups of furan ring of Vit-C in the bond formation to Ti in TiO_2 of the modified surface. [21-23] The bands associated to CH_2 wagging, CH deformation, CH_2 torsion, ring vibrations modes and C-C ring stretching are found at lower wavenumber concerning their location in the parent molecule (Vit-C), supporting the idea of formation of a complex between Vit-C and Ti species of TiO_2. Moreover, the intensity of the band at 819 cm^{-1} associated with C-C ring stretching is lessened when compared with the corresponding band of the RS spectrum of Vit-C. Overlapping and broadening of bands in the following regions: 400-680 cm^{-1}, 950-1080 $cm^{-1,}$ and 1230-1400 cm^{-1} was also observed.

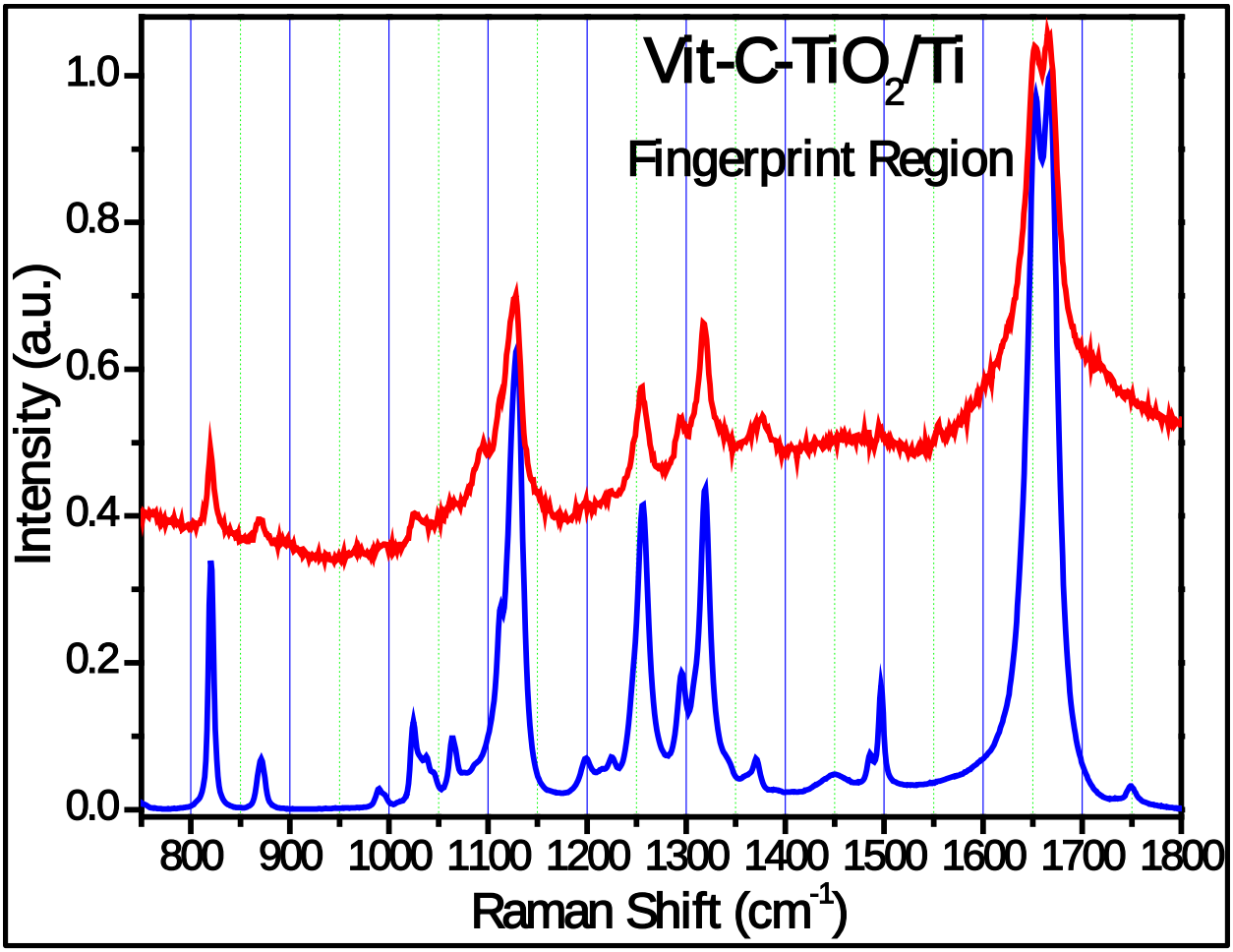

Figure 6.5. Region of 750-1800 cm^{-1} of the RS spectrum of a) Vit-C and b) Vit-C-TiO_2/Ti.

Regarding the bands associated with -C-OH, it can be noted that some decrease in intensities and the majority were shifted to lower frequencies. The disappearance of the band at 1112 cm^{-1} associated with stretching of C-O-C bond is noticeable. Similarly, four new bands are found in the RS spectrum of Vit-C-TiO_2/Ti. They are as follows: a shoulder at 1095 cm^{-1} that is associated to C-O-Ti, a very weak band at 893 cm^{-1}, associated to symmetric C-O-C stretching, a weak band at 377 cm^{-1} related to torsion of C-OH group [20, 24], and another weak band at 518 cm^{-1} associated to -OH wagging [24] in the complex formed between Vit-C and TiO_2 using the -OH groups in 2 and 3 position of enediol bond. Figure 6.6a and 6.6b shows the RS spectra of Vit-C and Vit-C-TiO_2/Ti, corresponding to low frequencies in the 150-750 cm^{-1} region. Table 6.2 shows the above Raman assignments.

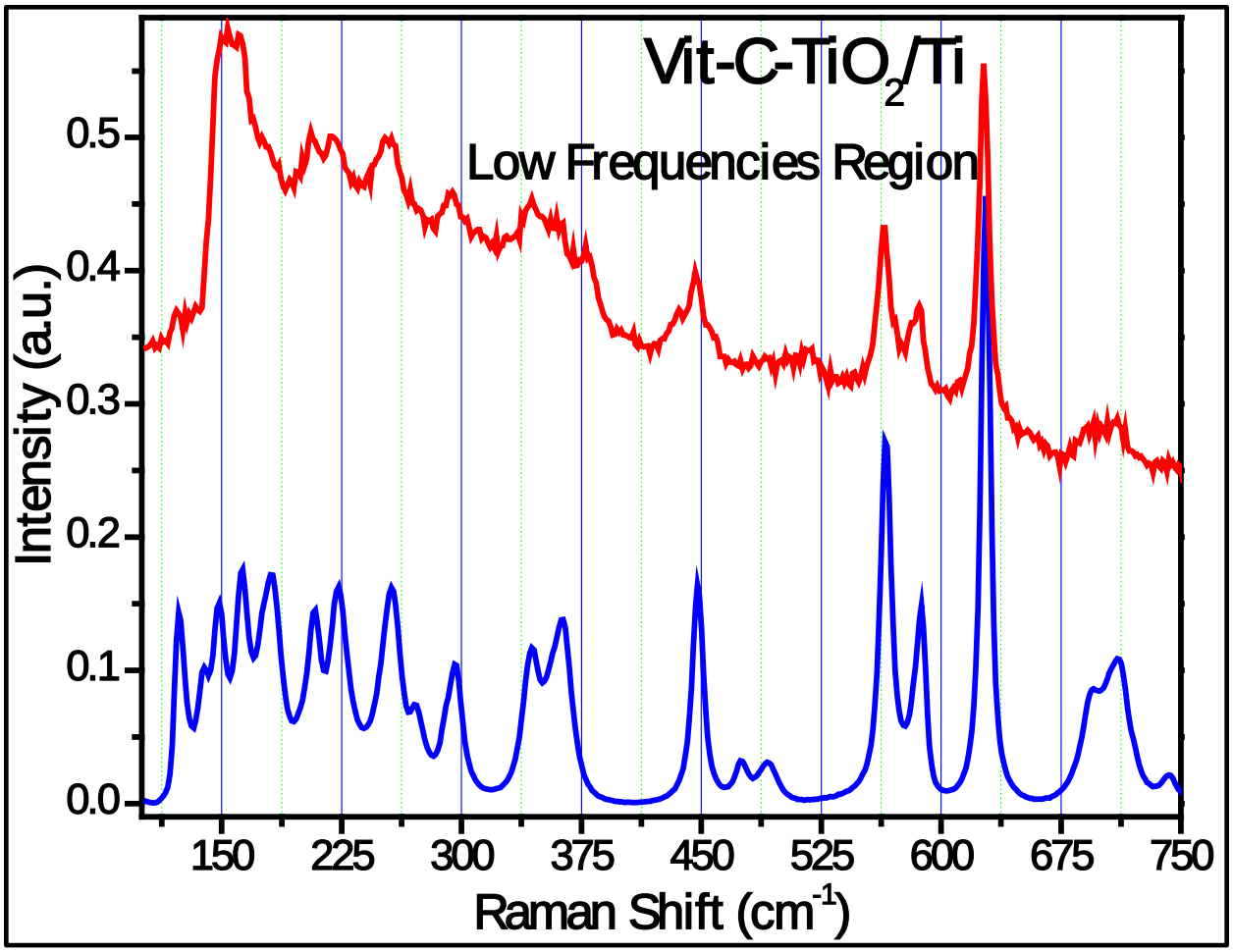

Figure 6. 6. Region of 150-750 cm^{-1} of the RS spectrum of a) Vit-C and b) Vit-C-TiO_2/Ti.

Table 6. 2. Raman frequencies of Vit-C-TiO_2/Ti

Raman Shift (cm^{-1})	Proposed Assignment
1095 (s)	Stretch of C-O-Ti bond
893 (vw)	Symmetric C-O-C stretching
518 (w)	Wagging of-OH group
377 (w)	Torsion of C-OH group

(vs)=very strong, (s)=strong, (m)=medium, (w)=weak, (vw)= very weak, (ms)=medium sharp

The formation of the complex between the organic ligand and the substrate was demonstrated by comparing the RS spectra of Vit-C (Figure 6.2) and Vit-C-TiO_2/Ti (Figures 6.3 to 6.6). Based on the spectroscopic data the decrease of intensities and the shape of -OH groups belonging to 2,3-enediol have drastically decreased in such manner that it is difficult to distinguish their location in the 3250-3450 cm^{-1} region. The above suggests that the mentioned -OH groups are not pure now, but they are complexed with Ti species of TiO_2. [22-26] Similarly, the overlapping, broadening and shifting to lower frequencies (specifically at 447, 564, 626, 819, 869, 1063, 1125, 1196, 1255, 1316, 1369 and 1496 cm^{-1}) for the majority of band confirm the hypothesis of bidentate complex formation. [23] To infer the structure and bonding of adsorption of Vit-C on the substrate, it has into account the appearance of four new bands in definite positions (at 1095, 893, 518 and 377 cm^{-1}) evidencing the formation of new C-O-Ti bond. [22,27] Based on the above evidence a bidentate binding of Vit-C by using the two oxygen atoms belonging to 2,3-enediol can be suggested. In the five-membered

ring or chelate (Figure 6.7), the anionic oxygen is the electron donor. It has the angle configuration more favorable for the Ti atoms on the surface, with little distortion of angles and interatomic distances. Besides, this geometry stabilizes ring structure due to delocalization of the electron cloud in the 2,3-enediole bond, using the oxygen atom of C=O group and those bonding the Ti atom, and the C atoms in positions 1, 2 and 3 in the lactone ring. [23,28]

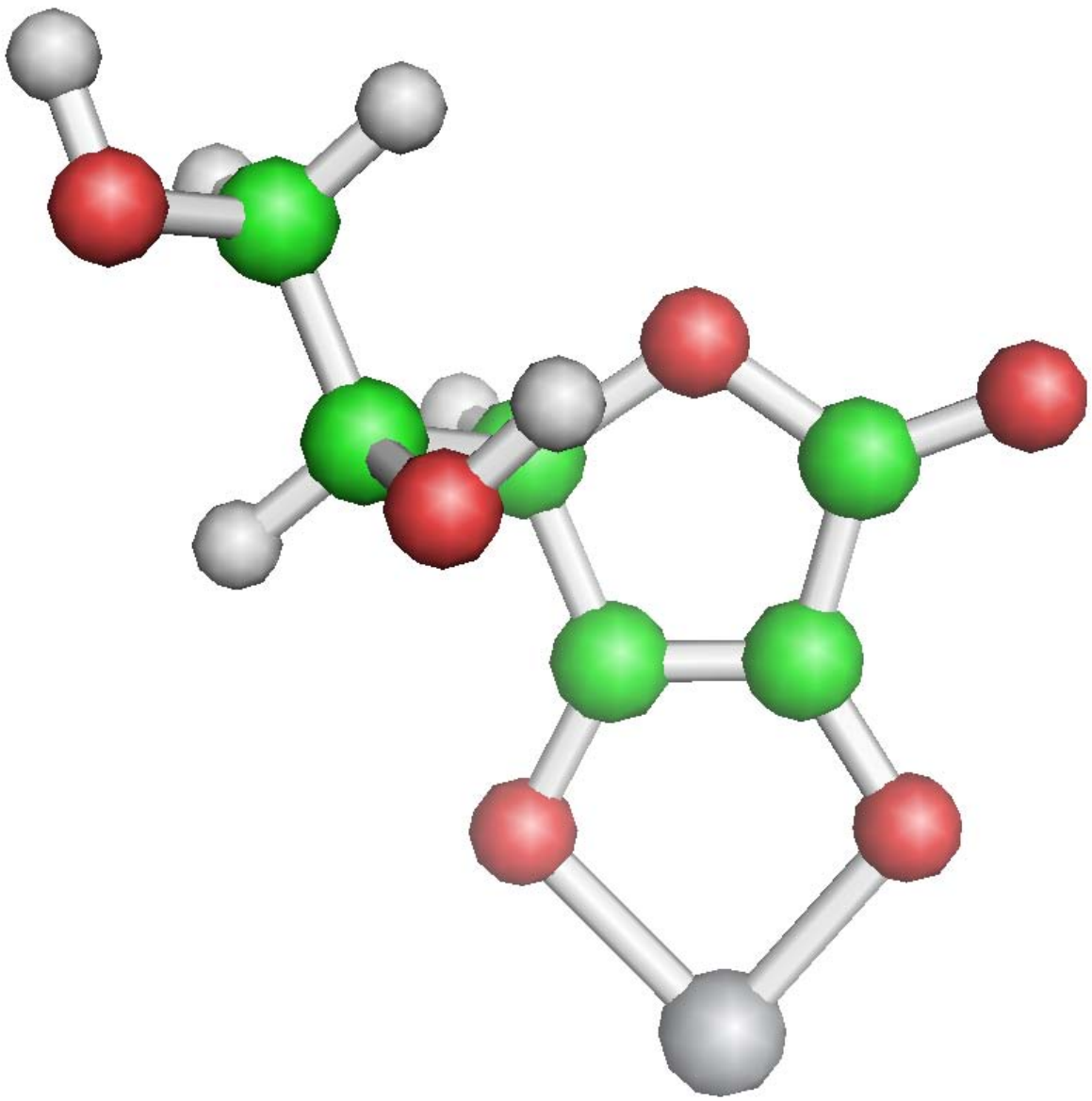

Figure 6.7. Proposed orientation of Vit-C on the functionalized TiO_2/Ti surface.

6.3.3 Bioactivity *"in vitro"* of Vit-C-TiO_2/Ti surface

Raman vibrational bands from HA layer developed on the Vit-C-TiO_2/Ti surface are shown in Figure 6.8c. Figures 6.8a and 6.8b correspond to RS spectra of Vit-C and HA, respectively. The characteristic peak of HA with the highest intensity can be appreciated in 961 cm^{-1}, which corresponds to the symmetric stretching vibrational mode of P-O bond in the PO_4^{3-} ion. This band practically dominates the spectrum of HA.

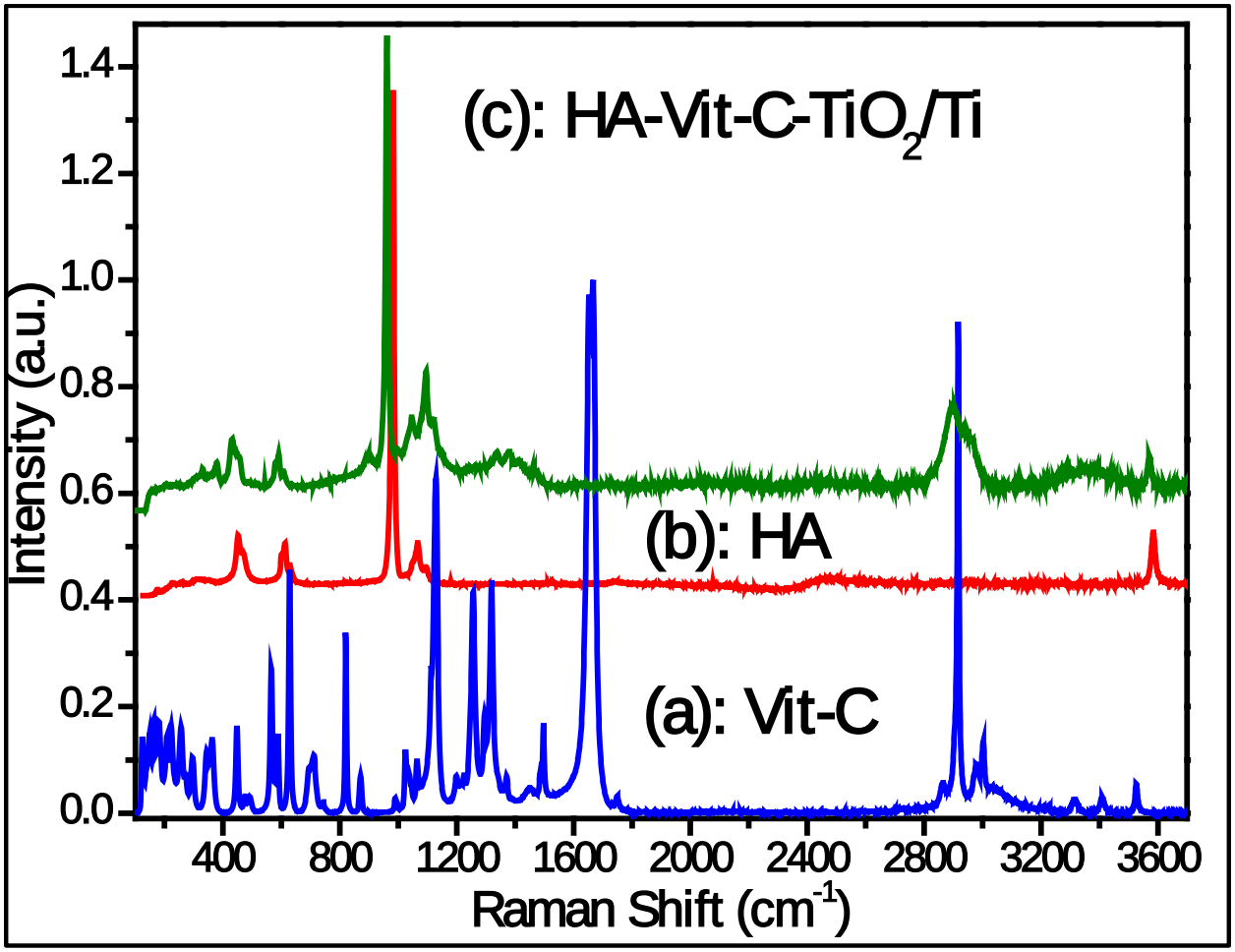

Figure 6. 8. RS spectrum of a) Vit-C, b) HA, and c) HA layer formed on Vit-C-TiO_2/Ti surface.

The other weak bands belonging to HA which normally appear in 415, 599 and 619 cm^{-1} are not observed in this case, due to possibly to the overlapping of bands that occurs in the 400-490 and 550-610 cm^{-1} regions (Figure 6.9c).

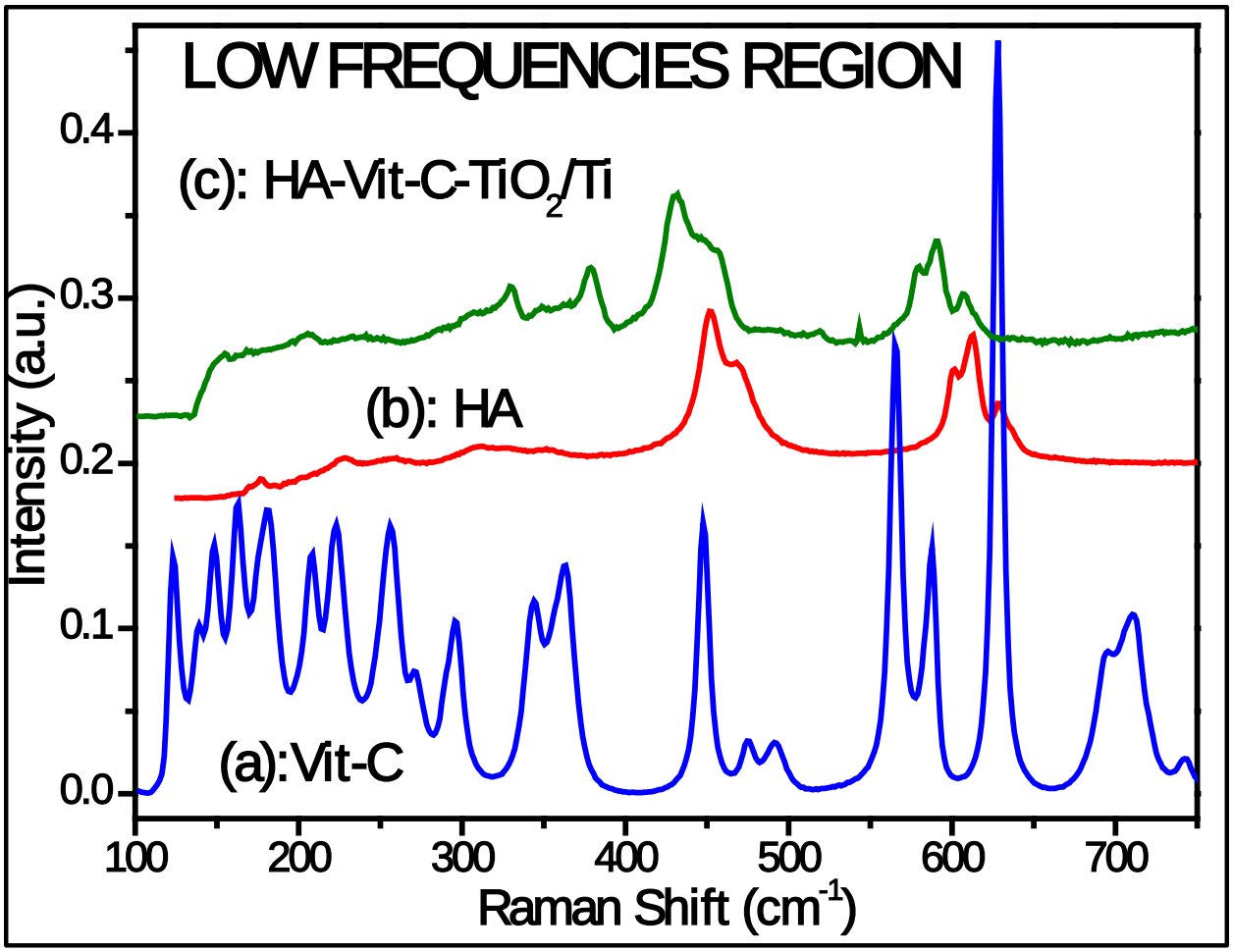

Figure 6. 9. RS spectrum. a) Vit-C, b) HA and c) HA layer formed on Vit-C-TiO_2/Ti surface in the low frequency region.

This indicates intermolecular interactions between HA and Vit-C of the derivatized surface, probably due to the formation of hydrogen bonds between the oxygen of phosphate group of HA and the –OH group of Vit-C. The same situation is expected in the case of $^{-}$OH of HA with the oxygen of Vit-C. Therefore, propitiating the broadening of bands in the above regions. Additionally, the sharp medium intensity band at 3570 cm^{-1} corroborates the bond stretching mode associated to –OH of HA. Likewise, the decreasing of a signal at 626 cm^{-1} corresponding to C=O group suggests that it could be exist a C-OH bond.

The sharpness and intensity of the above peaks suggest that phosphate groups are ordered structurally. [29-34] Another interesting feature of RS spectrum of HA on Vit-C-TiO_2/Ti has to do with a broad band in the 3200-3500 cm^{-1} region (Figure 6.10), indicating the interaction between oxygen atoms of 2,3-enediole bond with Ti ion of TiO_2 of modified surface yielding a coordination complex.

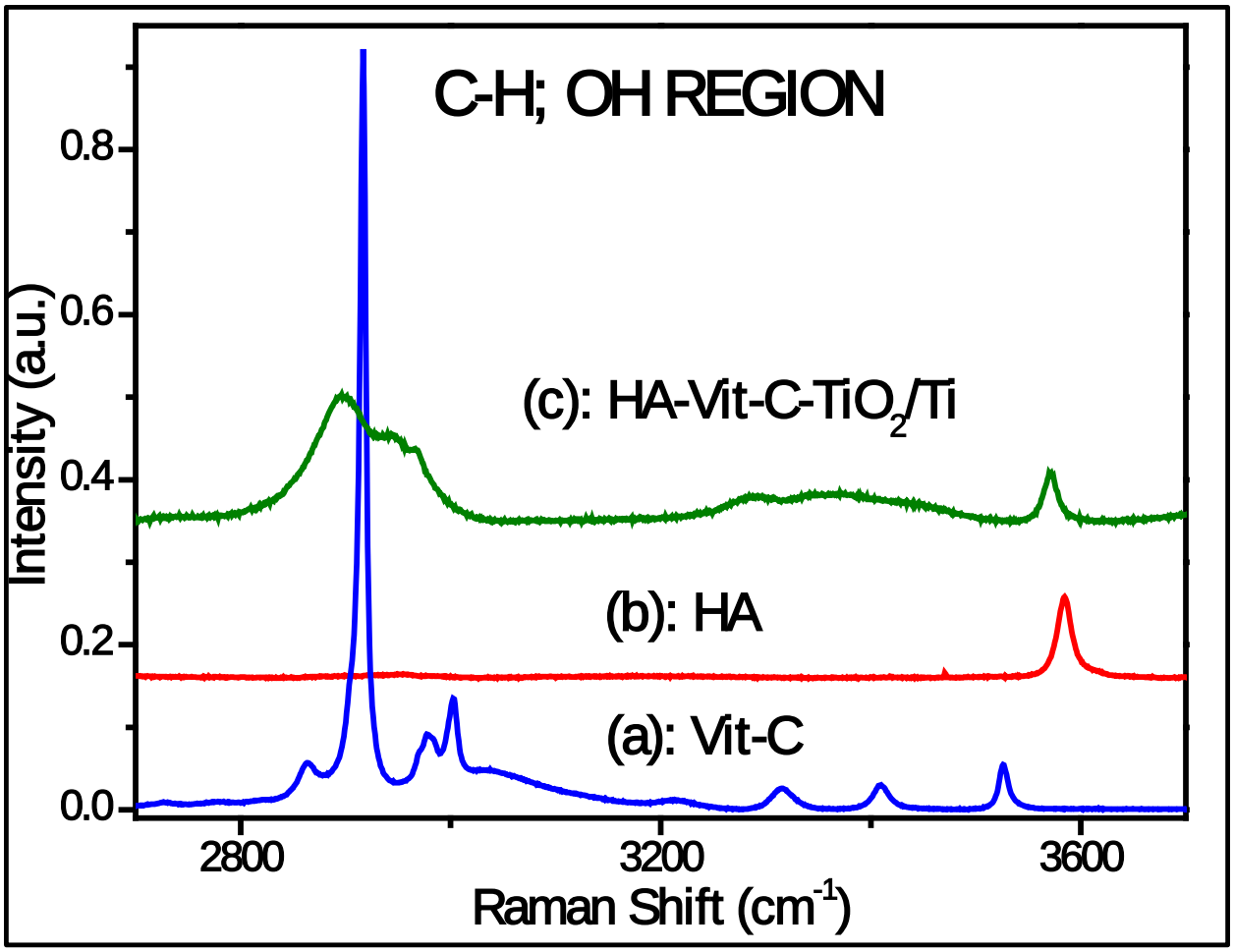

Figure 6. 10. RS spectrum of a) Vit-C, b) HA and c) HA layer formed on Vit-C-TiO_2/Ti surface

Furthermore, the absence of doublet in 1652 and 1666 cm^{-1} suggests that there is no C=C bond. Therefore, there is no delocalized electron density, but the single bond between C-2 and C-3 with oxygen atoms of TiO_2. This is supported by the existence of a band at 1094 cm^{-1} associated with C-O-Ti bond (Figure 6.11). [17-19] Another absent band is the corresponding to 1749 cm^{-1} related to C=O bond, [17,18] indicating a new hydrogen bond between the oxygen of AA and $^{-}$OH of HA as mentioned above. [17-19]

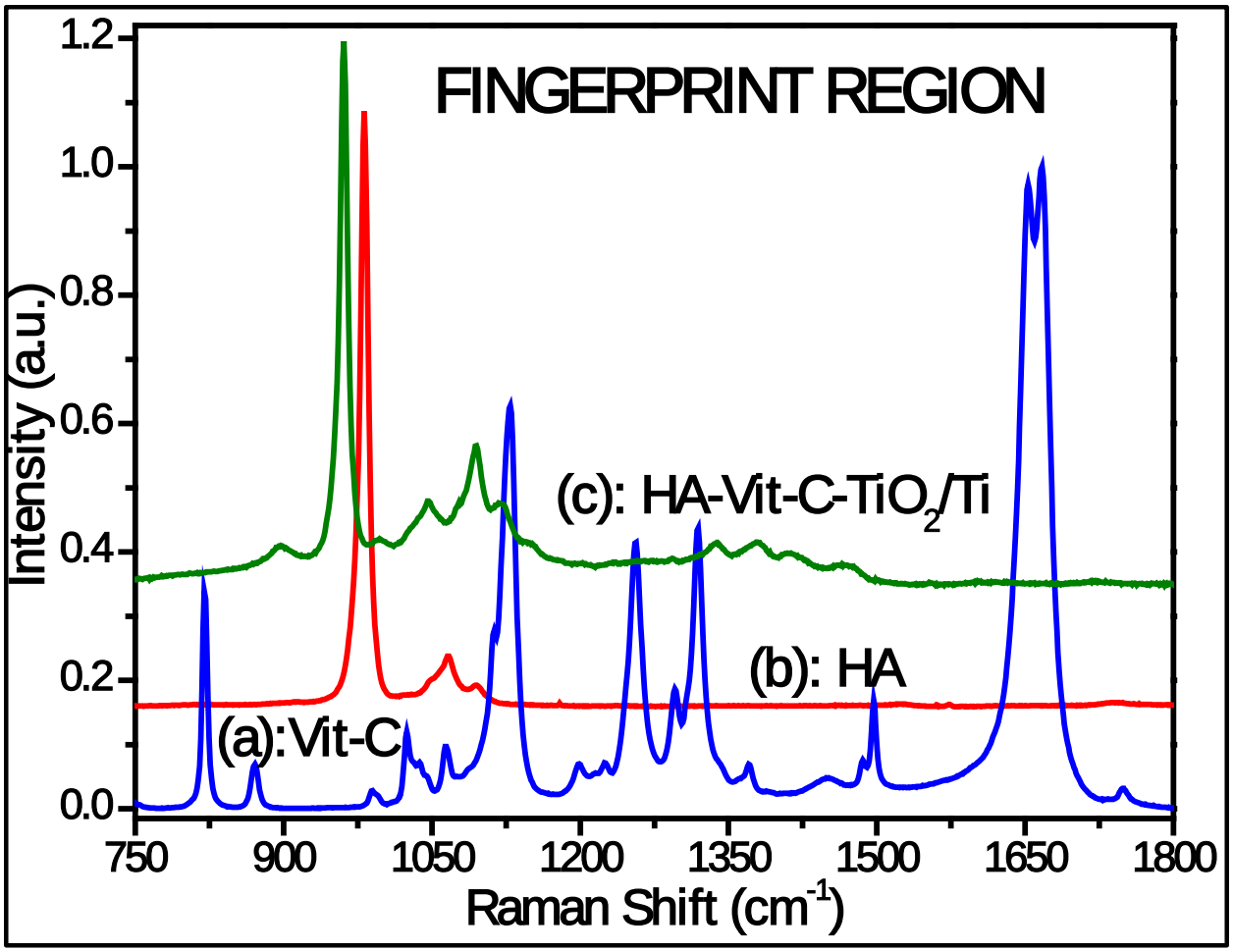

Figure 6. 11. RS spectrum of a) Vit-C, b) HA and c) HA layer formed on Vit-C-TiO_2/Ti surface.

This is confirmed by the absence of the band at 626 cm^{-1} associated with C=O in-plane deformation. [20] The ring structure is confirmed by analyzing the presence of weak bands at 378, 578, 591, 894 and 999 cm^{-1}. [17,18,20] Besides, the C-O-C bond inside the ring is evidenced analyzing the weak bands at 1094 and 1123 cm^{-1} [17,18,20] The weak bands are associated to -C-OH in-plane deformation (at 430 and 448 cm^{-1}), C-OH bending modes (at 1046 cm^{-1}), and -C-OH in-plane bond (at 1478 cm^{-1}). [17-19]

The CH bond and CH_2 group can be associated to a strong band centered at 2892 cm^{-1} (C-H stretching mode), and to the very weak bands at 1336, 1381 and 1413 cm^{-1} related to scissors vibration mode for CH_2 group, wagging CH deformation and CH in-plane rocking, respectively. [20]

The absence of the prominent bands at 1652 and 1666 cm^{-1} enables to clarify the disappearance of C=C bond, as well as the lack of a band at 1749 cm^{-1} related to C=O group. On the other hand, it has been corroborated the ring structure and the C-O-C bond through their correspond bands at 1094 and 894 cm^{-1}, respectively. Equally, the new hydrogen bonds have been elucidated analyzing the bands related to it (mainly at 1046 and 448 cm^{-1}). One possible interpretation to the above has to do with the adsorption of HA onto functionalized Ti surface is done through Vit-C using hydrogen bond between -C-OH group of Vit-C and the oxygen atoms of the PO_4^{3-} group, the -C-O group of Vit-C, and the hydrogen of $^{-}$OH of HA, with the Vit-C molecule anchored to TiO_2/Ti surface through -C-O-Ti bonds of 2,3-enediole. Lastly, based on the expressed above, and on the results of the micro RS studies it can be suggested the chemical structure depicted in the Figure 6.12, where it can be seen in more detail the above intermolecular interactions.

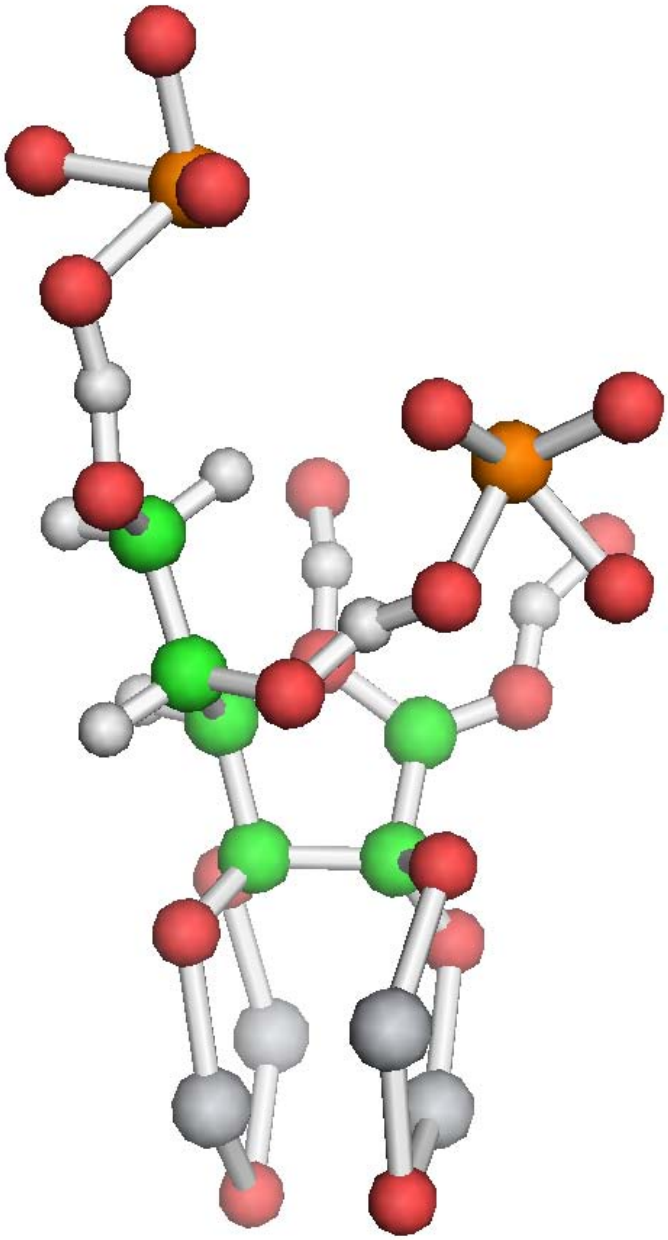

Figure 6. 12. Proposed chemical structure of HA-Vit-C-TiO_2/Ti

Acknowledgments

The authors express sincere appreciation to the faculty members and supporting personnel of the Departments of Bioengineering and Chemistry of the Mayagüez Campus of the University of Puerto Rico for their collaboration during all project stages.

Conflict of Interest

The authors report there are no conflicts of interest.

6.4 Conclusions

A TiO_2/Ti layer was developed on previously unmodified neat Ti plates. Vit-C was chemically adsorbed on this surface. RS spectroscopy was employed to obtain information regarding chemical bonds formed between adsorbate and substrate as well as the intermolecular interactions. The vibrational information: wavenumber locations, intensities, and band profiles for the organic ligand adsorbate were analyzed. An a very intense doublet at 1653 and 1666 cm^{-1}, corresponding to C=C bond.

Complexation of Vit-C with TiO_2/Ti surface was evidenced by decreasing in Raman intensities and shape of -OH groups of 2,3-enediol. Besides, the overlapping, broadening, and shifting to lower frequencies for the majority of the bands appear to be characteristic of the changes in the ring structure found in Vit-C when interacting with TiO_2/Ti surface directly to form a bidentate complex. Also, the appearance of four new bands supports the statement about the formation of the new C-O-Ti bond, where the two oxygen atoms of 2,3-enediol are the electron donors to form a bidentate binding

with Ti belonging to TiO_2/Ti surface. The new ring is stabilized because of delocalization of electron cloud in the 2,3-enediol bond facilitated by the oxygen atom of the C=O group.

HA layer developed on the Vit-C-TiO_2/Ti surface exhibited Raman vibrational bands confirming the adsorption and intermolecular interactions of HA the surface. The strong doublet at 1749 cm^{-1} is absent suggesting a hydrogen bond between -C-OH group of Vit-C and the oxygen atoms of PO_4^{3-} group, the -C-O group of Vit-C, and the hydrogen of $^{-}$OH of HA. Furthermore, Raman bands located at 1094 and 894 cm^{-1} corroborated the ring structure and the C-O-C bond.

6.5 References

[1] B. M. Tolbert, M. Downing, R. W. Carlson, M. K. Knight, and E. M. Baker, “Chemistry and Metabolism of Ascorbic Acid and Ascorbate Sulfate,” *Ann. N. Y. Acad. Sci.*, **258**(1): 48–69, 1975.

[2] P. Neta, R. E. Huie, S. Mosseri, L. V. Shastri, J. P. Mittal, P. Maruthamuthu and S. Steenken, “Rate constants for reduction of substituted methylperoxyl radicals by ascorbate ions and N,N,N’, N’-tetramethyl-p-phenylenediamine,” *J. Phys. Chem.*, **93**(10): 4099–4104, 1989.

[3] S. Zapata and J. P. Dufour, “Ascorbic, Dehydroascorbic and Isoascorbic Acid Simultaneous Determinations by Reverse Phase Ion Interaction HPLC,” *J. Food Sci.*, **57**(2): 506–511, 1992.

[4] R. N. Allen, M. K. Shukla, D. Reed, and J. Leszczynski, “Ab initio study of the structural properties of ascorbic acid (vitamin C),” *Int. J. Quantum Chem.*, **106**(14): 2934–2943, 2006.

[5] R. Amorati, G. F. Pedulli, and L. Valgimigli, “Kinetic and thermodynamic aspects of the chain-breaking antioxidant activity of ascorbic acid derivatives in non-aqueous media,” *Org. Biomol. Chem.*, **9**(10): 3792–3800, 2011.

[6] A. K. Schlueter and C. S. Johnston, “Vitamin C: Overview and Update,” *J. Evid. Based. Complementary Altern. Med.*, **16**(1): 49–57, 2011.

[7] B. N. Ames, M. K. Shigenaga, and T. M. Hagen, “Oxidants, antioxidants, and the degenerative diseases of aging,” *Proc. Natl. Acad. Sci.*, **90**(17): 7915-7922, 1993.

[8] D. E. Henson, G. Block, and M. Levine, “Ascorbic Acid: Biologic Functions and Relation to Cancer,” *JNCI J. Natl. Cancer Inst.*, **83**(8): 547–550, 1991.

[9] Y. Ogata and Y. Kosugi, “Spectrophotometric Determination of L-Ascorbic Acid,” *Bull. Chem. Soc. Jpn.*, **42**(8): 2282–2286, 1969.

[10] S. J. Padayatty, A. Katz, Y. Wang, P. Eck, O. Kwon, J. H. Lee, S. Chen, C. Corpe, A. Dutta, S. K. Dutta, and M. Levine, “Vitamin C as an Antioxidant: Evaluation of Its Role in Disease Prevention,” *J. Am. Coll. Nutr.*, **22**(1): 18–35, 2003.

[11] O. Arrigoni and M. C. De Tullio, “Ascorbic acid: much more than just an antioxidant,” *Biochim. Biophys. Acta - Gen. Subj.*, **1569**(1-3): 1–9, 2002.

[12] J. M. Jamison, J. Gilloteaux, H. S. Taper, and J. L. Summers, “Evaluation of the In Vitro and In Vivo Antitumor Activities of Vitamin C and K-3 Combinations against Human Prostate Cancer,” *J. Nutr.*, **131**(1): 158S–160S, 2001.

[13] S. Park, S. S.Han, C. H. Park, E. R. Hanm, S. J. Lee, H. K. Park, S. H. Lee, W. S. Kim, C. W. Jung, K. Park, H. D. Riordan, B. F. Kimler, K. Kim, and J. J. Lee, “l-Ascorbic acid induces apoptosis in acute myeloid leukemia cells via hydrogen peroxide-mediated mechanisms,” *Int. J. Biochem. Cell Biol.*, **36**(11): 2180–2195, 2004.

[14] C. I. Rivas, J. C. Vera, V. H. Guaiquil, F. V. Velásquez, O. A. Bórquez-Ojeda, J .G. Cárcamo, I. I. Concha, and D. W. Golde, “Increased Uptake and Accumulation of Vitamin C in Human Immunodeficiency Virus 1-infected Hematopoietic Cell Lines,” *J. Biol. Chem.*, **272**(9): 5814–5820, 1997.

[15] T. Kokubo and H. Takadama, “How useful is SBF in predicting in vivo bone bioactivity?,” *Biomaterials*, **27**(15): 2907–2915, 2006.

[16] C. A. Manrique-Bastidas, P. Sundaram, P. R., N. Mina, and S. P. Hernandez-Rivera, “Functionalization of Titanium Surfaces with Lysine: a Micro Raman Study of TiO_2-Lysine Intermolecular Interactions”, Manuscript in progress, 2019.

[17] L. C. Bichara, H. E. Lanús, C. G. Nieto, and S. A. Brandán, “Density Functional Theory Calculations of the Molecular Force Field of l-Ascorbic Acid, Vitamin C,” *J. Phys. Chem. A*, **114**(14): 4997–5004, 2010.

[18] C. Yohannan Panicker, H. Tresa Varghese, and D. Philip, “FT-IR, FT-Raman and SERS spectra of Vitamin C,” *Spectrochim. Acta Part A Mol. Biomol. Spectrosc.*, **65**(3-4): 802–804, 2006.

[19] E. G. Ferrer and E. J. Baran, “Reduction of vanadium(V) with ascorbic acid and isolation of the generated oxovanadium(IV) species,” *Biol. Trace Elem. Res.*, **83**(2): 111-119, 2001.

[20] G. Socrates, “Infrared and Raman Characteristic Group Frequencies, Tables and Charts.” Third Ed., John Wiley & Sons, Ltd., 2001.

[21] T. Kamegawa, S. Matsuura, H. Seto, and H. Yamashita, “A Visible-Light-Harvesting Assembly with a Sulfocalixarene Linker between Dyes and a Pt-TiO_2 Photocatalyst,” *Angew. Chemie Int. Ed.*, **52**(3): 916–919, 2013.

[22] Y. Ou, J.-D. Lin, H.-M. Zou, and D.-W. Liao, “Effects of surface modification of TiO_2 with ascorbic acid on photocatalytic decolorization of an azo dye reactions and mechanisms,” *J. Mol. Catal. A Chem.*, **241**(1-2): 59–64, 2005.

[23] T. Rajh, J. M. Nedeljkovic, L. X. Chen, O. Poluektov, and M. C. Thurnauer, “Improving Optical and Charge Separation Properties of Nanocrystalline TiO_2 by Surface Modification with Vitamin C,” *J. Phys. Chem. B*, **103**(18): 3515–3519, 1999.

[24] P. J. Larking, “IR and Raman Spectroscopy Principles and Spectral Interpretation”, Elsevier Inc., 2011.

[25] E. H. Mert, Y. Yalcin, M. Kilic, N. San and Z. Cinar, “Surface Modification of TiO_2 with Ascorbic Acid for Heterogeneous Photocatalysis: Theory and Experiment,” *Journal of Advanced Oxidation Technologies*, **11**(2): 199-207, 2008.

[26] A. Umer, S. Naveed, N. Ramzan, M. S. Rafique, and M. Imran, “A green method for the synthesis of Copper Nanoparticles using L-ascorbic acid ,” *Matéria (Rio de Janeiro)*, **19**(3): 197–203, 2014.

[27] G. Lui, J.-Y. Liao, A. Duan, Z. Zhang, M. Fowler, and A. Yu, “Graphene-wrapped hierarchical TiO_2 nanoflower composites with enhanced photocatalytic performance,” *J. Mater. Chem. A*, **1**(39): 12255–12262, 2013.

[28] A. P. Xagas, M. C. Bernard, A. Hugot-Le Goff, N. Spyrellis, Z. Loizos, and P. Falaras, “Surface modification and photosensitisation of TiO2 nanocrystalline films with ascorbic acid,” *J. Photochem. Photobiol. A Chem.*, **132**(1-2): 115–120, 2000.

[29] B. Mihailova, B. Kolev, C. Balarew, E. Dyulgerova, and L. Konstantinov, “Vibration spectroscopy study of hydrolyzed precursors for sintering calcium phosphate bio-ceramics,” *J. Mater. Sci.*, **36**(17): 4291–4297, 2001.

[30] G. R. Sauer, W. B. Zunic, J. R. Durig, and R. E. Wuthier, “Fourier transform raman spectroscopy of synthetic and biological calcium phosphates,” *Calcif. Tissue Int.*, **54**(5): 414–420, 1994.

[31] H. Tsuda and J. Arends, “Raman Spectra of Human Dental Calculus,” *J. Dent. Res.*, **72**(12): 1609–1613, 1993.

[32] B. O. Fowler, M. Markovic, and W. E. Brown, “Octacalcium phosphate. 3. Infrared and Raman vibrational spectra,” *Chem. Mater.*, **5**(10): 1417–1423, 1993.

[33] G. Penel, N. Leroy, P. Van Landuyt, B. Flautre, P. Hardouin, J. Lemaitre, and G. Leroy, “Raman microspectrometry studies of brushite cement: in vivo evolution in a sheep model,” *Bone*, **25**(2), Supplement 1, p. 81S–84S, 1999.

[34] F. Barrere, C. A. van Blitterswijk, K. de Groot, and P. Layrolle, “Nucleation of biomimetic Ca–P coatings on Ti6Al4V from a SBF×5 solution: influence of magnesium,” *Biomaterials*, **23**(10): 2211–2220, 2002.

Chapter 7

Spectroscopic Investigation of Cholecalciferol (VITAMIN-D) Adsorbed on TiO_2/Ti Surfaces: Biocompatibility and Osseointegration of Titanium

Abstract

The modification, oxidation, and subsequent functionalization of Ti surfaces was carried out with cholecalciferol (Vit-D). The functionalized Ti surfaces were then coated with hydroxyapatite (HA) to investigate possible intermolecular interactions between the adsorbed chemical species and the substrate. Analysis of Raman scattering (RS) measurements allowed to characterize the chemical structure and spatial orientation of complexes formed between Vit-D and the TiO_2/Ti surfaces as well as potential binding between HA and the functionalized Ti surfaces. The emergence of a band at 1095 cm^{-1} was attributed to the formation of a C-O-Ti bond. On the other end, the disappearance of bands at 1261, 1073 and 479 cm^{-1} corresponding to the –OH group in the spectra of Vit-D-TiO_2/Ti indicated that probably the TiO_2 is interacting with the –OH group of Vit-D. Furthermore, the dominant band of Vit-D spectrum at 1647 cm^{-1} assigned to C=C stretching vibration mode band decreased significantly in intensity and shifted to lower wavenumber (1640 cm^{-1}), indicating a possible interaction of C=C with TiO_2/Ti surfaces, and therefore, yielding a new bond. Concerning the functionalized Ti surface coated

with HA, the bands at 961 and 3571 cm^{-1} indicate the formation of HA onto it. Besides, the mentioned bands were instrumental when elucidating the intermolecular interactions between HA and Vit-D of functionalized Ti surface, in such way that it is suggested that the formation of hydrogen bond between the –OH group of Vit-D and the oxygen atoms of the phosphate group of HA.

Keywords

Functionalization, cholecalciferol, titanium surfaces, hydroxyapatite, titanium coating, Raman spectroscopy, osseointegration

7.1 Introduction

Cholecalciferol or vitamin D_3 (Vit-D; Figure 7.1), is classified as fat a soluble steroid hormone, and it is an essential nutrient. This group of biochemical exist in diverse forms such as ergocalciferol (vitamin D_2) and Vit-D. It was discovered by McCollum in 1922. [1,2] Biosynthesis of Vit-D is carried out when the skin (containing cholesterol) is exposed to sunlight. The 7-dehydrocholesterol (7-DHC) is photoactivated by UV from sunlight to produce VIT-D. VIT-D is hydroxylated in the liver and kidney to form the active metabolite: 1,25-dihydroxycholecalciferol (1,25-$[OH]_2D_3$), called calcitriol. [3]

Vit-D plays a significant role in homeostasis of calcium, that is, in the absorption and use of calcium in the intestine and kidney. [4-6] Besides, it enhances the bone reabsorption and decreases calcium and phosphate excretion, increasing blood plasma concentration. Vit-D has been used in the prevention and treatment of osteoporosis. [7-13]

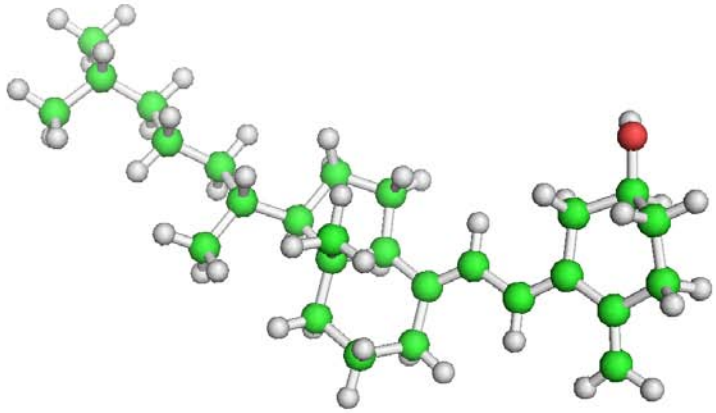

Figure 7. 1. Chemical structure of Vit-D.

At old age in humans, the biosynthesis rate of 7-DHC decreases. Therefore, its conversion to VIT-D is diminished, producing excessive bone resorption and a deficiency for new bone tissue formation. [14-16] All age groups belonging to different populations worldwide have a high prevalence of Vit-D deficiency, due to inadequate dietary intake, together with insufficient sunlight exposure. [17-20]

Thus, an investigation of the effects of Vit-D in the osseointegration process of titanium (Ti) implants is imperative. [21-23] Vit-D treatment can be a feasible approach focusing on functionalizing bioactive Ti surfaces to enhance osseointegration and fixation of implants in compromised patients. Ti is the most commonly used material to bone-implant, due to its excellent physical and biological properties (density, high mechanical strength, and excellent corrosion resistance). [21] Modification of Ti surfaces by using Vit-D can improve the quality and quantity of bone around Ti implant resulting in benefits such as: improving osseointegration, reducing treatment times and financial costs, and resulting in an improved lifetime quality.

The primary purpose of this research was to functionalize the oxidized Ti surfaces with Vit-D to elucidate potential intermolecular interactions between the modified Ti surfaces and Vit-D. Likewise, hydroxyapatite (HA) layer was developed on the functionalized Ti surfaces to analyze its chemical bonding with the bioactive coating. To accomplish the pursued goal, Raman scattering (RS) microspectroscopy was used as a highly sensitive, efficient, and robust analytical spectroscopic technique.

7.2 Materials and methods

Neat Ti plates (99.99%, Thermo-Fisher Scientific, Waltham, MA, USA) with dimensions of 10 mm x 10 mm x 2 mm were used as substrates for functionalization. The Ti surfaces were roughened using silicon carbide (SiC) grinding paper. The plates were then consecutively bathed with acetone, absolute ethanol, and deionized (DI) water in an ultrasonic bath for 15 min each. Once the Ti surfaces were cleaned, they were dried in a desiccator overnight before modification and functionalization. A mixture of 30 mL nitric acid (HNO_3, 40 wt.%) and 70 mL DI water was used for etching the Ti surfaces. The dried Ti substrates were etched for 2 min. Etched Ti surfaces were oxidized by immersing and soaking them in a hydrogen peroxide solution (H_2O_2, 30% wt.) for 24 h.

A 10.0 mM cholecalciferol solution was used to incubate and functionalize the TiO_2/Ti surfaces at room temperature. Total incubation process lasted 6 days. At the end of 3rd day, samples were rinsed with water and ethanol to eliminate any interferences. Functionalized Vit-D-Ti surfaces (Vit-D-TiO_2/Ti) were left in the air overnight to dry them.

The methodology described by Kokubo and coworkers to prepare Simulated Body Fluid (SBF) were implemented. [24] Vit-D-TiO_2/Ti samples were immersed and soaked in SBF for 28 days monitoring the precipitation of HA from SBF. The above procedure was used to evaluate the *in vitro* bioactivity of Vit-D-TiO_2/Ti to form an HA layer on the substrates.

RS was used to spectroscopically analyze the oxidized Ti surfaces, the organic ligand (Vit-D), and the functionalized plates. The reference samples were the two room temperature stable crystalline phases of TiO_2 (anatase and rutile). RS spectra were acquired by an InVia™ Raman spectrometers (Renishaw, LLC., West Dundee, IL). The spectrometers were interfaced to Leica DM2500 microscopes, and 50x Leica objectives were used to focus the laser beam on the sample surfaces for collecting the scattered light. Ten (10) accumulations were averaged with an exposure time of 10 s each. Two excitation sources were used: 532 nm and 785 nm diode pumped lasers (Cobolt AB, Solna, Sweden).

The Raman spectrometers were calibrated before each set of measurements based on 520.65 cm^{-1} Raman shift peak of polycrystalline silicon (Si). Characteristic Raman signatures were marked, and a baseline correction was applied to all spectra. Laser power at the samples was controlled to avoid sample degradation upon irradiation.

7.3 Results and discussion

7.3.1 Raman spectroscopic features of Vit-D

The full RS spectrum of Vit-D is shown in Figure 7.2. Figures 7.3 and 7.4 show the RS spectrum of Vit-D at low frequencies and C-H, O-H region, respectively. Table 7.1 shows the Raman shifts observed with their respective tentative assignments. The 2700-3100 cm^{-1} is composed for two strong bands that are overlapping among them, and they correspond to the C-H stretching vibration mode, where the band at 2866 cm^{-1} is associated to symmetric stretching of CH_2 group, and band at 2934 cm^{-1} is related to

chain-end CH_3 symmetric stretching mode. [25-29] The Raman spectrum is dominated by a prominent peak at 1647 cm^{-1}, which originates from C=C stretching vibration. [27,29,30] The band at 1436 cm^{-1} corresponds to CH_2 scissoring mode and deformation of CH_3 group. Similarly, a low-intensity band at 1323 cm^{-1} was observed, corresponding to CH_2 group and =CH bending. [31] The observed band at 1158 cm^{-1} is associated with the stretching vibration of single C-C bonds. [32,33] A considerable number of bands resulting from C-C backbone vibrations are observed in the 800-1000 cm^{-1} region. The bands in the 500-800 cm^{-1} region correspond to characteristic ring stretching. [27,34] With regards to –OH group, it can be distinguished two strong bands at 1073 and 1261 cm^{-1} associated to –C–OH bonding. Weak bands at 441 and 479 cm^{-1} are assigned to –OH wagging. [31]

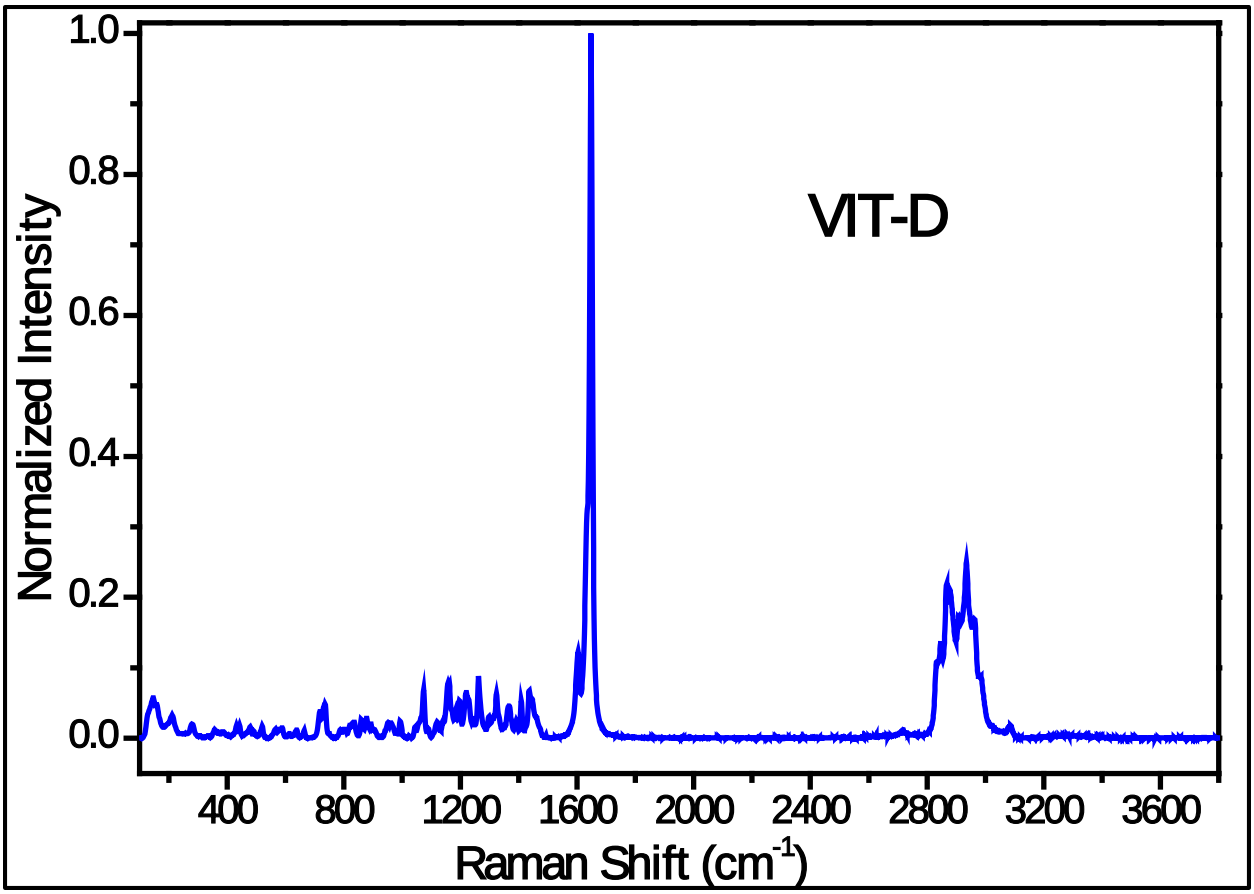

Figure 7.2. RS spectrum of Vit-D, full spectrum

Table 7. 1. Raman frequencies of Vit-D

Raman Shift (cm^{-1})	**Proposed Assignment**
2866 (s)	symmetric stretching of the CH_2 group
2934 (s)	chain-end CH_3 symmetric stretching mode
1647 (vs)	C=C stretching vibration
1436 (s)	CH_2 scissoring mode and to deformation of the CH_3
1323 (m)	CH_2 group and =CH bending
1158 (m)	stretching vibration of single C-C bond
1073 (s) and 1261 (s)	–C–OH bonding
800-1000	C-C backbone vibrations
500-800	ring stretching
441 (w) and 479 (w)	OH wagging

(vs) = very strong, (s) = strong, (m) = medium, (w) = weak, (vw) = very weak

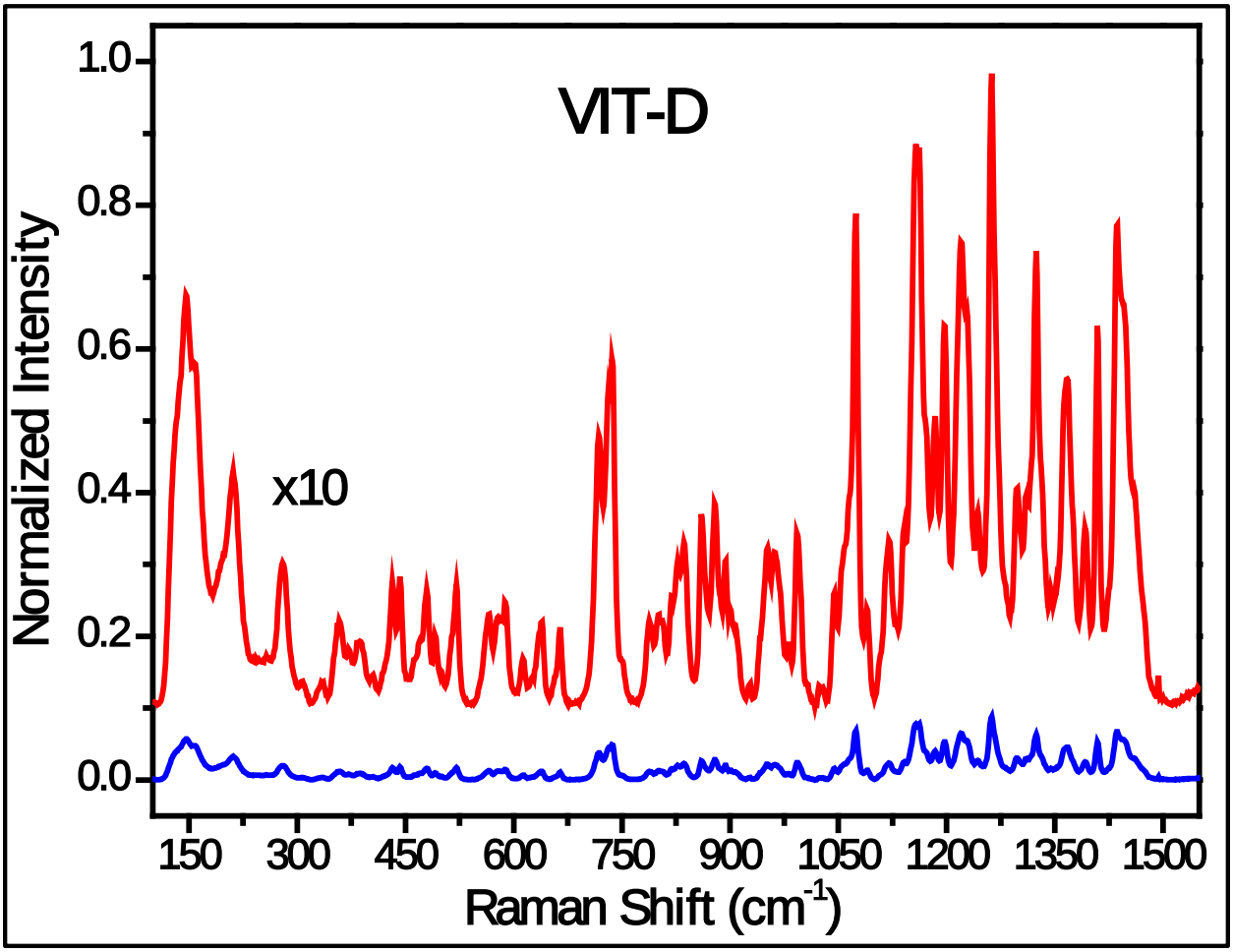

Figure 7. 3. RS spectrum of Vit-D: low frequencies and fingerprint regions.

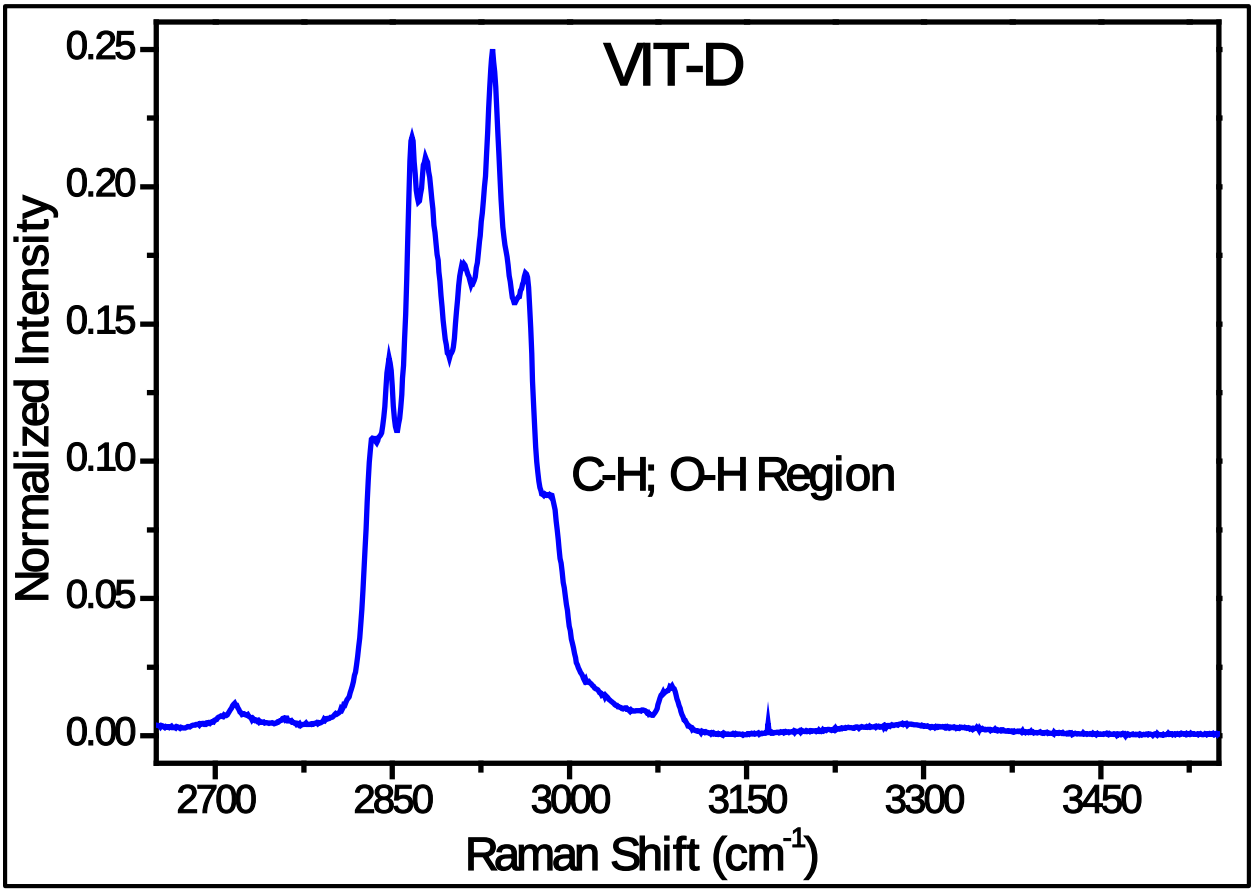

Figure 7.4. RS spectrum of Vit-D: C-H and O-H region.

7.3.2 Functionalization of Ti surface with Vit-D

Figure 7.5 and 7.6 show the full RS spectrum of TiO_2/Ti substrates functionalized with Vit-D and the 2700-3600 cm^{-1} region, respectively. It can be noted that the main bands at 2866 and 2934 cm^{-1} are on a broad peak centered about 2896 cm^{-1} corresponding to C-H stretching vibration mode. A possible explanation for the broadening and overlapping in this region has to do with the proximity of -CH group to the modified Ti surface and interactions with TiO_2 of modified Ti surface. About the above, the very broad band in the 3200-3550 cm^{-1} suggests, possibly, the formation of a coordination complex between C=C belonging to Vit-D and TiO_2 of TiO_2/Ti surface. When analyzing the spectrum in 200-2000 cm^{-1} (Figure 7.7) it can be seen that the dominant band in the Raman spectrum of Vit-D (Figure 7.2) attributed to C=C stretching vibration mode at 1647 cm^{-1} is now a low-intensity band and shifted to lower wavenumber (1640 cm^{-1}) [27,29,30] possibly due to the interaction of C=C with the TiO_2/Ti surface [35,36] resulting in a new bond, and therefore in a delocalization of the double bond, because of decreasing the electron density in the C=C bond. The above can be corroborated by analyzing the Figure 7.7, where it can be appreciated that the band located at 1323 cm^{-1} related to =CH bending has disappeared because there is an overlapping of bands in the 1200-1500 cm^{-1} region. Similarly, a new band at 1095 cm^{-1} has been found in the RS spectrum of Vit-D-TiO_2/Ti, and it can be suggested that it is associated with C-O-Ti bond. [35,36] Also, two new bands corresponding to -C-O torsion and C-C-O appear at 378, and 250 cm^{-1} were formed. Bands in the 1100-1400 cm^{-1} are assigned to characteristic vibrations of CH_2 in the Vit-D molecule. Likewise, the bands in the 800-1000 cm^{-1} correspond to the ring, corroborating its stability.

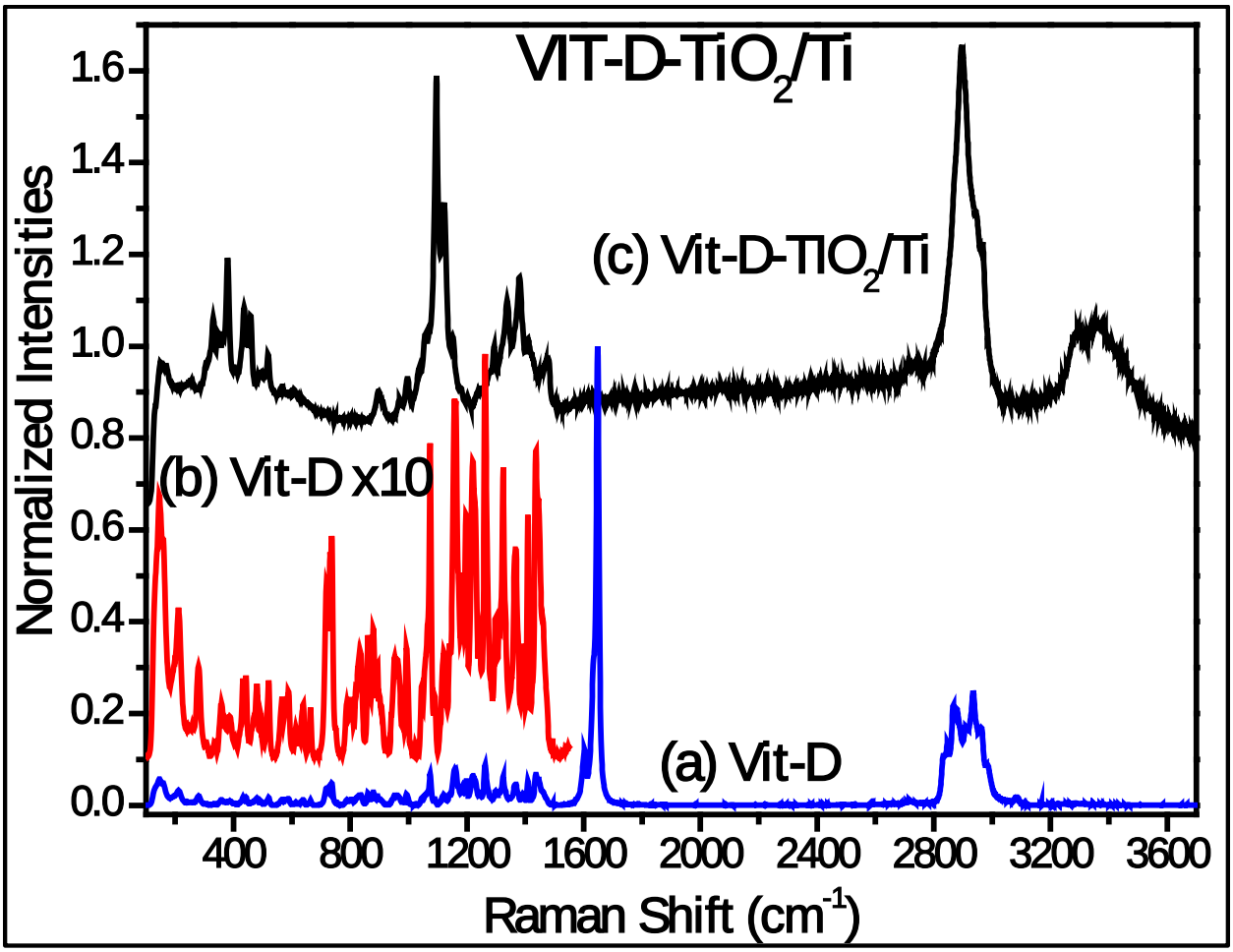

Figure 7.5. RS spectrum of TiO_2/Ti surface functionalized with Vit-D (full spectrum).

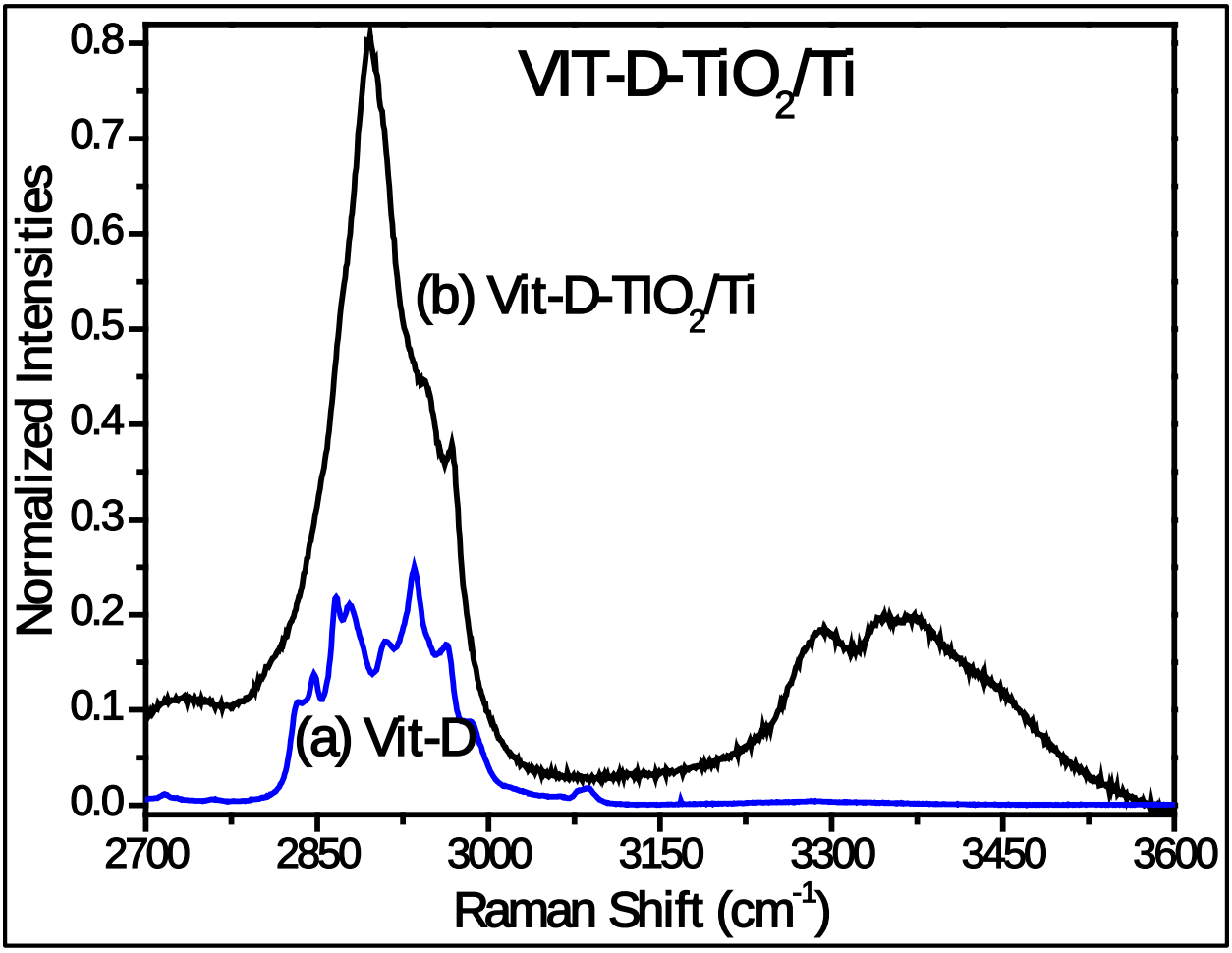

Figure 7.6. RS spectrum of TiO_2/Ti surface functionalized with Vit-D (CH, OH region).

When comparing the Raman spectra of organic ligand Vit-D (Figure 7.2) with Vit-D-TiO_2/Ti (Figures 7.5 to 7.7) a decrease in the number of bands as well as their overlapping and broadening. On the other hand, the characteristic of Vit-D-TiO_2/Ti Raman spectrum consists of the shift of bands corresponding to CH_2 wagging, CH deformation, CH_2 torsion, ring vibration modes and C-C ring stretching to lower wavenumbers. This supports the idea of formation of a complex between Vit-D and Ti ion of TiO_2.

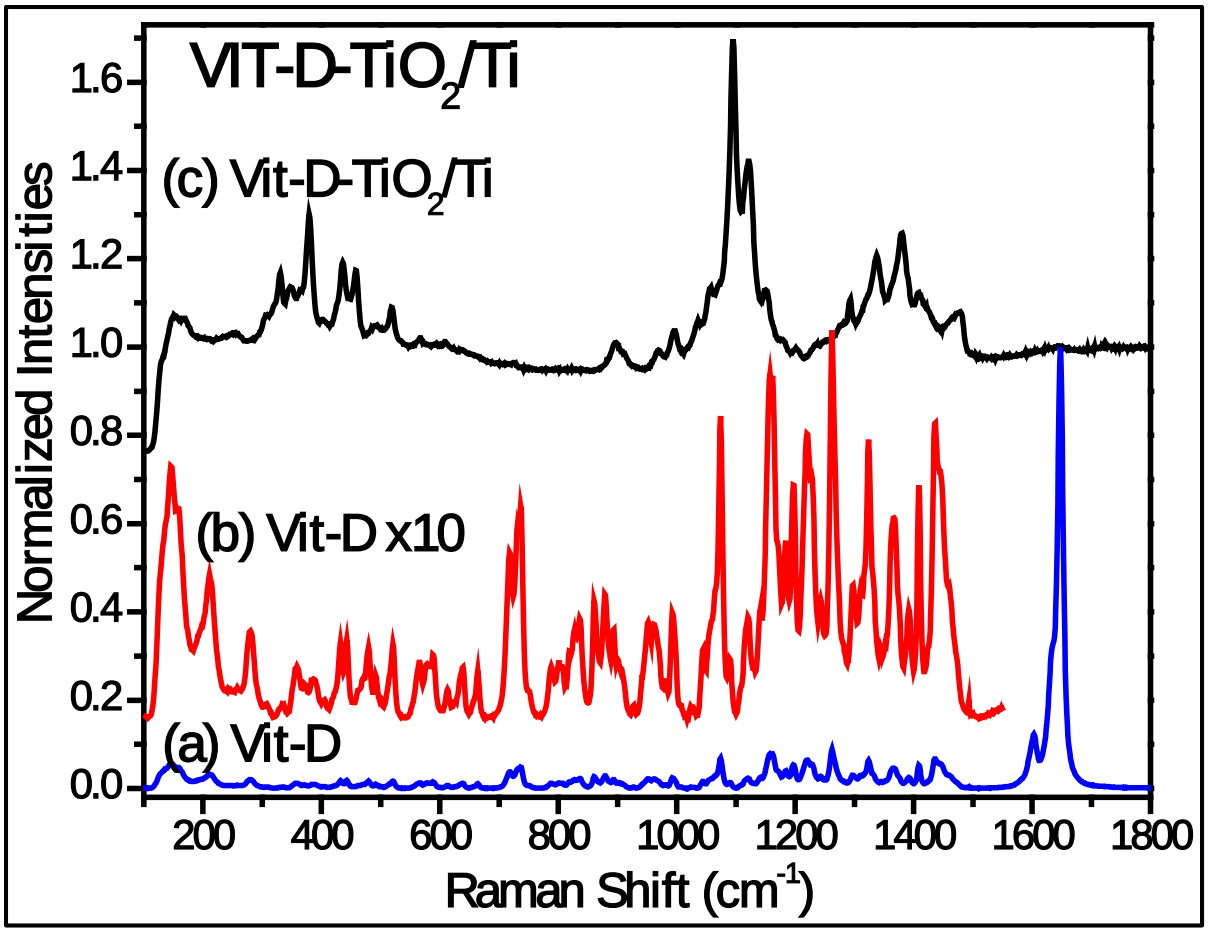

Figure 7.7. RS spectrum of TiO_2/Ti surface functionalized with Vit-D (100-1800 cm^{-1} region).

The above mentioned about broadening, overlapping and shift of bands in conjunction with the finding of new bands give clues about complexation of TiO_2/Ti with C=C bonds in the Vit-D molecule to form C-O-Ti bond. [35,36,37] Finally, based on the above arguments it can be suggested that the coating of modified Ti surface can be represented as a VIT-D-TiO_2 complex where the chemical bond and hence the intermolecular interactions are made through C-O-Ti bond regarding C=C bond. Consequently, the most probable suggested structure for adsorption of Vit-D on modified Ti surface is indicated in Figure 7.8, where it can be observed the intermolecular interactions of the above groups and Ti ion of modified Ti surface.

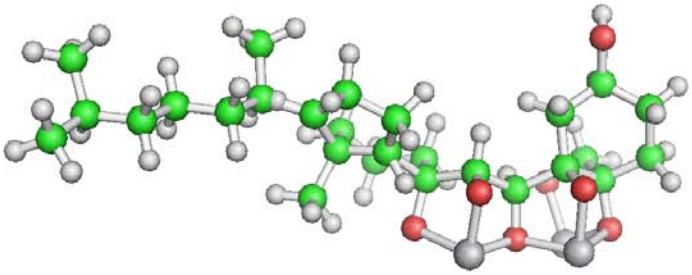

Figure 7.8. The proposed orientation of Vit-D on the functionalized TiO_2/Ti surface.

7.3.3 Bioactivity *"in vitro"* of Vit-D-Ti surface

The RS spectrum of the HA layer developed on the Vit-D-TiO2/Ti surfaces is shown in Figures 7.9, 7.10 and 7.11. The strong peak at 961 cm^{-1} dominates the full region spectrum. In the same way the characteristic bands of RS spectrum of HA at 415, 599 and 619 cm^{-1} were observed.

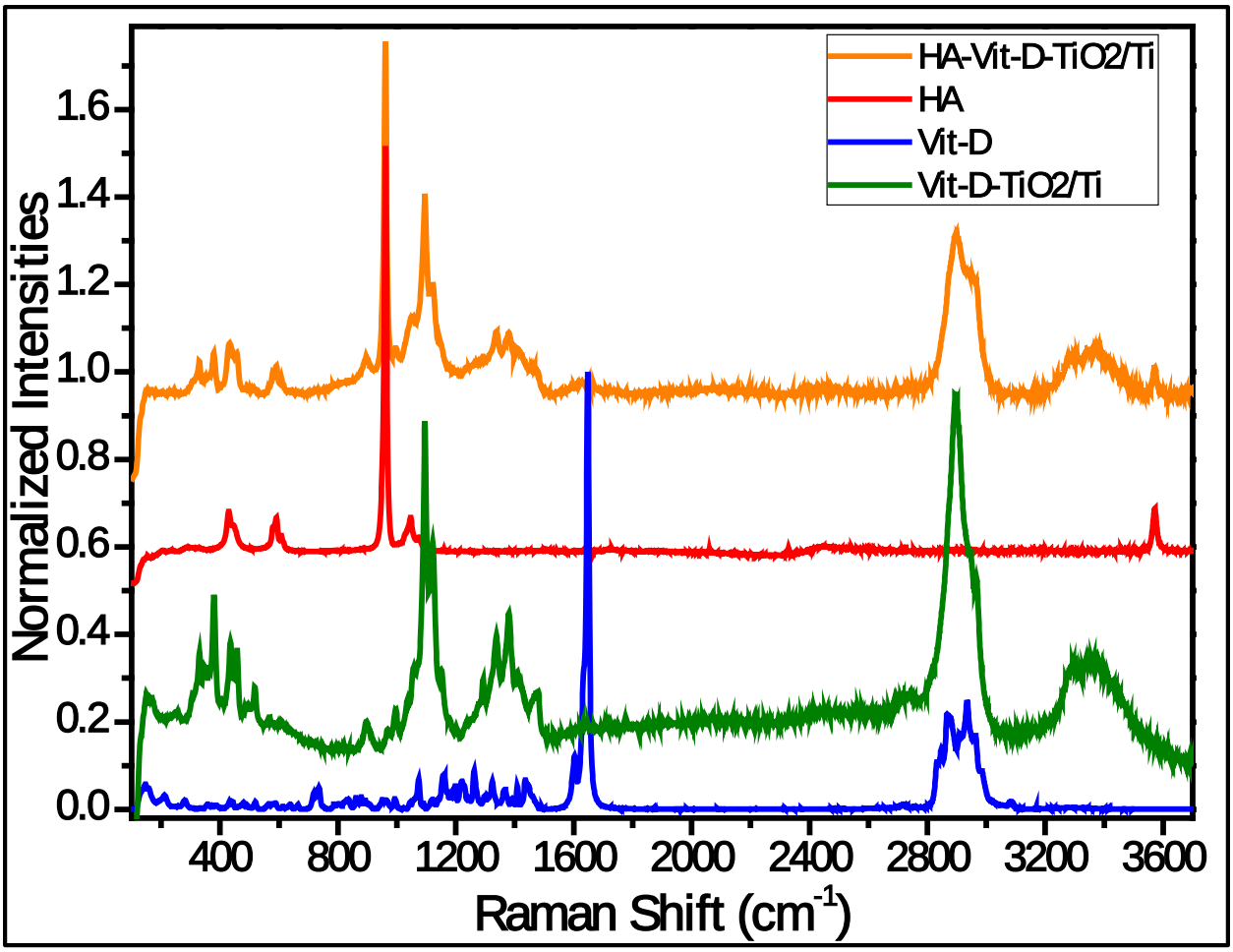

Figure 7. 9. RS spectrum of formed HA on functionalized VIT-D-TiO_2/Ti surface: full spectrum.

.

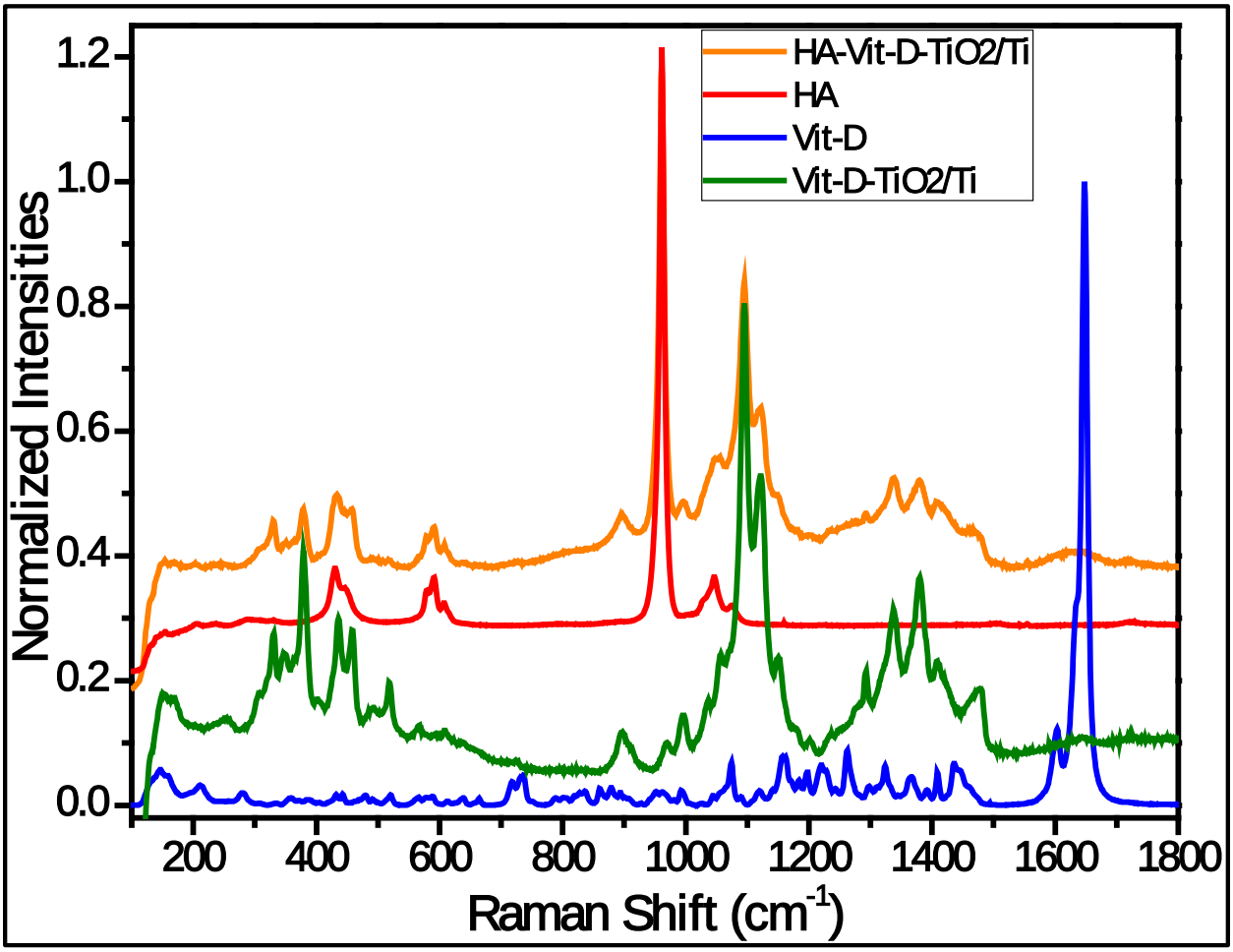

Figure 7.10. RS spectrum of formed HA on functionalized VIT-D-TiO_2/Ti surface (100-1800 cm^{-1} region).

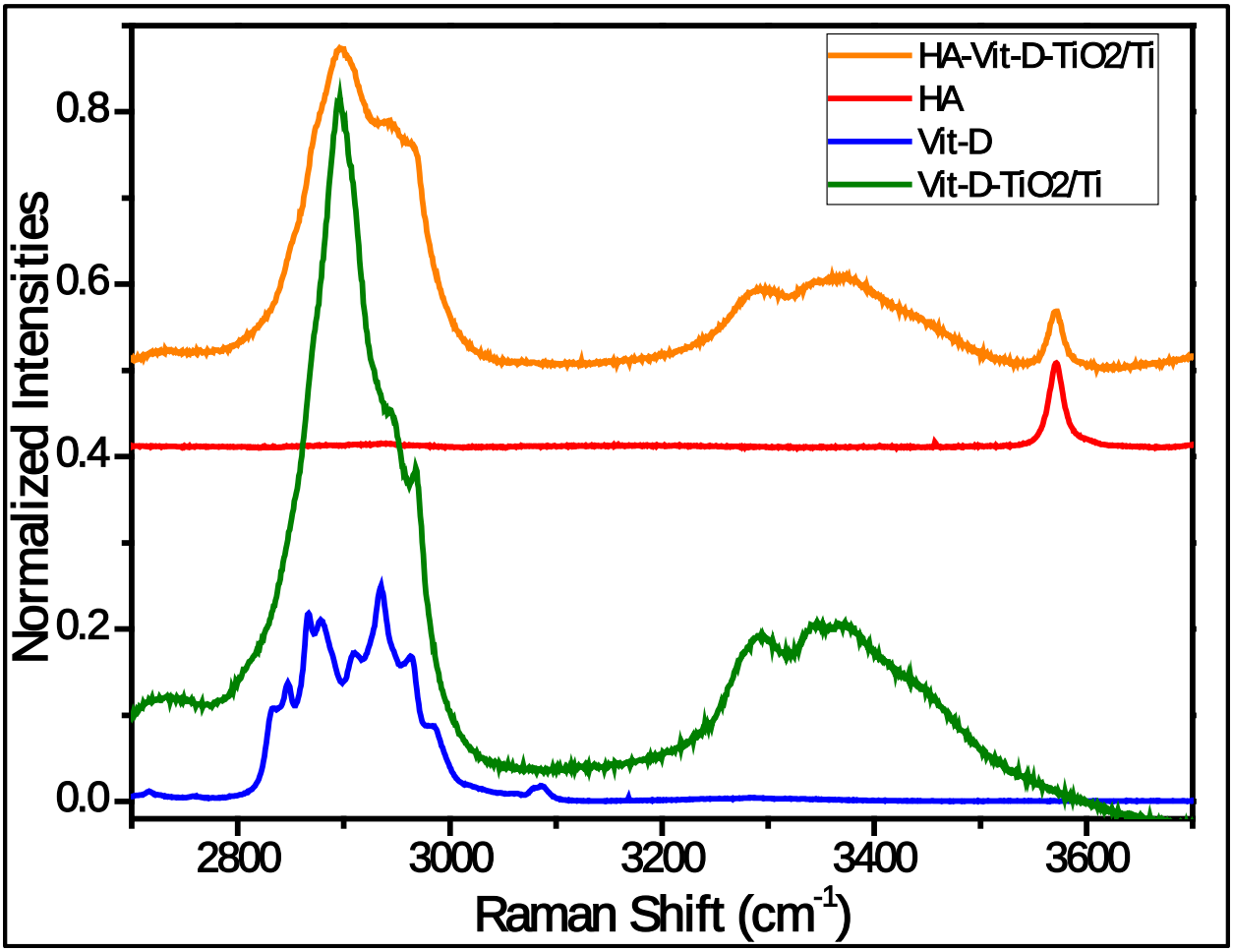

Figure 7.11. RS spectrum of formed HA on functionalized VIT-D-TiO_2/Ti surface (CH, OH region).

The band at 3571 cm^{-1} confirms the presence of –OH group of HA. The presence of water is discarded when verifying the absence of its characteristic band at 630 cm^{-1}. Also, it can be verified the structural order of phosphate groups observing the sharpness and intensity of peaks at 961 and 3571 cm^{-1}. [38-43] The above can be corroborated by observing that at 1647 cm^{-1} there is a very weak band associated to the C=C bond in Vit-D, and it can be inferred that single bond between C atoms belonging to the double bond and the oxygen atoms of TiO_2 are formed. Likewise, the band at 1095 cm^{-1} confirms the C-O-Ti bond. [35,36]

Other bands absent at 1261, 1073 and 479 cm^{-1} relative to –OH group normally appearing in the RS spectrum of Vit-D, suggest the formation of hydrogen bond between –OH and oxygen atoms of PO_4^{3-}. The stability of rings in the Vit-D molecule can be confirmed with the presence of weak bands at 378, 578, 591, 896 and 994 cm^{-1}. [27,31,34] The weak bands at 434 and 457 cm^{-1} are associated with -C-OH in-plane deformation. Similarly, in the region 1100-1400 cm^{-1} there are some bands overlapping among them, and they correspond to $-CH_2$ vibration modes in the Vit-D molecule. [31] When analyzing the 2800-3100 cm^{-1} region, a strong, broad band with overlapped peaks associated with C-H stretching vibration mode was found. Its broadening is possibly due to the proximity of -CH group with TiO_2/Ti surface.

Finally, RS measurements helped to clarify the adsorption and intermolecular interactions of HA with Vit-D on modified TiO_2/Ti surface. The absence of a strong band at 1647 cm^{-1} suggests that Vit-D is complexed with TiO_2/Ti surface, which is supported by the strong band at 1095 cm^{-1} corresponding to C-O-Ti bond, keeping the ring structure. Furthermore, the fixation of HA onto Vit-D-TiO_2/Ti surface can be related to

the hydrogen bond between the –OH group of Vit-D and oxygen atoms of the phosphate group of HA. Based on the discussion the suggested chemical structure for the complex is shown in Figure 7.12.

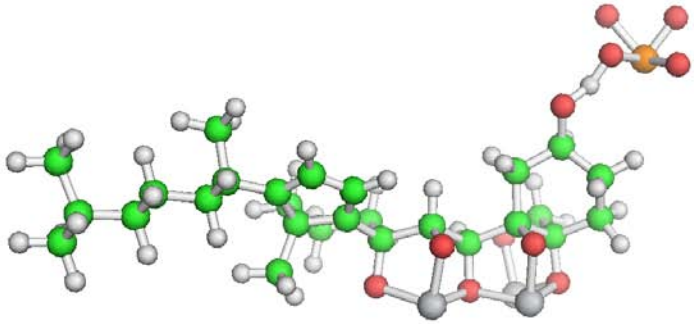

Figure 7. 12. Proposed chemical structure of HA-VIT-D onto the functionalized Ti surface.

7.4 Conclusions

Vit-D was used to coat and functionalize the TiO_2/Ti surfaces, which were obtained from modified neat Ti plate. RS spectroscopy was used to identify the types of intermolecular interactions between the organic ligand adsorbate and the substrates. Vibrational data obtained showed a very strong peak at 1647 cm^{-1}, originating from C=C stretching vibration, which dominates the RS spectrum of Vit-D. The ring structure part in the Vit-D molecule was verified by the bands in the 500-800 cm^{-1} region. Two bands at 1073 and 1261 cm^{-1} were associated with the existence of –OH group.

The most characteristic features of RS spectrum of Vit-D-TiO_2/Ti surfaces have to do with the decrease in the number of vibrational bands as well as profuse overlapping and broadening. The appearance of new bands and shifting of peaks to lower wavenumbers, related to aliphatic chain and C-C ring, supports the hypothesis about the formation of a complex between Vit-D and Ti species belonging to TiO_2/Ti surface, where intermolecular interactions are controlled by the C=C bond involved in the creation of C-O-Ti bond. The strong band at 1647 cm^{-1} corresponding to C=C vibration which is absented and the new strong peak at 1095 cm^{-1} support the complexation of Vit-D with TiO_2/Ti surface.

The adsorption and intermolecular interactions of HA with Vit-D-TiO_2 /Ti surface were analyzed using RS measurements. The characteristic bands of RS spectrum of HA at 415, 599 and 619 cm^{-1} were observed. Intermolecular interactions, possibly through hydrogen bonds between the oxygen of PO_4^{3-} of HA and -OH group of Vit-D,

favoring enhancement of bands and consequently their overlap can be related to fixation of HA.

Acknowledgments

The authors express sincere appreciation to the faculty members and supporting personnel of the Departments of Bioengineering and Chemistry of the Mayagüez Campus of the University of Puerto Rico for their collaboration during all project stages.

Conflict of Interest

The authors report there are no conflicts of interest.

7.5 References

[1] M. F. Holick, “Resurrection of vitamin D deficiency and rickets,” *J. Clin. Invest.*, **116**(8): 2062–2072, 2006.

[2] K. Rajakumar, “Vitamin D, Cod-Liver Oil, Sunlight, and Rickets: A Historical Perspective,” *Pediatrics*, **112**(2): e132-e135, 2003.

[3] M. F. Holick, “Vitamin D Deficiency,” *N. Engl. J. Med.*, **357**(3): 266–281, 2007.

[4] S. Christakos, M. Hewison, D. G. Gardner, C. L. Wagner, I. N. Sergeev, E. Rutten, A. G. Pittas, R. Boland, L. FerruVit-Di, and D. D. Bikle, “Vitamin D: beyond bone,” *Ann. N. Y. Acad. Sci.*, **1287**(1): 45–58, 2013.

[5] L. F. Cooper, “Systemic effectors of alveolar bone mass and implications in dental therapy,” *Periodontol. 2000*, **23**(1): 103–109, 2000.

[6] M. van Driel, M. Koedam, C. J. Buurman, M. Roelse, F. Weyts, H. Chiba, A. G. Uitterlinden, H. A. P. Pols, and J. P. T. M. van Leeuwen, “Evidence that both

1α,25-dihydroxyvitamin D_3 and 24-hydroxylated D_3 enhance human osteoblast differentiation and mineralization," *J. Cell. Biochem.*, **99**(3): 922–935, 2006.

[7] I. Nemere, N. Garbi, G. Hammerling, and K. J. Hintze, "Role of the 1,25D_3-MARRS receptor in the 1,25$(OH)_2D_3$-stimulated uptake of calcium and phosphate in intestinal cells," *Steroids*, **77**(10): 897–902, 2012.

[8] R. St-Arnaud, "The direct role of vitamin D on bone homeostasis," *Arch. Biochem. Biophys.*, **473**(2): 225–230, 2008.

[9] L. G. Raisz, C. L. Trummel, M. F. Holick, and H. F. Deluca, "1,25-Dihydroxycholecalciferol: A Potent Stimulator of Bone Resorption in Tissue Culture," *Science*, **175**(4023): 768-769, 1972.

[10] T. Suda, N. Takahashi, N. Udagawa, E. Jimi, M. T. Gillespie, and T. J. Martin, "Modulation of Osteoclast Differentiation and Function by the New Members of the Tumor Necrosis Factor Receptor and Ligand Families," *Endocr. Rev.*, **20**(3): 345–357, 1999.

[11] A. Shiraishi, S. Higashi, H. Ohkawa, N. Kubodera, T. Hirasawa, I. Ezawa, K. Ikeda, and E. Ogata, "The Advantage of Alfacalcidol Over Vitamin D in the Treatment of Osteoporosis," *Calcif. Tissue Int.*, **65**(4): 311–316, 1999.

[12] H. Orimo, M. Shiraki, Y. Hayashi, T. Hoshino, T. Onaya, S. Miyazaki, H. Kurosawa, T. Nakamura, and N. Ogawa, "Effects of 1α-hydroxyvitamin D_3 on lumbar bone mineral density and vertebral fractures in patients with postmenopausal osteoporosis," *Calcif. Tissue Int.*, **54**(5): 370–376, 1994.

[13] S. Sairanen, M. Kärkkäinen, R. Tähtelä, K. Laitinen, P. Mäkelä, C. Lamberg-Allardt, and M. J. Välimäki, "Bone Mass and Markers of Bone and Calcium Metabolism in Postmenopausal Women Treated with 1,25-Dihydroxyvitamin D (Calcitriol) for Four Years," *Calcif. Tissue Int.*, **67**(2): 122–127, 2000.

[14] R. I. Kelley, "Diagnosis of Smith-Lemli-Opitz syndrome by gas chromatography/mass spectrometry of 7-dehydrocholesterol in plasma, amniotic fluid and cultured skin fibroblasts," *Clin. Chim. Acta*, **236**(1): 45–58, 1995.

[15] J. MacLaughlin and M. F. Holick, "Aging decreases the capacity of human skin to produce vitamin D3.," *J. Clin. Invest.*, **76**(4): 1536–1538, 1985.

[16] G S. Tint, M. Irons, E. R. Elias, A. K. Batta, R. Frieden, T. S. Chen, and G. Salen, “Defective Cholesterol Biosynthesis Associated with the Smith-Lemli-Opitz Syndrome,” *N. Engl. J. Med.*, **330**(2): 107–113, 1994.

[17] H. Glerup, K. Mikkelsen, L. Poulsen, E. Hass, S. Overbeck, J. Thomsen, P. Charles, and E. F. Eriksen, “Commonly recommended daily intake of vitamin D is not sufficient if sunlight exposure is limited,” *J. Intern. Med.*, **247**(2): 260–268, 2000.

[18] L. M. Hall, M. G. Kimlin, P. A. Aronov, B. D. Hammock, J. R. Slusser, L. R. Woodhouse, and C. B. Stephensen, “Vitamin D Intake Needed to Maintain Target Serum 25-Hydroxyvitamin D Concentrations in Participants with Low Sun Exposure and Dark Skin Pigmentation Is Substantially Higher Than Current Recommendations,” *J. Nutr.*, **140**(3): 542–550, 2010.

[19] H. M. Macdonald, A. Mavroeidi, W. D. Fraser, A. L. Darling, A. J. Black, L. Aucott, F. O’Neill, K. Hart, J. L. Berry, S. A. Lanham-New, D. M. Reid, “Erratum to: Sunlight and dietary contributions to the seasonal vitamin D status of cohorts of healthy postmenopausal women living at northerly latitudes: a major cause for concern?,” *Osteoporos. Int.*, **22**(9): 2473–2474, 2011.

[20] P. Lips, “Vitamin D physiology,” *Prog. Biophys. Mol. Biol.*, **92**,(1): 4–8, 2006.

[21] K. James, L. Audrey, W. C. J., P. Sil, and N. Ichiro, “Vitamin D and Bone Physiology: Demonstration of Vitamin D Deficiency in an Implant Osseointegration Rat Model,” *J. Prosthodont.*, **18**(6): 473–478, 2009.

[22] F. Alvim-Pereira, C. C. Montes, G. Thomé, M. Olandoski, and P. C. Trevilatto, “Analysis of association of clinical aspects and vitamin D receptor gene polymorphism with dental implant loss,” *Clin. Oral Implants Res.*, **19**(8): 786–795, 2008.

[23] S. Jingushi, A. Iwaki, O. Higuchi, Y. Azuma, T. Ohta, J. Shida, T. Izumi, T. Ikenoue, Y. Sugioka, and Y. Iwamoto, “Serum 1α,25-Dihydroxyvitamin D_3 AVit-Dumulates into the Fracture Callus during Rat Femoral Fracture Healing,” *Endocrinology*, **139**(4): 1467–1473, 1998.

[24] T. Kokubo and H. Takadama, “How useful is SBF in predicting in vivo bone bioactivity?,” *Biomaterials*, 27(15): 2907–2915, 2006.

[25] W. W. Morris, J. B. Wilkie, S. W. Jones, and L. Friedman, “Differentiation of Vitamins D_2 and D_3 by Infrared Spectrophotometry”, *Anal. Chem.*, **34**(3): 381–384, 1962.

[26] N. Toyran and F. Severcan, “Infrared Spectroscopic Studies on the Dipalmitoyl Phosphatidylcholine Bilayer Interactions with Calcium Phosphate: Effect of Vitamin D_2” *Spectroscopy*., **16**(3-4): 399–408, 2002

[27] C. Krafft, L. Neudert, T. Simat, and R. Salzer, “Near infrared Raman spectra of human brain lipids,” *Spectrochim. Acta Part A Mol. Biomol. Spectrosc.*, **61**(7): 1529–1535, 2005.

[28] J. L. Suhalim, C. Chung, M. B. Lilledahl, R. S. Lim, M. Levi, B. J. Tromberg, and E. O. Potma, “Characterization of Cholesterol Crystals in Atherosclerotic Plaques Using Stimulated Raman Scattering and Second-Harmonic Generation Microscopy,” *Biophys. J.*, **102**(8): 1988–1995, 2012.

[29] S. Bresson, M. El Marssi, and B. Khelifa, “First investigations of two important components of low density lipoproteins by Raman spectroscopy: the cholesteryl linoleate and arachidonate,” *Vib. Spectrosc.*, **34**(2): 231–241, 2004.

[30] T. J. Ro, J. F. Brennan III, T. C. Bakker, R. Wolthuis, R. C.M. van den Hoogen, J. J. Emeis, A. van der Laarse, A. V. G. Bruschke, G. J. Puppels, “Raman spectroscopy for quantifying cholesterol in intact coronary artery wall,” *Atherosclerosis*, **141**(1): 117–124, 1998.

[31] G. Socrates, “Infrared and Raman Characteristic Group Frequencies, Tables and Charts.” Third Ed., John Wiley & Sons, Ltd., 2001.

[32] E. Kočišová, A. Antalík, and M. Procházka, “Drop coating deposition Raman spectroscopy of liposomes: role of cholesterol,” *Chem. Phys. Lipids*, **172-173**: 1–5, 2013.

[33] P. Le Cacheux, G. Ménard, H. Nguyen Quang, N. Q. Dao, A. G. Roach, and D. Dron, “Quantitative determination of free and esterified cholesterol concentrations in cholesterol-fed rabbit aorta using near-infrared- Fourier Transform-Raman

spectroscopy," *Spectrochim. Acta Part A Mol. Biomol. Spectrosc.*, **52**(12): 1619–1627, 1996.

[34] M. Muratore, "Raman spectroscopy and partial least squares analysis in discrimination of peripheral cells affected by Huntington's disease," *Anal. Chim. Acta*, **793**: 1–10, 2013.

[35] T. A. Nijhuis, T. Visser, and B. M. Weckhuysen, "The Role of Gold in Gold–Titania Epoxidation Catalysts," *Angew. Chemie Int. Ed.*, **44**(7): 1115–1118, 2005.

[36] A. Ruiz, B. van der Linden, M. Makkee, and G. Mul, "Acrylate and propoxy-groups: Contributors to deactivation of Au/TiO_2 in the epoxidation of propene," *J. Catal.*, **266**(2): 286–290, 2009.

[37] G. Lui, J.-Y. Liao, A. Duan, Z. Zhang, M. Fowler, and A. Yu, "Graphene-wrapped hierarchical TiO_2 nanoflower composites with enhanced photocatalytic performance," *J. Mater. Chem. A*, **1**(39): 12255–12262, 2013.

[38] B. Mihailova, B. Kolev, C. Balarew, E. Dyulgerova, and L. Konstantinov, "Vibration spectroscopy study of hydrolyzed precursors for sintering calcium phosphate bio-ceramics," *J. Mater. Sci.*, **36**(17): 4291–4297, 2001.

[39] G. R. Sauer, W. B. Zunic, J. R. Durig, and R. E. Wuthier, "Fourier transform raman spectroscopy of synthetic and biological calcium phosphates," *Calcif. Tissue Int.*, **54**(5): 414–420, 1994.

[40] H. Tsuda and J. Arends, "Raman Spectra of Human Dental Calculus," *J. Dent. Res.*, **72**(12): 1609–1613, 1993.

[41] B. O. Fowler, M. Markovic, and W. E. Brown, "Octacalcium phosphate. 3. Infrared and Raman vibrational spectra," *Chem. Mater.*, **5**(10): 1417–1423, 1993.

[42] G. Penel, N. Leroy, P. Van Landuyt, B. Flautre, P. Hardouin, J. Lemaitre, and G. Leroy, "Raman microspectrometry studies of brushite cement: in vivo evolution in a sheep model," *Bone*, **25**(2), Supplement 1, p. 81S–84S, 1999.

[43] F. Barrere, C. A. van Blitterswijk, K. de Groot, and P. Layrolle, "Nucleation of biomimetic Ca–P coatings on Ti6Al4V from a SBF×5 solution: influence of magnesium," *Biomaterials*, **23**(10): 2211–2220, 2002.

Chapter 8

Conclusions and Future Work

8.1 Conclusions

Functionalization of Ti surfaces with biological molecules was successfully achieved. The subsequent *"in vitro"* development of a HA layer on each of the derivatized TiO_2/Ti substrates, which was the main objective of this work, which was also effectively accomplished as per the spectroscopic interpretation of the RS data for all the stages of the established protocol

First, characterization of important intermolecular interactions between adsorbates (Lys, Asp, Vit-C, Vit-D3, and HA) and the functionalized Ti surface was done using micro Raman spectroscopy. Second, based on the spectroscopic evidence, the most probable spatial orientation of the adsorbates interacting with the surface were suggested, and therefore the chemical structure of the biological species coating the TiO_2/Ti surface. Third and probably most important, the spectroscopic evidence points to the direction that the target molecules chosen as adsorbate ligands are very good candidates to functionalize the modified Ti surface, hence promoting the *"in vitro"* formation of a HA layer on the TiO_2/Ti surface.

Regarding TiO_2/Ti surfaces functionalized with Lys, structural and chemical information about the intermolecular interactions between it and the host TiO_2/Ti

substrate was obtained by means of RS. RS data of the interaction at different pH values could suggests that Lys formed with TiO_2/Ti surface via its carboxylic group forming a a bridged structure complex. Further complexation is possible with the neighboring ammonium group. An HA layer was developed onto Lys-TiO_2/Ti surface, as evidence by spectroscopic data. Interaction with the host substrate can be attributed to formation of H-bonds or to longer range electrostatic binding involving calcium ions. These weak interactions are probably responsible for adhesion of the important mineralization HA layer on the Lys–TiO_2/Ti surfaces.

In relation to Asp adsorbed on the TiO_2/Ti surfaces, it was inferred that –COOH groups of Asp formed bridged surface complexes with the host substrate. Based on the Raman data, it appears that the ammonium group remained oriented far from the TiO_2/Ti surfaces. The above suggests that Asp molecule is at angle with respect to TiO_2/Ti surfaces. Also RS data was used to verify that HA coating developed on Asp-TiO_2/Ti surfaces. The adsorption of HA onto TiO_2/Ti surfaces was probably mediated by hydrogen bonds between –COOH groups of Asp and oxygen atoms belonging to PO_4^{3-}.

Formation of bidentate complex TiO_2/Ti surface with Vit-C was also evidenced. This was deduced from the change of the band shape of –OH groups of 2,3-enediol in conjunction with new bands and changes in the ring structure evidenced the above. Vit-C-TiO_2/Ti surface allowed the formation of an HA layer, as confirmed by RS based on specific spectroscopic bands corresponding to interactions between –C-OH group of Vit-C and the oxygen atoms of of PO_4^{3-} group and C-O group of Vit-C and $^{-}$OH of HA.

Vit-D was the other biological molecule used to functionalized TiO_2/Ti surface. Here, the appearance of new bands and shifting of peaks to lower wavenumbers in the Raman Shift scale of the aliphatic chain and C-C ring supports the hypothesis of the formation of complex between Vit-D and TiO_2/Ti surface together with the formation of a C-O-Ti bond. RS measurements suggested that there are intermolecular interactions between HA and Vit-D-TiO_2 /Ti surface.

8.2 Future work

In order to absolutely assign the observed vibration bands for each one of the adsorbates on the Ti surface and therefore to understand better why some signals appear and other do not in the obtained spectra, it is highly recommended to carry out isotopic labelling of the target biomolecules that have been postulated as good candidates for functionalizing the TiO_2/Ti surfaces. These experiments could be accompanied by *ab initio* calculations and by molecular mechanics modeling of the systems studied.

Even though the *"in vitro"* results of functionalized Ti surface have been very good, it is advisable to perform *"in vivo"* research in order to confirm their efficiency and roles in cellular systems. The protocols described should be modified to improve bioactivity of the coated Ti surface to enhance the *"in vivo"* osseointegration.

It is very important to point out that the evaluation of functionalized Ti surfaces is important to medical and health sciences but that other science and engineering fields, such as bioengineering and molecular biology can contribute significantly to expand the

knowledge about this important applied field and help to interpret the results of the *"in vivo"* experiments. Biostatistics will probably also play an important role also..